

CALIPSO Level 3 Stratospheric Aerosol Profile Product: Version 1.00 Algorithm Description and Initial Assessment

Jayanta Kar^{1,2}, Kam-Pui Lee^{1,2}, Mark A. Vaughan², Jason L. Tackett^{1,2}, Charles R. Trepte², David M. Winker², Patricia L. Lucker^{1,2}, Brian J. Getzewich^{1,2}

¹Science Systems and Applications Inc., Hampton, VA, USA

²NASA Langley Research Center, Hampton, VA, USA

Correspondence to: J. Kar (jayanta.kar@nasa.gov)

Abstract. In August 2018, the Cloud-Aerosol Lidar and Infrared Pathfinder Satellite Observation (CALIPSO) project released a new level 3 stratospheric aerosol profile data product derived from nearly 12 years of measurements acquired by the space-borne Cloud-Aerosol Lidar with Orthogonal Polarization (CALIOP). This monthly averaged, gridded level 3 product is based on version 4.2 of the CALIOP level 1B and level 2 data products, which feature significantly improved calibration that now makes it possible to reliably retrieve profiles of stratospheric aerosol extinction and backscatter coefficients at 532 nm. This paper describes the science algorithm and data handling techniques that were developed to generate the CALIPSO version 1.00 level 3 stratospheric aerosol profile product. Further, we show that the ~~retrieved~~ extinction profiles (retrieved using a constant lidar ratio of 50 sr) capture the major stratospheric perturbations in both hemispheres over the last decade resulting from volcanic eruptions, extreme smoke events, and signatures of stratospheric dynamics. Initial assessment of the product by inter-comparison with the stratospheric aerosol retrievals from the Stratospheric Aerosol and Gas Experiment III (SAGE III) on the International Space Station (ISS) indicates good agreement in the tropical stratospheric aerosol layer (30°N-30°S), where the average difference between zonal mean extinction profiles is typically less than 25% between 20 km and 30 km (CALIPSO biased high). However, differences can exceed 100% in the very low aerosol loading regimes found above 25 km at higher latitudes. Similarly there are large differences ($\geq 100\%$) within 2 to 3 kilometers above the tropopause which might be due to cloud contamination issues.

1. Introduction.

While the bulk of the global distribution of atmospheric aerosols is concentrated within the planetary boundary layer and free troposphere, the persistent aerosol burden in the stratosphere has long been known to have important implications for Earth's climate (Turco et al., 1980). Techniques for reliable detection of a background aerosol layer in the stratosphere date back to the early ~~sixties~~1960s (Junge and Manson, 1961). These aerosols are mostly liquid sulfate particles which are derived from precursor gases like SO₂ and carbonyl sulfide (OCS) transported from the troposphere (Thomason and Peter, 2006, Kremser et al., 2016, Thomason et al., 2018). In addition, intermittent volcanic eruptions and strong biomass burning events can inject sulfates, ash, and smoke into the stratosphere, which can last for long periods of time and exert significant climatic influences. For example, stratospheric perturbations from the Pinatubo volcano in 1991 lasted for several years (Chazette et al., 1995, Robock, 2000, Deshler, 2008). While eruptions of the same scale as Pinatubo have not taken place in the last 25 years or so, there is evidence that a large number of smaller eruptions ~~have~~has been significantly affecting the stratosphere with implications for the climate system (Vernier et al., ~~2011~~2011a, Solomon et al., 2011). Thus it is very important to monitor the stratospheric aerosol loading over the long term. ~~As such~~In pursuit of this goal, stratospheric aerosol measurements have been made ~~from~~using numerous techniques, including ground based ~~lidar~~,lidars and balloon borne in situ samplers, as well as multi-sensor aircraft measurements ~~for a long time~~ (, since the mid-twentieth century (Junge et al., 1961, Northam et al., 1974, Hoffman et al., 1975, McCormick et al., 1984, Gramms and Fiocco, 1986, Brock et al., 1993, Beyerle et al., 1994, Jaeger and Deshler 2002).

Most of our current knowledge of the global distribution of stratospheric aerosols comes from satellite measurements. ~~The earliest such measurements were carried out by the Stratospheric Aerosol Measurement II (SAM II) on board the Nimbus 7 spacecraft which provided the vertical profiles of aerosol extinction at 1 μm and in particular from~~were followed by the Stratospheric Aerosol and Gas Experiment (SAGE) series of instruments (Chu and McCormick, 1979, Kent and McCormick, 1984, Mauldin et al., 1985; Chu et al., 1993; Damadeo et al., 2013). The basic principle employed in these instruments is solar occultation, wherein the vertical profile of stratospheric aerosols is retrieved from measurement of sunlight as the rays pass through the

atmosphere during sunrise and sunset events as observed from the orbiting spacecraft. Stratospheric aerosols have been characterized using this technique from SAGE instruments on Earth Radiation Budget Satellite (ERBS) and Meteor-3M as well as from the International Space Station (ISS). ~~Another~~ Among other space-borne ~~instrument~~ instruments that ~~uses~~ have used this technique ~~is~~ are the Polar Ozone and Aerosol Measurement (POAM II, POAM III, Glaccum et al., 1996, Lucke et al., 1999) and Measurement of Aerosol Extinction in the Stratosphere and Troposphere Retrieved by Occultation (MAESTRO, McElroy et al., 2009). In addition, the Optical Spectrograph and InfraRed Imager System (OSIRIS) and the Ozone Mapping and Profiler Suite (OMPS) have used a limb scatter technique to obtain the aerosol extinction profiles (Bourassa et al., 2012, Chen et al., 2018).

A novel and pioneering technique to retrieve aerosol profiles from space came about with the launch of the Cloud-Aerosol Lidar and Infrared Pathfinder Satellite Observation (CALIPSO) mission in April 2006, with a two-wavelength, polarization-sensitive elastic backscatter lidar as the primary payload (Winker et al., 2010). For over 12 years the Cloud-Aerosol Lidar with Orthogonal Polarization (CALIOP) has been providing ~~vertically-resolved~~ profiles of aerosol and cloud extinction globally. The primary measurement from a space-borne elastic backscatter lidar consists of ~~the~~ attenuated backscatter ~~measurements from~~ coefficients of the aerosols and clouds in the atmosphere. The strong backscatter from the tropospheric aerosols, combined with CALIOP's relatively strong signal-to-noise ratio (SNR), has been exploited to provide accurate extinction profiles in the troposphere (Young and Vaughan, 2009, Winker et al., 2013, Young et al., 2013, 2016, 2018). In comparison, the aerosol loading in the stratosphere is much lower with correspondingly smaller SNR. As such, retrieving stratospheric aerosol information was not originally a principal target of the CALIPSO mission. However, early results indicated that it might be possible to obtain such information with ~~adequate~~ sufficient averaging of the data (Thomason and Pitts, 2007, Vernier et al., 2009).

One of the issues impacting the retrieval of stratospheric aerosol extinction was the realization that the standard calibration altitude of CALIOP, which was originally fixed at 30-34 km (Powell et al., 2009), was not completely free of aerosols and thus applying the molecular normalization technique at these altitudes would bias the aerosol extinction profiles (Vernier et al., 2009). This issue has since been addressed with the release of the version 4 (V4) family of CALIPSO data products in November 2016. In this version, the calibration altitude for the

nighttime 532 nm data which is the primary calibration for all of CALIOP measurements (all the other measurements like the daytime data as well as the 1064 nm data are calibrated relative to the 532 nm nighttime calibration) was raised to 36-39 km, where the aerosol loading is expected to be negligible (Kar et al., ~~2018~~2018a). This largely removed the aerosol contamination issue, making reliable retrievals of stratospheric aerosols possible. Accordingly, a stand-alone CALIPSO stratospheric aerosol **profile** product was developed which uses the V4 level ~~1B~~ and level 2 data from the CALIOP measurements. This is a level 3 monthly averaged product gridded in latitude (5°), longitude (20°) and altitude (900 m). In what follows, we describe the overall algorithm and its implementation in detail in section 2. Section 3 then presents a comprehensive assessment of the quality and capabilities of this new data product, including analyses of the temporal and spatial evolution of specific stratospheric features captured by the product and inter-comparisons with extinction retrievals from SAGE III on ISS. Discussion and concluding remarks are given in section 4 and section 5 respectively.

2. Overall design of the **level 3** stratospheric aerosol profile product

2.1 Motivation for a CALIPSO stratospheric product

The CALIPSO **level 3** stratospheric aerosol **profile** product is built primarily from the V4 level ~~1B~~ 532 nm attenuated backscatter profiles (https://eosweb.larc.nasa.gov/project/calipso/cal_lid_11-standard-v4-10) As mentioned above, the most fundamental change in V4 level 1 data was the ~~new~~improved calibration of the 532 nm nighttime data (Kar et al., ~~2018~~2018a). The consequences of this change are illustrated in Figure 1, which shows the **median values of** zonally averaged attenuated scattering ratios at 30-34 km from **version 3 (V3)** and V4 for the month of May 2009.

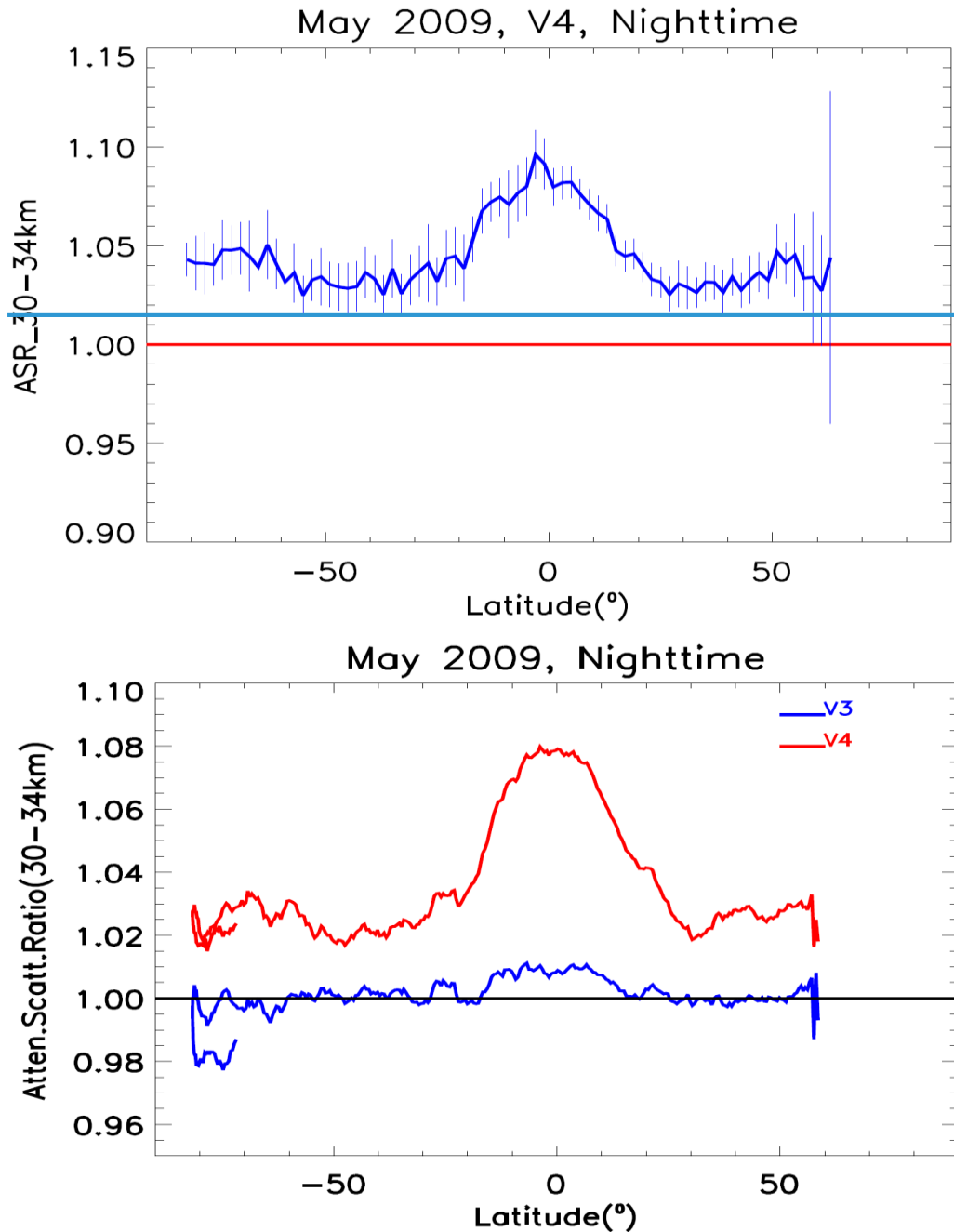


Figure 1. Zonally Median values of zonally and vertically (over 30-34 km) averaged 532 nm attenuated scattering ratios for May 2009 nighttime data from V3 and V4 (blue). Data over the South Atlantic Anomaly were excluded. The data are binned over 2° in latitude and the error bars represent the standard error. A 10-point smoothing of the mean scattering ratios over this latitude interval data has been applied.

As shown in Eq. (1), the attenuated scattering ratios, $R'(z)$, are computed as the ratio of the measured attenuated backscatter coefficients, $\beta'_{\text{measured}}(z)$, which contain contributions from both

molecular and particulate backscatter ($\beta_m(z)$ and $\beta_p(z)$, respectively), and the attenuated backscatter coefficients calculated from modeled profiles of molecular number densities, $\beta'_{\text{modeled}}(z)$ (Vaughan et al., 2009).

$$R'(z) = \frac{\beta'_{\text{measured}}(z)}{\beta'_{\text{modeled}}(z)} = \frac{(\beta_m(z) + \beta_p(z)) T_m^2(z) T_{O_3}^2(z) T_p^2(z)}{\beta_{m,\text{modeled}}(z) T_{m,\text{modeled}}^2(z) T_{O_3,\text{modeled}}^2(z)} = \left(1 + \frac{\beta_p(z)}{\beta_{m,\text{modeled}}(z)} \right) T_p^2(z) \quad (1)$$

5 In this expression, $T_X^2(z)$ represents the two-way transmittance (i.e., signal attenuation) between the lidar and altitude z for air molecules ($X = m$), ozone ($X = O_3$), and particulates ($X = p$). In ~~version 3 (V3)~~, the calibration region was fixed at 30-34 km, with the assumption that the aerosol loading in this region was negligible (Powell et al., 2009); i.e., $\beta_p(z) \approx 0$ and $T_p^2(z) = 1$. This assumption essentially ~~forced~~ the V3 attenuated scattering ratios in the region to one. For
 10 the V4 data release, the calibration region was raised to 36-39 km, with the concomitant assumption that the mean scattering ratio at these higher altitudes is 1.01 ± 0.01 . The V4 ~~data~~ attenuated scattering ratios now (correctly) show significant aerosol in the altitude region used for the V3 calibration, with a **strong** maximum appearing over the tropics (Figure 1). The V4 data also capture the seasonal variation of these scattering ratios (Kar et al., ~~2018~~2018a, see their Figure 12).
 15 This improved calibration in V4, now accurate to about 1.6%, provides the motivation for the development of the CALIPSO stratospheric product, as it enables the retrieval of aerosol extinction coefficients in regions previously (but incorrectly) assumed to be aerosol-free. (Kar et al., 2018a).

2.2 Design and algorithm description

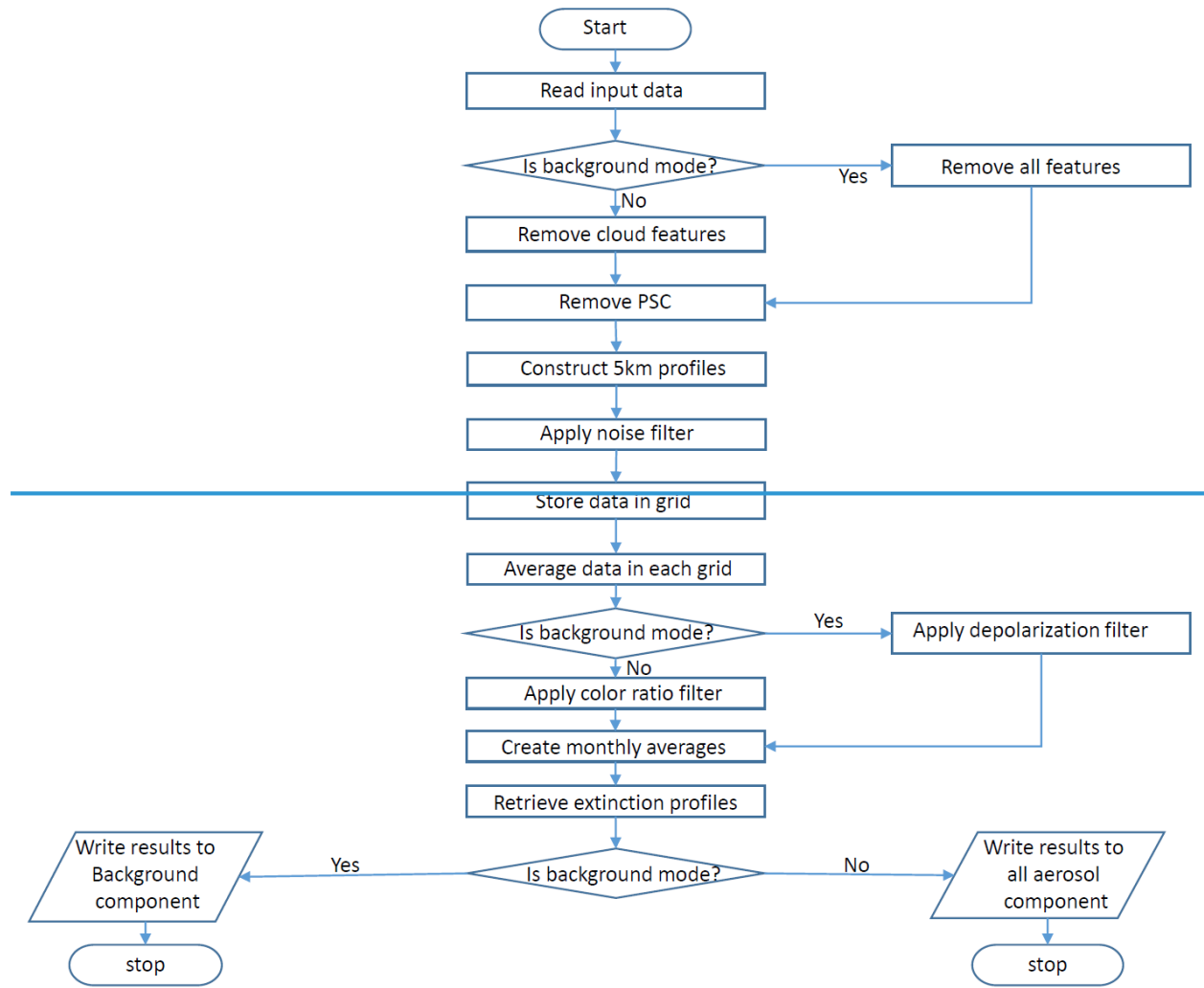
The level 3 stratospheric aerosol profile product reports height-resolved monthly mean
 20 profiles of aerosol backscatter and extinction coefficients on a uniform spatial grid that extends 5° in latitude (from 85°N to 85°S), 20° in longitude (from 180°W to 180°E), and 900 m in altitude. ~~This grid was chosen to allow for adequate averaging of the data to compensate for the lower~~ Given the low SNR in the ~~stratosphere while retaining some level of zonal information. Note that the range of altitudes to be covered in the stratosphere at various latitudes~~ stratospheric backscatter
 25 measurements, it is necessary to average the data substantially, both spatially and temporally. Averaging the backscatter data over 5° in latitude increases the SNR by a factor of 40 (compared to single shot profiles) and provides a reasonable depiction of stratospheric aerosol distribution. This is also consistent with the early results of Thomason et al. (2007), who used the early

CALIPSO measurements together with data from 8.2 the CALIPSO simulator (Powell, 2005) to show that averaging the data over 5° in latitude and about 1 km to 36 km, the latter being the lower limit of the calibration region, in the vertical resulted in fairly representative stratospheric distribution. Further, spatial distributions of stratospheric species tend to be zonally symmetric (e.g. Kremser et al., 2016). In order to capture the signature of any possible longitudinal variation, e.g., the Asian Tropopause Aerosol Layer (ATAL) which occurs over Asia every summer during the monsoon months, we have used a longitudinal grid of 20° . The altitude resolution of the CALIOP level 1 profiles varies over this with altitude range, going from 60 m between 8.23 km and 20.2 km to 180 m between 20.2 km and 30.1 km and finally to 300 m between 30.1 km and 40.0 km. In order to achieve a uniform altitude resolution, the vertical grid resolution was set to 900 m. Note that the tropopause can occur below 8.3 km at high latitudes, but the vertical resolution of level 1 profiles changes again below this altitude and the lower limit was kept at 8.3 km as a trade-off between computational complexity and the stratospheric information content, while the upper limit was set at 36 km, which is the lower limit of the calibration region. The tropopause heights were taken from the Modern-Era Retrospective analysis for Research and Applications 2 (MERRA-2) reanalyses as in all V4 products (Gelaro et al., 2017). In the current version of the stratospheric aerosol product we use only nighttime data as they have significantly better SNR as compared to the daytime data (Hunt et al., 2009).

Each level 3 stratospheric aerosol file reports two distinct realizations of the monthly averaged data products. The first of these is the “background” mode, which is designed to represent the long-term background stratospheric aerosol loading. In order to achieve this, we need to remove all readily detectable perturbations within the stratosphere; i.e., such as overshooting cirrus clouds, polar stratospheric clouds (PSCs), and strongly scattering injections of smoke, volcanic ash, and other aerosol species which are detected using the layer detection algorithm implemented in the CALIOP level 2 data processing (Vaughan et al., 2009). The second realization is the “all aerosols” mode which is designed to represent the time history of aerosol loading in the stratosphere resulting from all possible sources. In this case, the cirrus clouds and PSCs are still removed, exactly as is done for the background mode, but however, subject to various quality assurance tests, the aerosol layers detected in the level 2 analyses are retained. Details of the averaging algorithms and the various data filtering schemes are provided in the following sections.

2.2.1 Gridding and filtering

The overall design of the **level 3 stratospheric aerosol** product is shown in Figure 2. To begin with, three input files are required for each granule under consideration. A CALIOP granule comprises half an orbit of data either from the daytime or the nighttime part of the orbit and divided by the day-night terminator. As noted in section 1, the primary input files used for **this the present** product **is are** the lidar level 1B file, with the corresponding level 2 5 km merged layer and PSC mask files (Pitts et al., 2009) used for filtering. While the level 1B and level 2 merged layer files are based on V4, the currently available level 2 PSC files are based on V3. The latter is only available as a daily file and not for each granule separately. The 5 km merged layer file is a new product in V4 that reports the locations of all aerosol and cloud layers detected at both 5 km (also 20 km and 80 km) and single shot (333m) resolution (Vaughan et al., 2016).



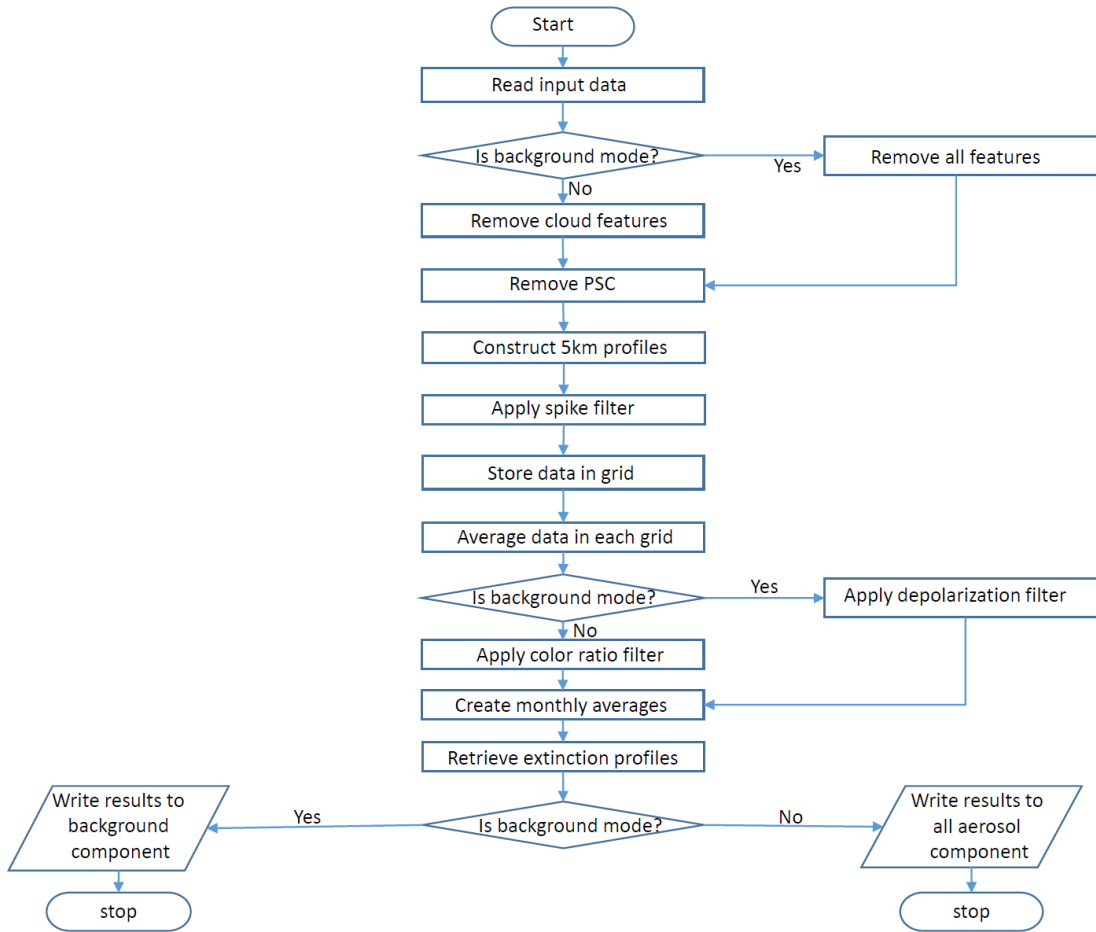


Figure 2. Overall Flowchart illustrating the overall design of the CALIPSO level 3 stratospheric aerosol profile product.

5

In the “background mode”, clearing the features detected in the level 2 analyses is done by removing all the level 1B (L1B) attenuated backscatter values (for 15 consecutive L1B profiles) **belowbeginning at** the top of the uppermost cloud or aerosol layers detected above the local tropopause using the layer heights reported in the 5 km merged layer file... Not only are signals from within the boundary of the layers removed, the backscatter values at all altitudes below the layers are also removed to avoid issues in correcting for signal attenuation from overlying layers. While the attenuated backscattered signals within and below these layers are removed, this step will retain values which fall below the minimum detectable attenuated backscatter threshold of the CALIPSO layer detection algorithm (McGill et al., 2007). In this sense, the retrieved extinction in this mode will reflect only the aerosol loading below this threshold. Similarly, the signals below

10

15

the uppermost PSC layers are also removed using the PSC mask file for the PSC-active months in the two hemispheres (December through March in the Arctic and May through October in the ~~Antarctica~~Antarctic). The PSC mask files report the occurrence of PSCs in both ~~the~~ hemispheres (Pitts et al., 2007, 2009) and are reported for a single day on a 5 km horizontal and 180 m vertical grid for nighttime conditions only.

After clearing all level 2 and PSC layers detected above the local tropopause, all L1B attenuated backscatter values below the tropopause are removed. Further, all L1B profiles within the South Atlantic Anomaly (SAA) region are also removed. In this region, between approximately the equator and 50°S in latitude and 20°E to 80°W in longitude (in the operational algorithm a polygon is used), the Van Allen belts come down to their lowest altitude (< 200 km), thus exposing the satellite sensors to high fluxes of energetic charged particles which are trapped within the belts (Hunt et al., 2009, Noel et al., 2014). Large amplitude noise excursions are often observed in attenuated backscatter profiles within this area, thus degrading the already low SNR in the stratosphere. Consequently, data over the SAA are not included when calculating the level 3 stratospheric aerosol product.

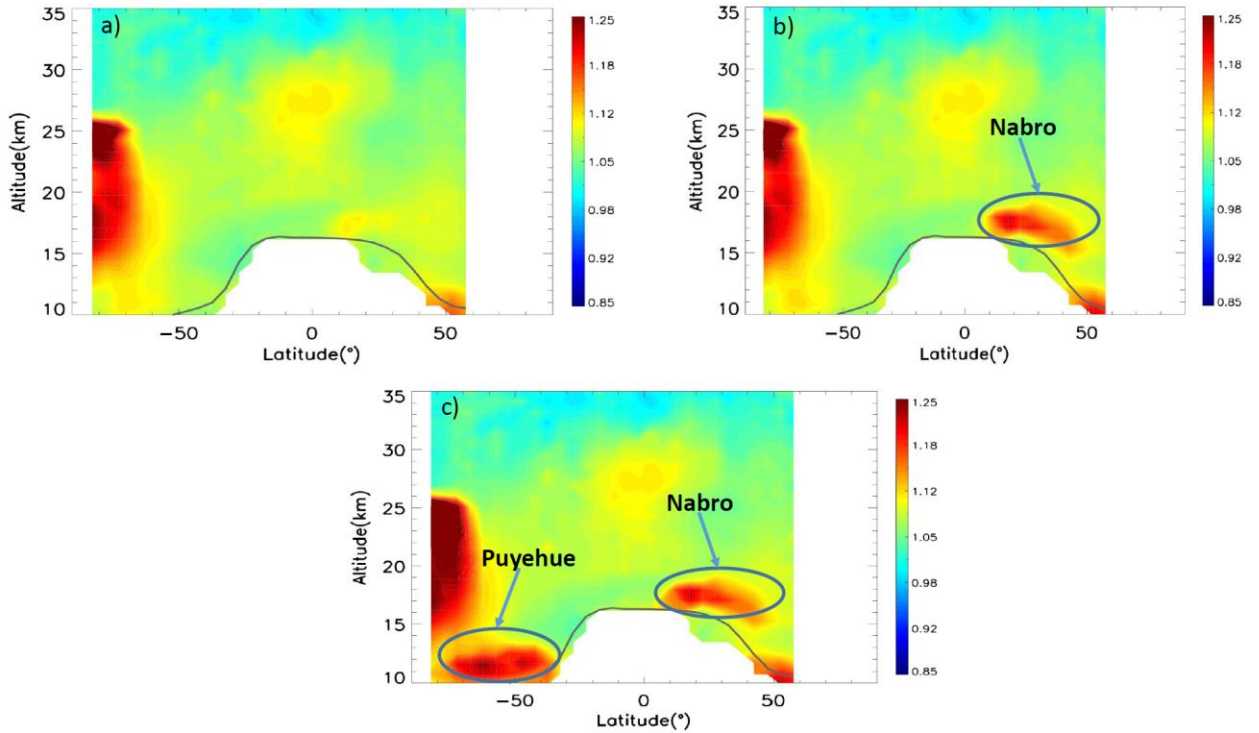
When creating the “all aerosol” mode of the stratospheric aerosol product, it is necessary to remove any clouds and PSCs, much the same way as for the background case, but retain the detected layers classified as aerosols by the CALIPSO cloud-aerosol discrimination (CAD) algorithm (Liu et al. 2009, 2019). It should be mentioned that the CAD algorithm was also modified in V4 in order to be compatible with the new V4 532 nm calibration (Liu et al., 2019). In fact, the CAD algorithm was extended to the stratosphere for the first time in V4. Up until V3, any layer in the stratosphere was simply classified as a “stratospheric feature” and no distinction was made between clouds and aerosols, which is no longer the case in V4. However, even the V4 CAD algorithm may not perform very well at high altitudes because of low SNR leading to generally lower absolute values of CAD scores (Liu et al., 2019). In any case, in the stratospheric altitudes above ~20 km, clouds are seldom observed (except in the polar regions) and uncertainties in the CAD algorithm are not likely to affect the stratospheric aerosol product. For this mode, only aerosol layers with acceptable CAD scores (-100 to -20) are retained within the stratosphere. Layers identified as aerosols but with unacceptably low CAD scores (between 0 and -20) are removed as if they were clouds or PSCs.

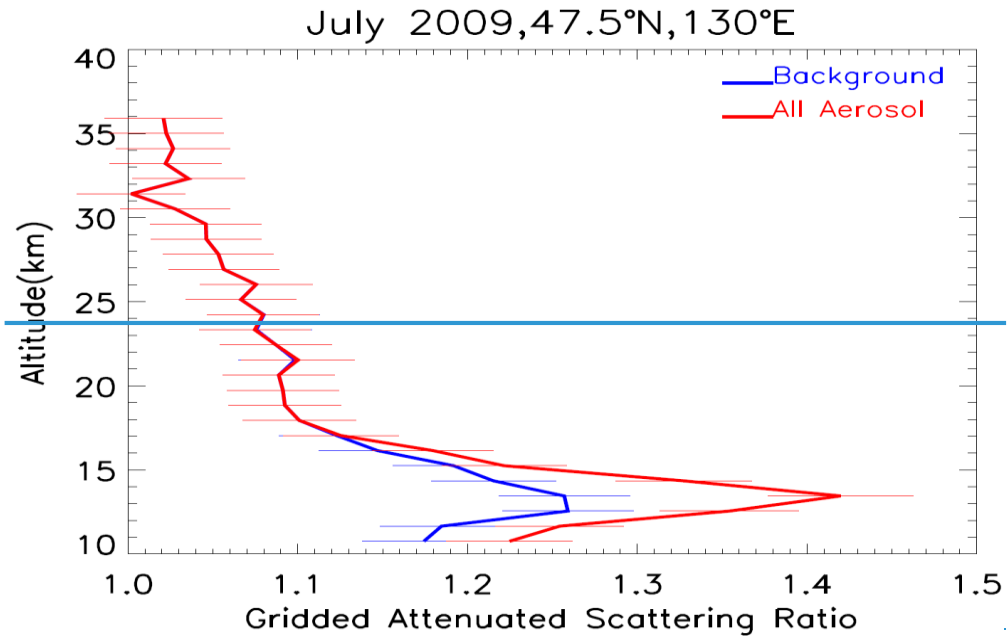
In the next step, a nominal 5 km resolution profile is constructed by taking the average of these 15 filtered L1B attenuated backscatter profiles. Subsequently, a noise filter is used to screen out strong outliers from these 5 km profiles that might otherwise lead to biases in high latitude and/or high altitude regions. The noise filter used for the current version of the product is a reconfigured version of the same filter that is used in the CALIPSO range dependent automated level 2 layer detection algorithm ~~and includes contributions from both~~. Essentially a range-invariant and range-dependent threshold array of attenuated scattering ratios is constructed, which incorporates noise from two types of sources. The first category is the range invariant noise and includes detector dark noise and noise from the solar background light. The second category is the range dependent noise from single shot measurements and is calculated from the molecular models. Using this range dependent threshold, outliers are removed (for details, see Vaughan et al., 2009, section 2c). After removing ~~thesethe~~ outliers, the 5 km profile is assigned to the appropriate spatial grid. This process is then repeated for all the profiles in the level 1B file. The resulting filtered 5 km profiles are then averaged to create a single mean attenuated backscatter profile for each grid cell.

In the final processing step for each granule, another quality screening is employed to identify and remove any lingering tenuous cirrus cloud in the lower stratosphere that might have escaped the layer detection mechanism due to low backscatter values. For the “background” mode, we can safely assume the background aerosols are uniformly spherical and thus have a near zero depolarization ratio. Since ice crystals in even the most tenuous cirrus violate this assumption, we use a threshold of 5% in volume depolarization ratio (ratio of the attenuated backscatter measured in the perpendicular and parallel channels at 532 nm (Hunt et al., 2009)) to detect weakly scattering residual clouds ~~(e.g., as described in Vernier et al., 2009)~~. However, for the “all aerosol” mode, this strategy will not work. This is because volcanic ash is typically non-spherical and has high volume depolarization values (~25-30%) and thus would be removed along with the cirrus clouds. On the other hand, attenuated color ratio values (i.e., the ratio of the total attenuated backscatter coefficients at 1064 nm and 532 nm) are generally larger for clouds as compared to ~~the~~ volcanic ash and thus may be used to filter out clouds while still retaining volcanic ash (Winker et al., 2012; Vernier et al., 2014). ~~The distribution of clouds and ash from the Puyehue-Cordon Caulle volcano (June 2011) at 17 km suggest that the two layer types can be discriminated reasonably well by using~~ We have used a threshold value of 0.5 in attenuated color ratio (Vernier et al., 2014). We

therefore use this threshold in attenuated color ratio in the “all aerosol” mode in an attempt to retain the volcanic ash in the “all aerosol” mode, instead of the rather than the filter on volume depolarization filter ratio. The effects of these filters in both modes are illustrated in Figure 3 using height-latitude cross sections of attenuated scattering ratios for the month of June 2011.

5





Figure

Figure 3.3. Zonally averaged height-latitude cross sections of attenuated scattering ratio for June 2011: a) after removing all detected layers and using a volume depolarization ratio filter (i.e., background aerosol only); b) including aerosol layers in the stratosphere detected by the level 2 algorithms with a 5% volume depolarization ratio filter applied; and c) including the level 2 aerosol layers but using an attenuated color ratio filter instead of the volume depolarization ratio filter. The white area in the northern high latitudes in summer indicates lack of nighttime data.

5

10 During this month two strong volcanic eruptions took place, Nabro in the northern hemisphere (June 13th, 13°N, 41°E) and Puyehue-Cordon Caulle in the southern hemisphere (June 4th, 40°S, 72°W). The composition of the Nabro plume was mostly sulfate while the composition of Puyehue-Cordon Caulle was mostly ash, at least initially (de Vries et al., 2014; Vernier et al., 2013). In the background mode (Figure 3a), removal of all detected layers combined with the application of the volume depolarization filter ensures that stratospheric perturbations from these two volcanoes are mostly excluded. Figure 3b shows the effect of including aerosol layers in the stratosphere with acceptable CAD scores ($|CAD| > 20$) while still using the volume depolarization filter. Now the Nabro plume can be clearly seen but not that of Puyehue-Cordon Caulle. This is because the sulfates in the Nabro plume have low volume depolarization ratios that fall below the threshold and are thus retained while the ash layers with high volume depolarization ratio from

15

20

Puyehue-Cordon Caulle are removed. On the other hand, including the aerosol layers but substituting an attenuated color ratio threshold of 0.5 in place of the volume depolarization ratio filter, as shown in Figure 3c (all aerosol mode), reveals both the Nabro (near 30°N) and Puyehue-Cordon Caulle plumes (near 50°S) quite clearly. Note the high scattering ratio values in the Antarctic latitudes between 15-km and 25-km. Because the PSC mask algorithm is optimized specifically for PSC detection, its increased sensitivity allows it to detect a considerably larger fraction of faint PSCs relative to the more generalized and generic level 2 feature detection algorithm. Since all PSC layers detected by the dedicated PSC detection algorithm were removed, what remains are the signatures of only those particles below the detectability threshold of the PSC mask data product. Note that the enhanced scattering ratios near 25-30 km represent the tropical reservoir of stratospheric aerosols (Trepte and Hitchman, 1992, Kremser et al., 2016). Further, the high scattering ratios near 50°N are likely due to the Grímsvötn volcano, which erupted in May 2011.

Using a constant threshold to discriminate between different classes of inherently noisy measurements can entail significant risk of misclassification. For example, using a higher attenuated color ratio acceptance threshold to ensure the identification of strong ash plumes (e.g., for Puyehue Cordon Caulle above) may result in a significant amount of cloud contamination. Similarly, an acceptance threshold set too low will likely exclude all clouds while simultaneously discarding much of the ash signal.

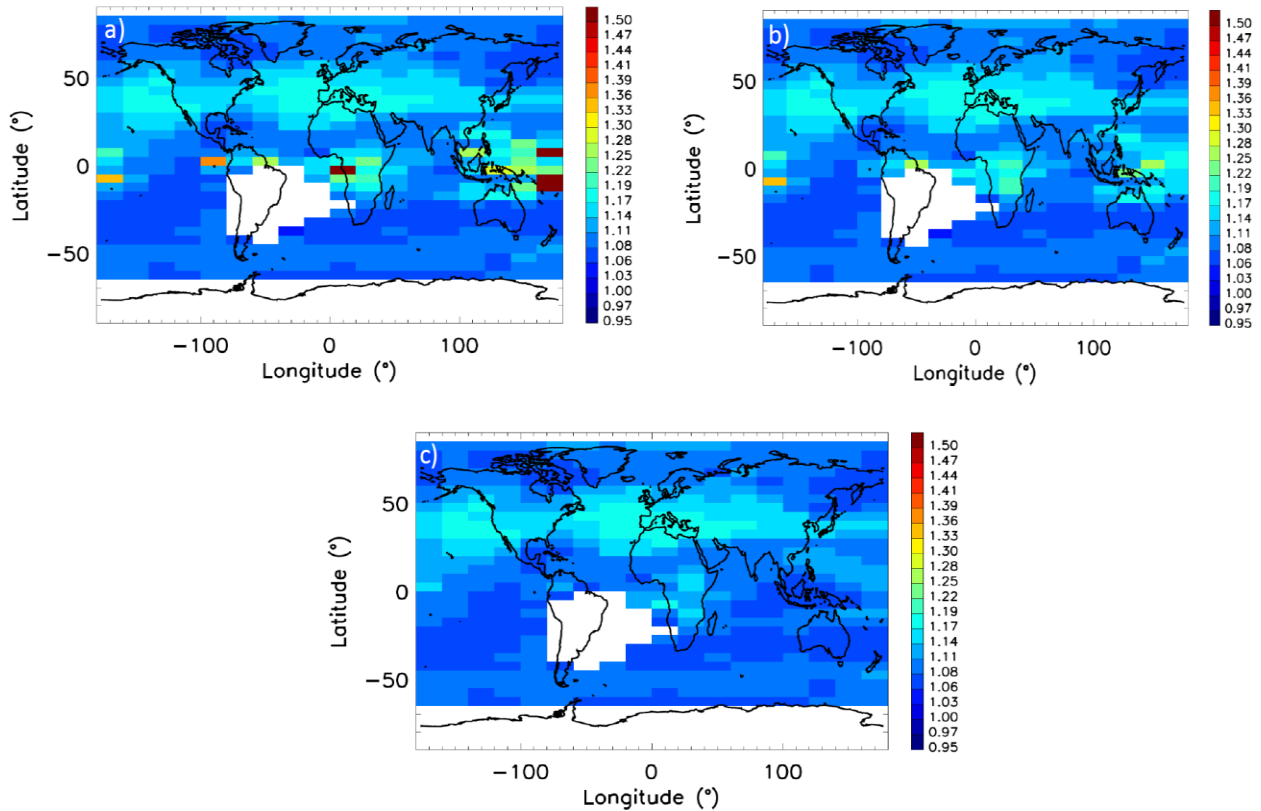


Figure 4: Attenuated scattering ratios at 17 km in December 2011, a) including all detected aerosol layers but before applying any filter to remove the thin cirrus clouds, b) including all detected aerosol layers after applying the filter in attenuated color ratio (the “all aerosol” mode) and c) excluding the detected layers and after applying the filter in volume depolarization ratio (the “background” mode).

The impact of using the attenuated color ratio and volume depolarization ratio filters on removing thin cirrus clouds in, respectively, the all aerosol and background only components is illustrated in Fig. 4 using the attenuated scattering ratios measured at 17 km during December 2011. In Fig. 4a, all the aerosol layers are retained, much like the “all aerosol” component, except that neither the volume depolarization ratio filter nor the attenuated color ratio filter is used. The high scattering ratios between about 30°N-55°N are due to the Nabro plumes which have spread around the northern hemisphere by December 2011. Apart from this band, high scattering ratios are also seen in a tropical band (between 25°S to 25°N) over the Western Pacific as well as over parts of Africa. These reflect the thin cirrus clouds occurring in the upper troposphere and lower

stratosphere near the tropopause (Sassen et al., 2009). Figure 4b shows the distribution in the “all aerosol” mode where the attenuated color ratio filter is used. Clearly a significant number of pixels with high scattering ratio (thin cirrus clouds) in the tropics has been removed while still retaining the volcanic aerosol signature. In Figure 4c we see the impact of the volume depolarization filter in the “background” mode. Now most of the cirrus clouds have been removed. Note that the aerosol signature has remained much the same in all three distributions. That is because by December 2011, there may not be many volcanic layers left, as such, yet enhanced scattering from the volcanic material is still present. This figure shows that for quiescent conditions or when the aerosol load is not very high (so that not many plumes are detectable as layers in CALIPSO L2 algorithm), the volume depolarization filter will do a better job of clearing the thin cirrus clouds, thus making the background component as the mode of choice. In any case, note that the thin cirrus clouds mostly affect the tropical latitudes and near the tropopause ~16-18 kms (Sassen et al., 2009). Note that both the volume depolarization ratio and attenuated color ratio filters are applied only below 25 km, as no cirrus is expected above this altitude.

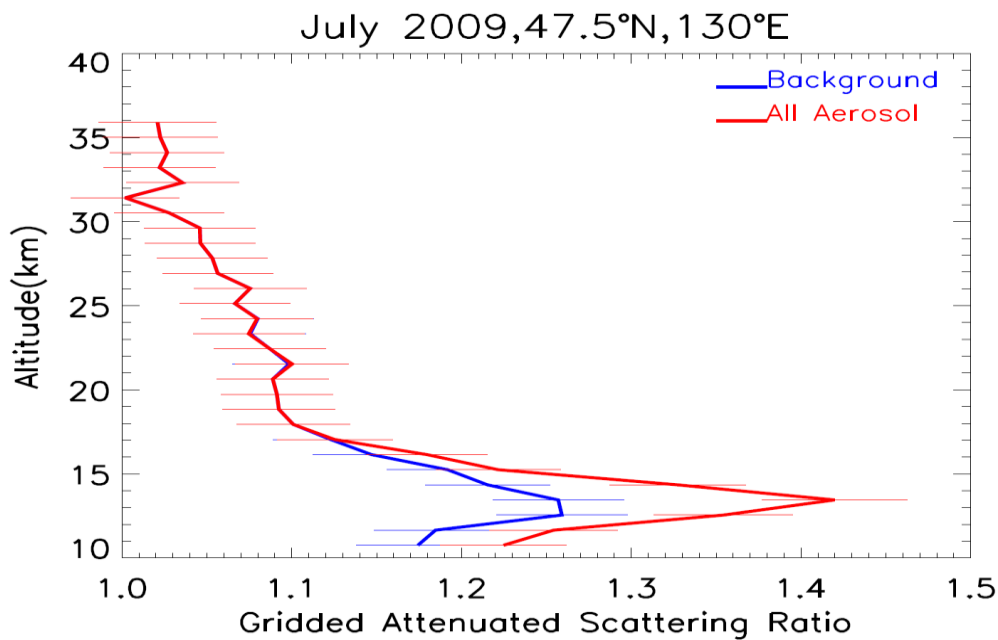
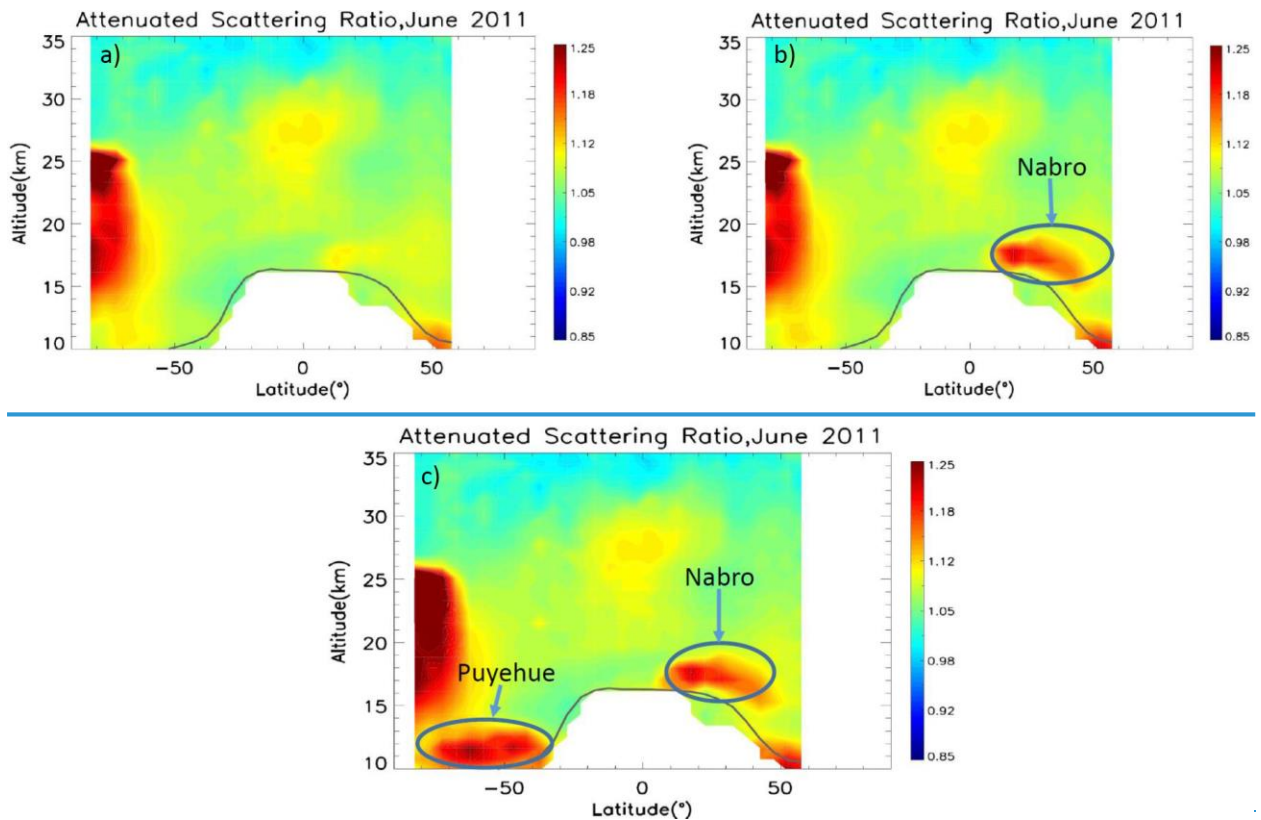


Figure 5. Profiles of attenuated scattering ratio at 47.5°N and 130°E in July 2009 for the background (blue) and all aerosol (red) components. The error bars represent computed uncertainties.

Figure 35 shows the profiles of attenuated scattering ratio for the background and all aerosol modes in July 2009 for the grid cell centered at 47.5°N and 130°E. The enhanced scattering ratio in the lower stratosphere between 10-km and 17-km is due to the inclusion of detected aerosol layers from the Sarychev volcano (48.1°N, 153.2°E), which erupted in June 2009. Note that backscatter from some of the Sarychev aerosols which fall below the minimum detectable backscatter threshold of the level 2 layer detection algorithm will contribute to the background profile.

After deriving the granule-averaged data, we create monthly averaged gridded profiles of attenuated backscatter by aggregating all profiles during each month of the mission. In addition to the attenuated backscatter coefficient profiles, profiles of molecular and ozone number densities, temperatures, and pressures reported in the L1B files are also averaged and gridded for use in the subsequent retrieval procedures.



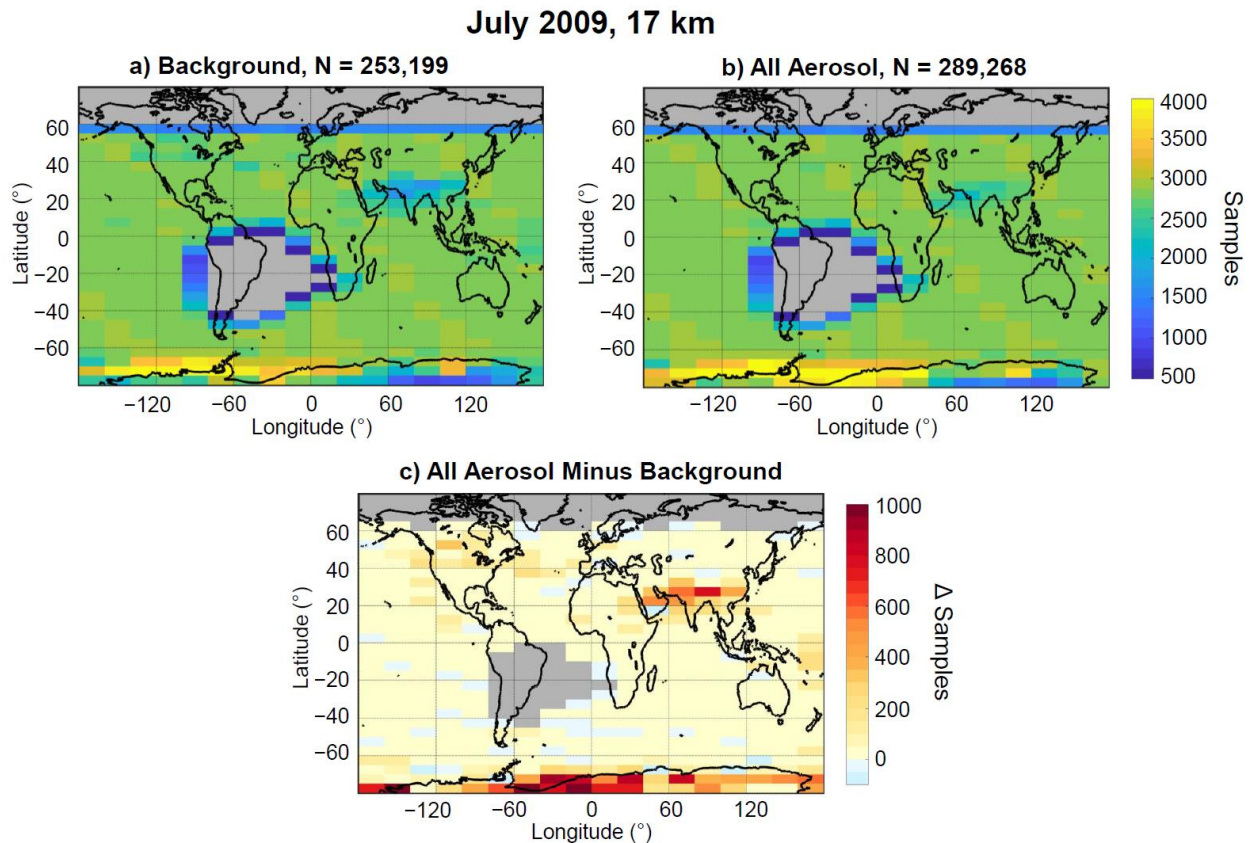


Figure 4. Zonally averaged height latitude cross sections of attenuated scattering ratio for June 2011 a) after removing all detected layers and using a depolarization filter, b) including only aerosol layers in the stratosphere with a depolarization filter and c) including aerosol layers but using a color ratio filter.

5

~~Figure 4 shows the effect of different filters on the height latitude cross sections of the gridded attenuated scattering ratio profiles for the month of June 2011. During this month two strong volcanic eruptions took place, Nabro in the northern hemisphere (June 13th, 13°N, 41°E) and Puyehue-Cordon Caulle in the southern hemisphere (June 4th, 40°S, 72°W). The composition of the Nabro plume was mostly sulfate while the composition of Puyehue-Cordon Caulle was mostly ash (de Vries et al., 2014; Vernier et al., 2013). In the background mode (Figure 4a), removal of all detected layers combined with the application of the depolarization filter ensures that stratospheric perturbations from these two volcanoes are mostly excluded. Figure 4b shows the effect of including aerosol layers in the stratosphere with acceptable CAD scores ($|CAD| > 20$) while still using the depolarization filter. Now the Nabro plume can be clearly seen but not that of~~

15

~~Puyehue-Cordon-Caulle. This is because the sulfates in the Nabro plume have low depolarization ratios that fall below the threshold and are thus retained while the ash layers with high depolarization ratio from Puyehue-Cordon-Caulle are removed. On the other hand, inclusion of the aerosol layers when using a color ratio threshold of 0.5 in Figure 4c (all aerosol mode) reveals both the Nabro and Puyehue-Cordon-Caulle plumes (near 50°S) quite clearly. Note the high scattering ratio values in the Antarctic latitudes between 15 km and 25 km. Since all PSC layers detected by the PSC mask product were removed, these are probably signatures of particles in the process of becoming PSCs.~~

10

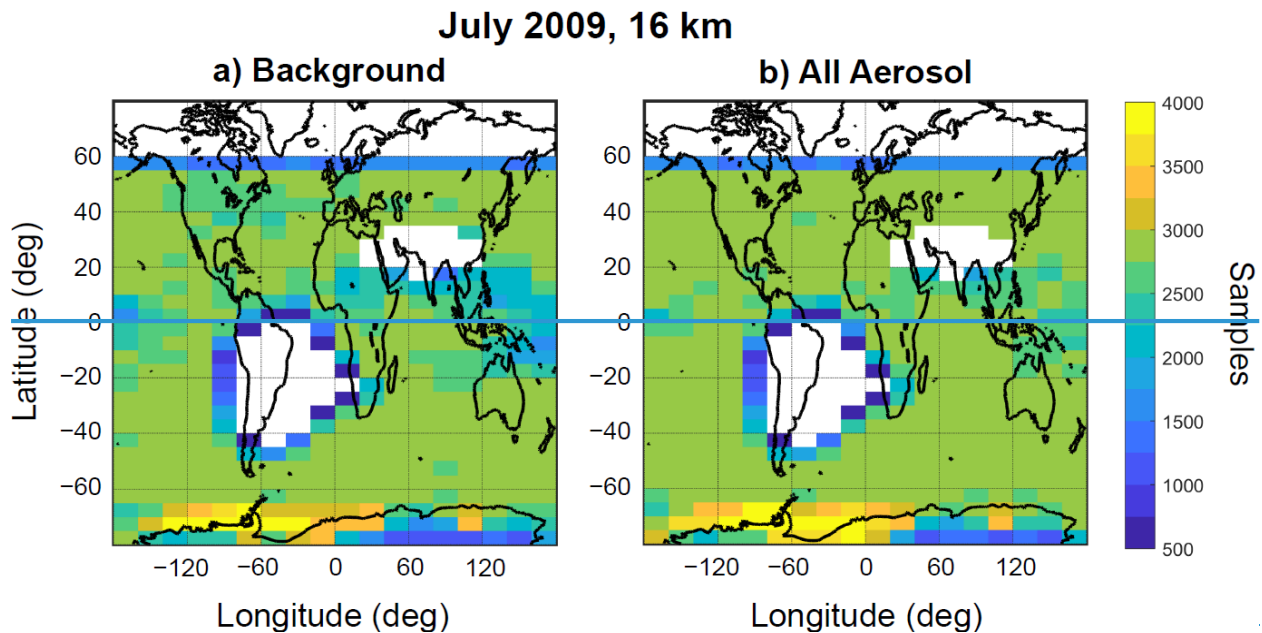


Figure 56. Number of samples contributing to a) background mode and b) all aerosol mode at 16 km and c) the difference between the two modes at 17 km in July 2009. Grid cells with < 50 samples are plotted in whitegrey.

15

Figure 56 depicts the spatial distribution of the number of samples that contributed to the two components at 16 km during July 2009. The whitegrey grid cells over South America and parts of South Atlantic Ocean correspond to the SAA, over which all data samples are rejected. The white grid cells over southeast Asia occur because the tropopause is higher than 16 km in this region. Higher number of samples for the all aerosol mode over the surrounding area might be related to the influence of deep convection during the Asian summer monsoon period. Higher number region reflects the signature of the aerosol in the Asian Tropopause Aerosol Layer

20

(ATAL, Vernier et al., 2011b). Higher number of samples in the all aerosol mode, albeit on a lesser degree, can also be seen over North America, which is likely related to the Sarychev volcano as mentioned above. Also note the high number of samples over parts of Antarctica. ~~This is again likely~~, partly from oversampling due to orbital configuration and related to small particles ~~which are in~~ below the ~~process forming~~ detectability of PSCs, by the PSC mask algorithm.

2.2.2 Retrieval of aerosol extinction profiles

The monthly mean profiles of gridded 532 nm attenuated backscatter coefficient (β'), constructed using the procedure described in the preceding section, along with gridded profiles of molecular backscatter coefficients (β_m), molecular extinction coefficients (α_m), and ozone absorption coefficients (α_{O_3}), are used to retrieve the particulate backscatter coefficient (β_p) using

$$\beta_p(z) = \beta'(z) / T_m^2(z) T_{O_3}^2(z) T_p^2(z) - \beta_m(z) \quad (2)$$

where,

$$T_m^2(z) T_m^2(z) = \exp\left(-2 \int_0^z \alpha_m(r') dr'\right) \exp\left(-2 \int_0^z \alpha_m(r') dr'\right), \quad (3a)$$

$$T_{O_3}^2(z) T_{O_3}^2(z) = \exp\left(-2 \int_0^z \alpha_{O_3}(r') dr'\right) \exp\left(-2 \int_0^z \alpha_{O_3}(r') dr'\right), \text{ and } (3b)$$

$$T_p^2(z) T_p^2(z) = \exp\left(-2 \eta_p S_p \int_0^z \beta_p(r') dr'\right). \quad (3c)$$

In these expressions, η_p is the particulate multiple scattering factor, S_p is the particulate lidar ratio (i.e., the extinction-to-backscatter coefficient ratio), and $T_m^2(z) T_m^2(z)$, $T_{O_3}^2(z) T_{O_3}^2(z)$, and $T_p^2(z) T_p^2(z)$ are, as previously defined, the molecular, ozone, and particulate two-way transmittances. The molecular backscatter coefficients and molecular and ozone two-way transmittances can be calculated from molecular model data (e.g., as described in Kar et al., 2018, 2018a). The molecular model used exclusively throughout the CALIPSO V4 data products is ~~the Modern Era Retrospective analysis for Research and Applications 2~~ (MERRA-2) provided by NASA's Global Modeling and Assimilation Office (Gelaro et al., 2017). For the CALIPSO stratospheric aerosol product, the particulate multiple scattering factor is taken as 1 for all species of stratospheric aerosols, consistent with the approach taken in the CALIPSO level 2 aerosol retrievals (Young et al., 2013; Young et al., 2016; Young et al., 2018).

Given an appropriate value of the lidar ratio, equations 2 and 3c can be solved iteratively to obtain estimates of $\beta_p(z)$ (Young and Vaughan, 2009). Estimates of particulate extinction coefficients are subsequently obtained using $\alpha_p(z) = S_p \times \beta_p(z)$. The V1.00 release of the level 3 stratospheric aerosol product uses a value of $S_p = 50$ sr for the stratospheric aerosol lidar ratio, which is a typical value used for stratospheric aerosols for background conditions and in absence of significant ash and sulfate injections from volcanoes (Trickl et al., 2013, Ridley et al., 2014, Sakai et al., 2016, Kremser et al., 2016, Khaykin et al., 2017). We also assume S_p to be constant at all latitudes and over the entire altitude range. Note that the lidar ratios could also be significantly different for stratospheric perturbations resulting from smoke intrusion from pyroCb events (Peterson et al., 2018, Khaykin et al., 2018). For this first version of CALIPSO stratospheric aerosol product we have used only a single lidar ratio. We also assume S_p to be constant at all latitudes and over the entire altitude range. The retrievals are carried out beginning at 36 km and extending downward to either 8.3 km or 1 km below the tropopause; processing stops when the higher of these two altitudes is reached. Extending the range below the tropopause, when possible, is intended to help in studies of the upper troposphere and lower stratosphere (UTLS). To guarantee uniform results across multiple CALIPSO data product levels, the level 2 CALIPSO extinction retrieval module is used to calculate the level 3 profiles of stratospheric aerosol extinction and backscatter coefficients and their uncertainties. The details of the retrieval process and uncertainty estimates are given in Young and Vaughan (2009) and Young et al. (2013, 2016, 2018) and are not repeated here.

3. Initial assessment of CALIPSO stratospheric aerosol product

In this section we assess the initial performance of the CALIPSO stratospheric aerosol product by first presenting the signatures of various stratospheric aerosol events as captured by the product and then making quantitative comparisons with observations from SAGE III on ISS.

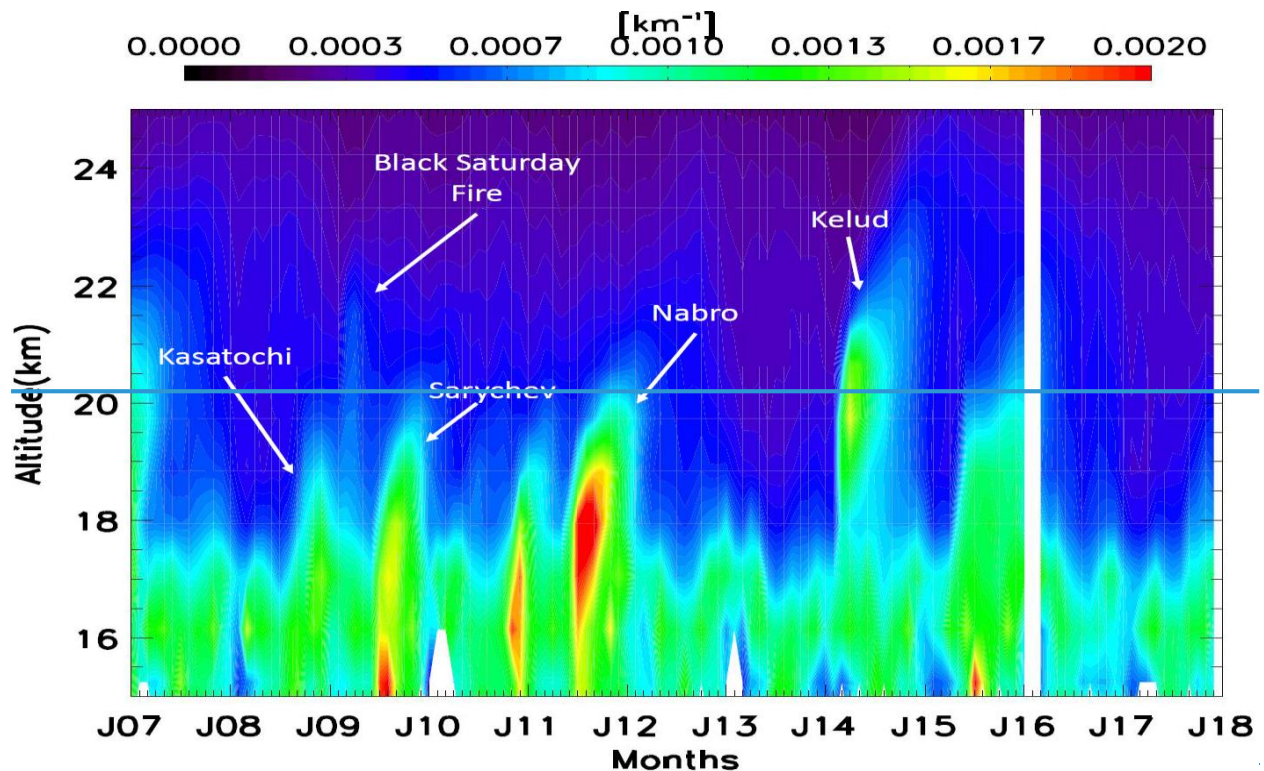
3.1. Signatures of stratospheric events and dynamics.

3.1.1 Effects of volcanic and smoke injections.

Volcanoes are one of the primary sources of stratospheric aerosols (e.g. Kremser et al., 2016). Ground based lidar studies have indicated a rising positive trend in the stratospheric sulfate aerosol

loading since the turn of the century which was initially attributed to anthropogenic emissions of SO₂ from coal burning in South East Asia (Hofmann et al., 2009). However, closer scrutiny suggests that the increase is instead related to emissions of SO₂ from a large number of moderate volcanic eruptions, as was ~~initially~~ subsequently suggested by Vernier et al. (2011, 2011a) based on analyses of CALIPSO data. Several volcanoes with stratospheric impacts have been recorded since the study by Vernier et al. (2011, 2011a). Volcanic signatures in CALIPSO data were examined more recently by Friberg et al. (2018).

Figure 67 shows the time-altitude cross section of the zonally averaged extinction coefficients between in the mid-high northern latitude (40°N-60°N), tropics (25°N-25°S to 25°N), and mid-high southern latitude (40°S-60°S) from the CALIPSO level 3 stratospheric aerosol product between January 2007 and December 2017. The signatures of many volcanoes are clearly evident in this image. While some of the volcanoes injected material only in the lower stratosphere (Kasatochi, Nabro etc.), the influence of some other volcanoes reached significantly higher, in particular Kelud in 2014, figure in all three latitude bands. The strongest extinctions are seen for Sarychev and Nabro in the northern hemisphere and Calbuco in the southern hemisphere. Note that the effects of some of the volcanoes can last for several months as they spread to other latitudes by isentropic transport.



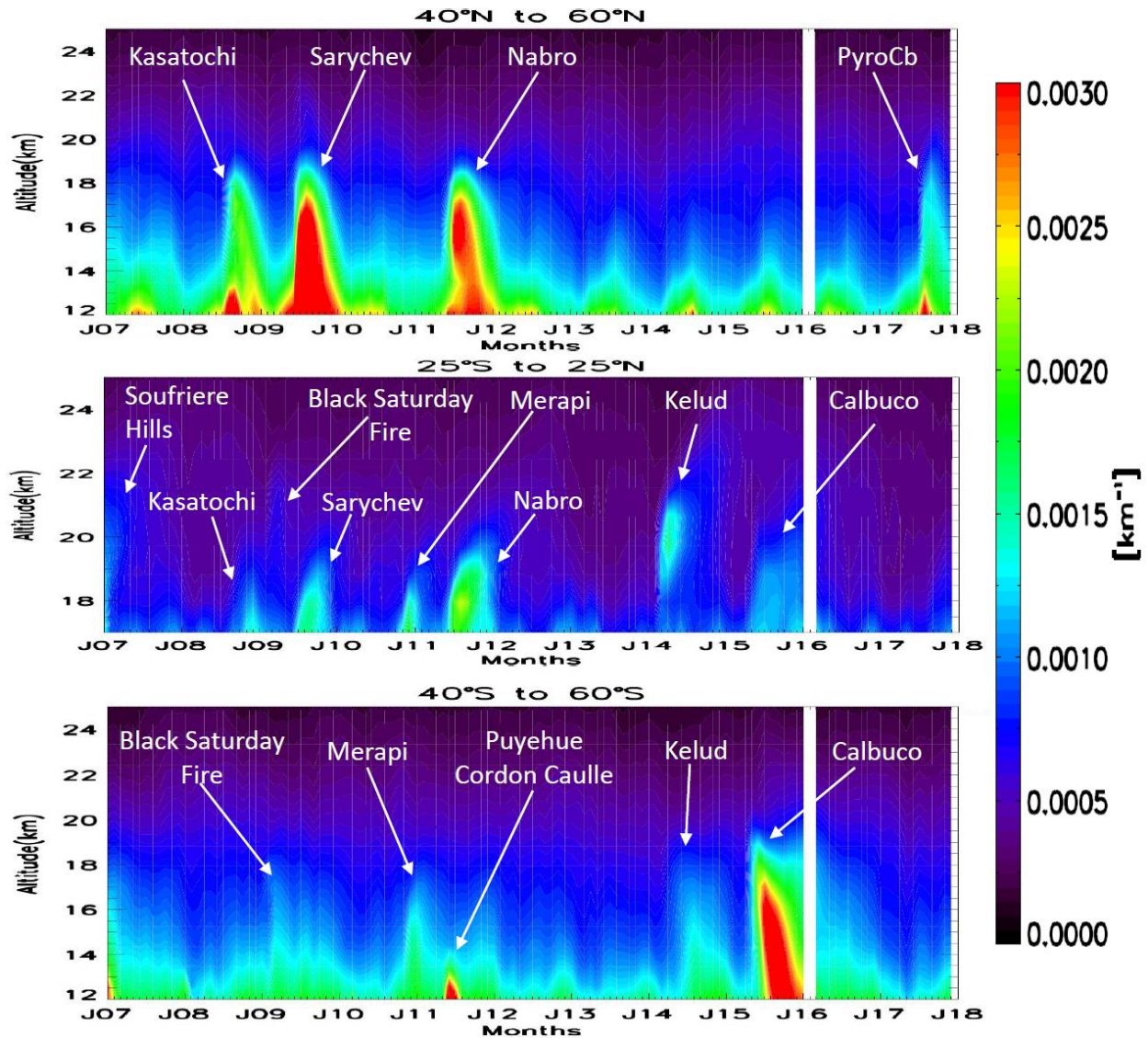


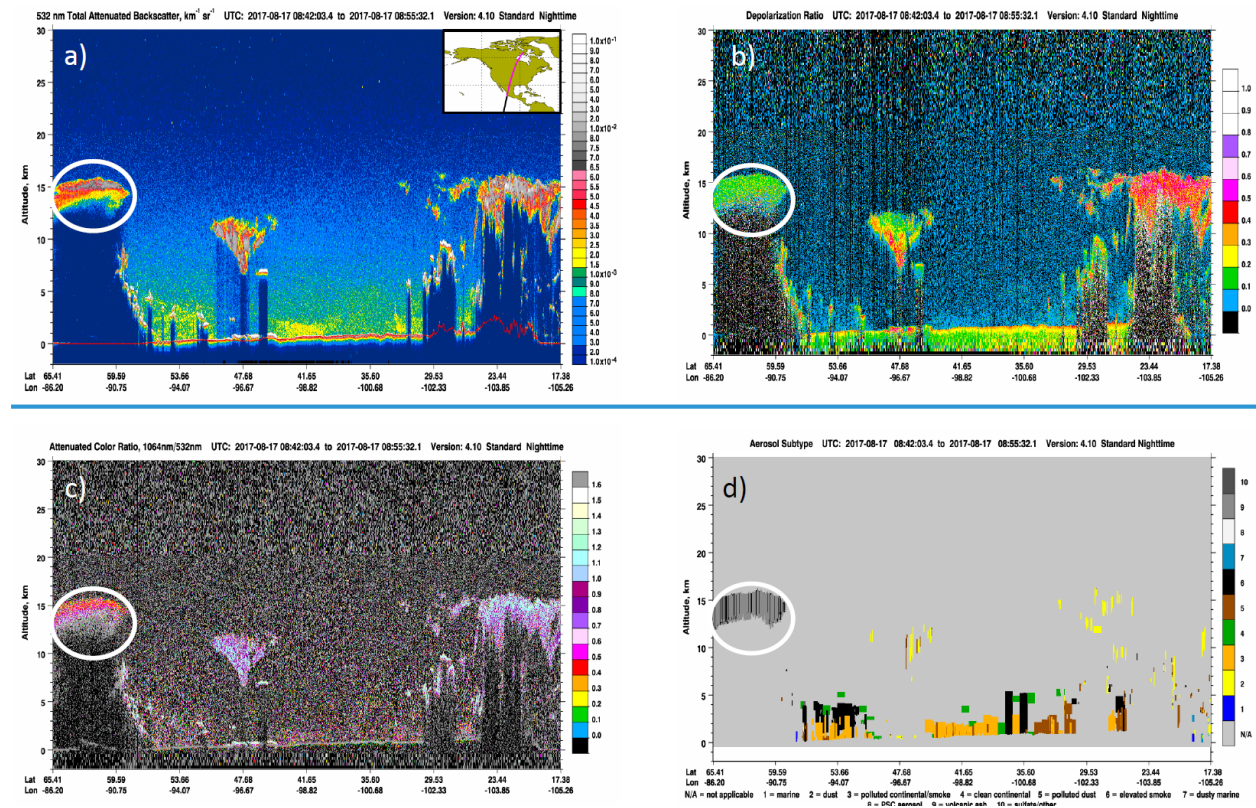
Figure 67. Time-altitude cross sections of the retrieved extinction coefficients, averaged between 25°S to 25°N, in all aerosol mode from January 2007 through December 2017, for a) mid-high northern latitudes, b) the tropics and c) mid-high southern latitudes. The white areas indicate missing data. Note that in the middle panel for the tropics, the altitude ranges from 17 km to 25 km, whereas the range is 12 km to 25 km in panels a) and c).

5

10

Apart from volcanic material, smoke from strong biomass burning events can also reach the stratosphere during the so-called pyrocumulonimbus events (Fromm et al., 2010; Peterson et al.,

2018). During the “Black Saturday” event, smoke from strong bushfires in Victoria, Australia on February 7, 2009 is known to have impacted the stratosphere. Plumes from this blaze eventually reached altitudes of 16–20 km and were readily visible in satellite imagery (de Laat et al., 2012; Glatthor et al., 2013). The signature of this event can also be quite clearly seen in Figure 6. These pyrocumulonimbus events seem to be increasing in frequency and currently there is a strong research focus on them (Peterson et al., 2018). identified in Figure 7b, reaching up to nearly 22 km. The signature of another strong pyroCb event can be seen at northern mid-high latitudes (top panel) in August-September, 2017. This event is discussed in detail below. Note the seasonal pattern of high extinction near 12-15 km in northern mid-high latitude summer, seen most clearly between 2012 and 2017. The reason for this is not entirely clear at this time, but could again be due to fire events. Cirrus cloud contamination could be another factor. However, the same pattern is also seen in the “background” mode (not shown) to a slightly lesser degree which suggests cloud contamination may not be very significant.



15

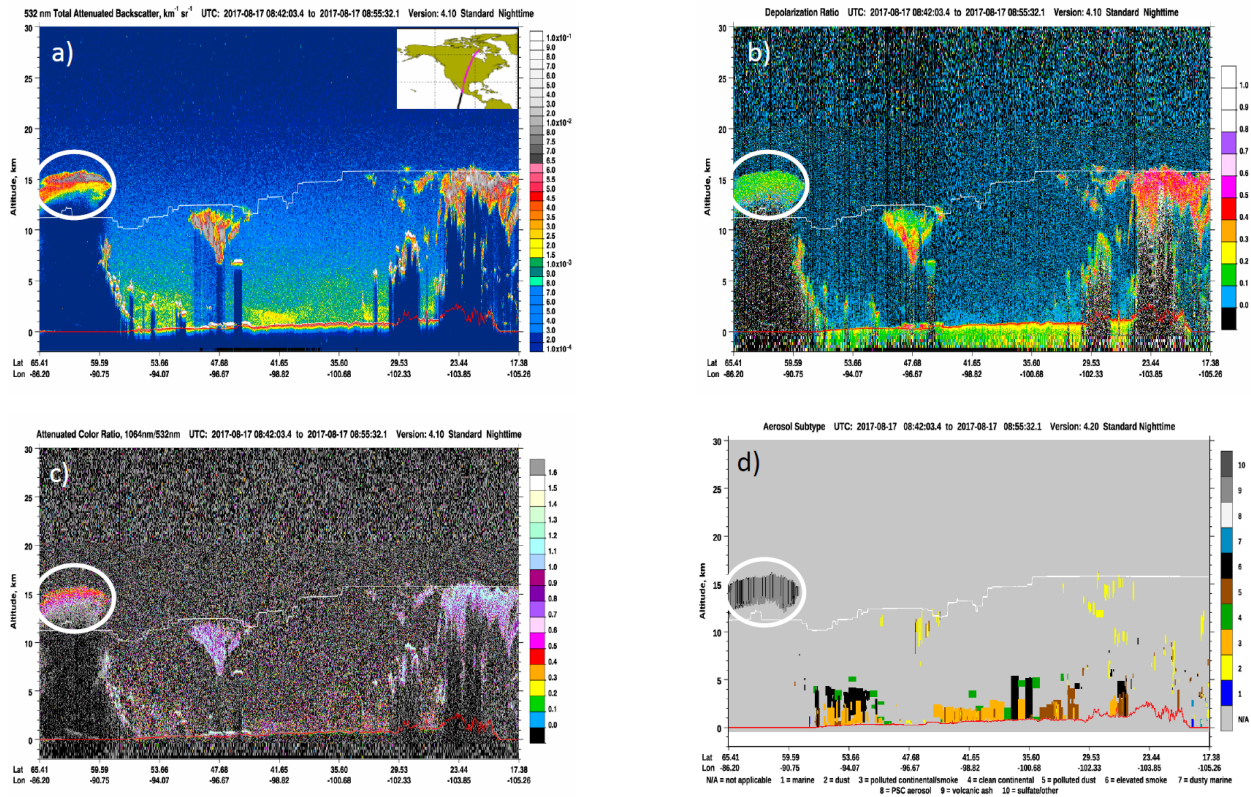


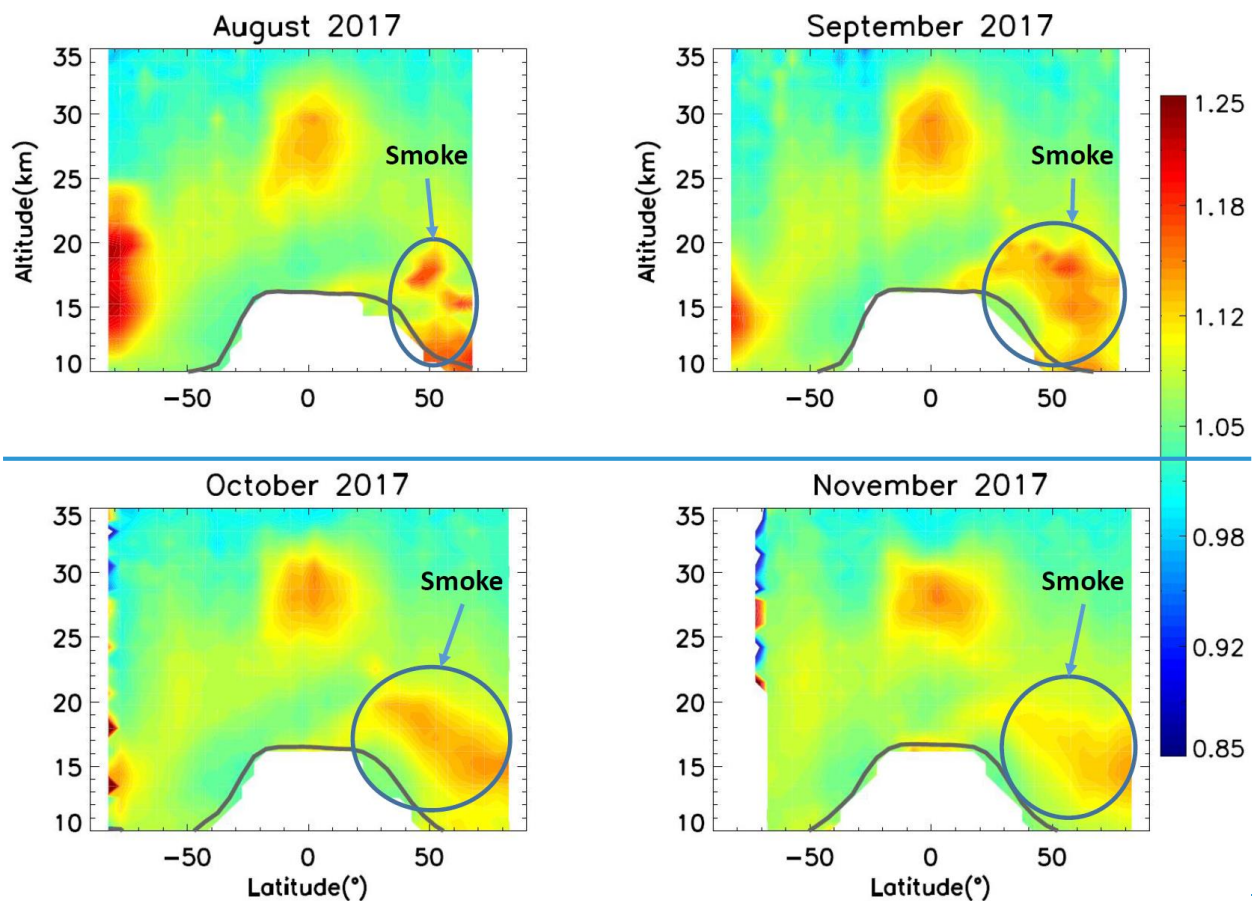
Figure 78. CALIPSO browse images of a) 532 nm total attenuated backscatter, b) 532 nm -volume depolarization ratio, c) attenuated backscatter color ratio (1064 nm / 532 nm) and d) aerosol subtypes for a pyroCb event over Canada on August 17, 2017. The smoke plume is shown in the white circles. The white lines indicate the MERRA-2 tropopause altitude.

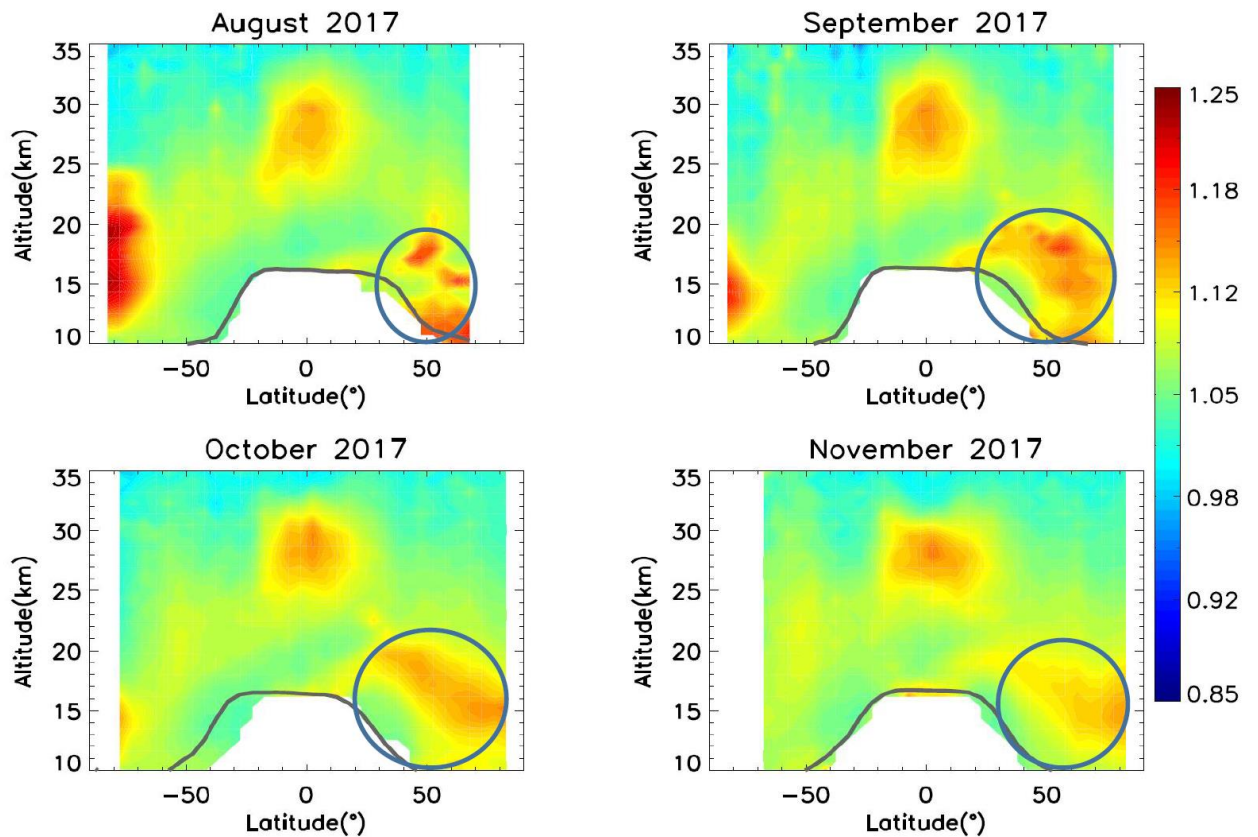
The extreme pyroCb event that occurred in August 2017 over British Columbia in Canada has been extensively studied recently and has been likened to volcanic perturbations in the stratosphere in terms of intensity and duration (Khaykin et al., 2018; Ansmann et al., 2018; Haarig et al., 2018, Peterson et al., 2018). Figure 78 shows an example of the CALIPSO measurements of this pyroCb event. The signature of the smoke plume is seen as extremely high attenuated backscatter (opaque at 532 nm) between 60°N and 65°N. The very high attenuated color ratio (~1.6) seen at the base of the plume (Figure 78c) is a tell-tale signature of smoke (e.g. Liu et al., 2008). The high volume depolarization ratio (≥ 0.1) seen in Figure 78b is somewhat unusual for smoke and suggests the presence of irregular soot particles and mineral dust and possibly some ice particles, with fast adiabatic lifting possibly retaining the initial irregular shapes (Haarig et al., 2018, Khaykin et al.,

2018). This high color ratio combined with the unusually high depolarization results in the plume being identified as a mixture of smoke and “volcanic ash” (Figure 7d8d), the latter being misclassifications by the CALIOP V4 level 2 scene classifier.

Figure 89 shows the height-latitude cross sections of CALIOP attenuated scattering ratios from the stratospheric aerosol product between August 2017 and November 2017 and captures the evolution of the aforementioned pyroCb event. After the original injection of smoke in August 2017 at mid-latitudes, the smoke spreads globally and to lower latitudes as can be seen in these monthly mean spatial distributions from the level 3 stratospheric aerosol product. As in Figure 3, the feature with high attenuated scattering ratio near 25-30 km seen in all the four panels is the signature of the tropical reservoir of stratospheric aerosols, maintained by a complex interplay of transport from the troposphere and stratospheric dynamics as well as microphysical processes including the Brewer-Dobson circulation, the QBO, evaporation and sedimentation (Trepte and Hitchman, 1992, Kremser et al., 2016).

15





5 **Figure 89.** Zonally averaged height-latitude cross section of the 532 nm attenuated scattering ratios from August 2017 through November 2017. The white areas in the northern high latitudes in August and the southern high latitudes in November indicate the lack of nighttime data due to continually changing day-night terminator times.

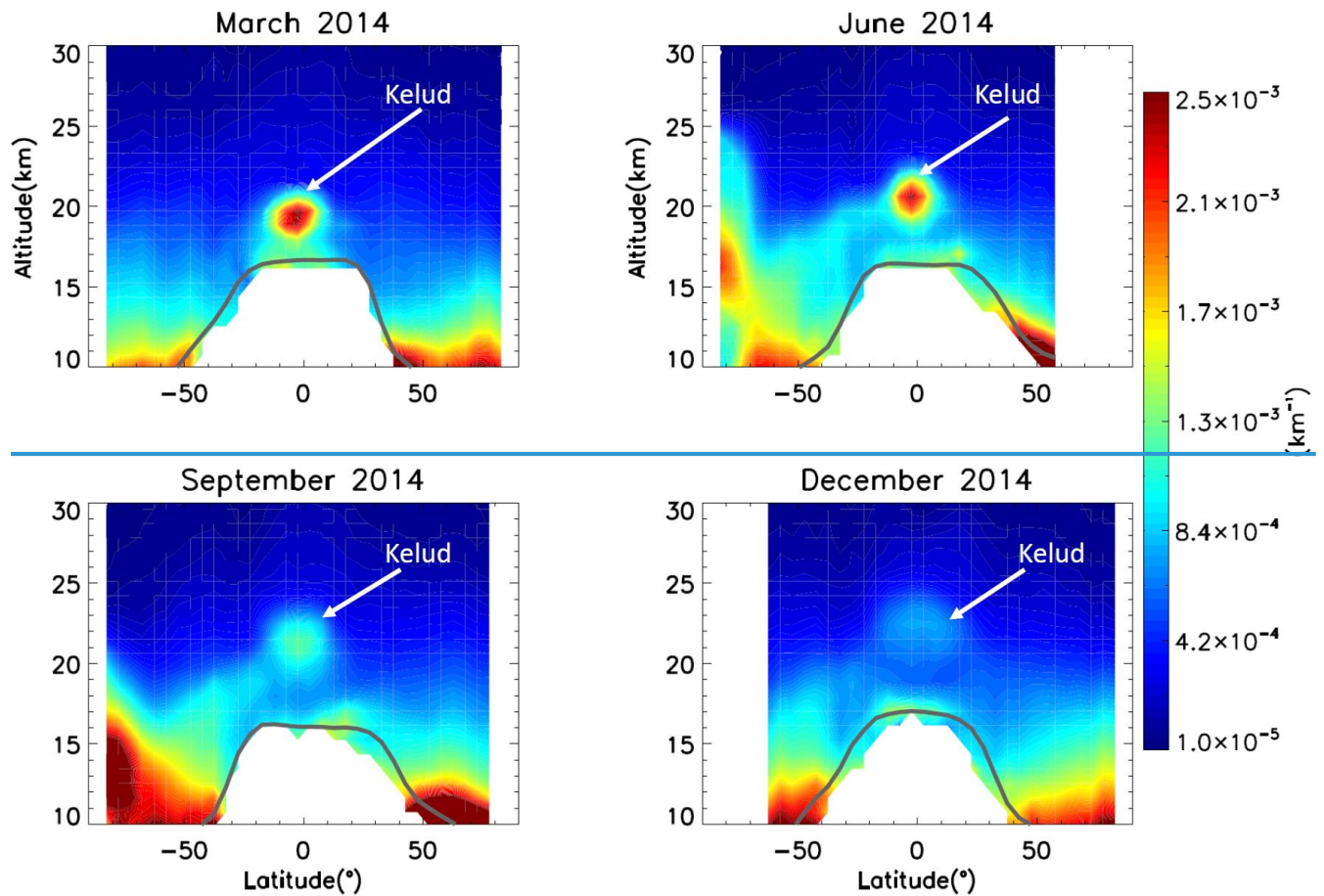
10

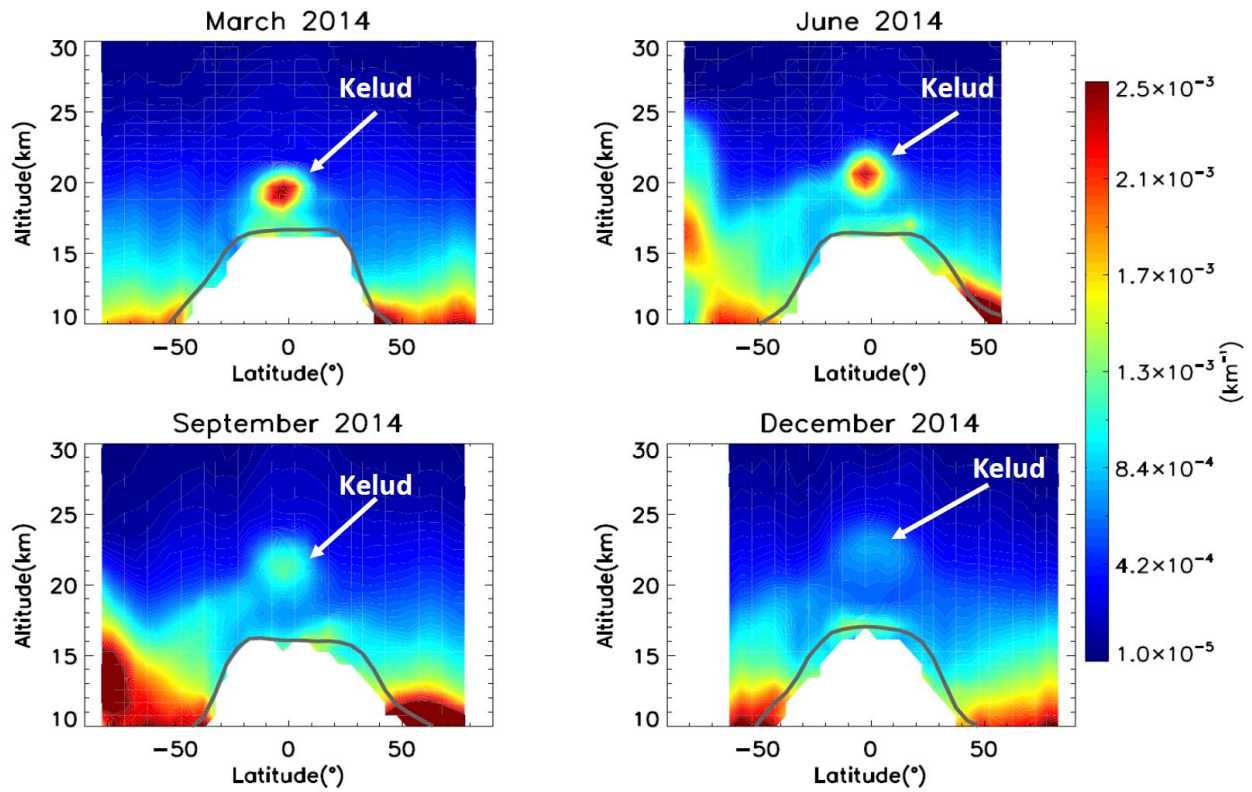
3.1.2. Signatures of stratospheric dynamics

15 Figure 910 shows the height-latitude cross section of the retrieved 532 nm extinction coefficients for the “all aerosol” mode from March to December 2014, which captures the evolution of the Kelud (April eruption (February 2014, 7.9°S, 112.3°E) eruption in altitude. The gradual lofting of the plume, with its top rising from around 17~21 km over the tropics in March to nearly ~24 km over in the same general location several months later, shows the signature of stratospheric dynamics in the CALIPSO stratospheric aerosol product. The persistence of the

stratospheric perturbation for several months is consistent with the results of Vernier et al. (2016) who found the presence of ash in the lower stratosphere 3 months after the Kelud eruption from balloon observations. Note the high extinction values near 50°N-60°N in the lower stratosphere (~10-15km). These are similar to the summer rise in extinctions at these latitudes as discussed earlier (Figure 7) and are possibly due to biomass burning effects but could also be related to possible cloud clearance issues. As also mentioned above, the high extinctions at high southern latitudes could be related to scattering from particles below the PSC detection threshold as well as to transported volcanic material from Kelud.

10





5 **Figure 910.** Zonally averaged height-latitude cross sections of 532 nm extinction coefficients (km^{-1}) in March, June, September and December of 2014. The white area in the northern high latitudes in June and in the southern high latitudes in December indicates lack of nighttime data.

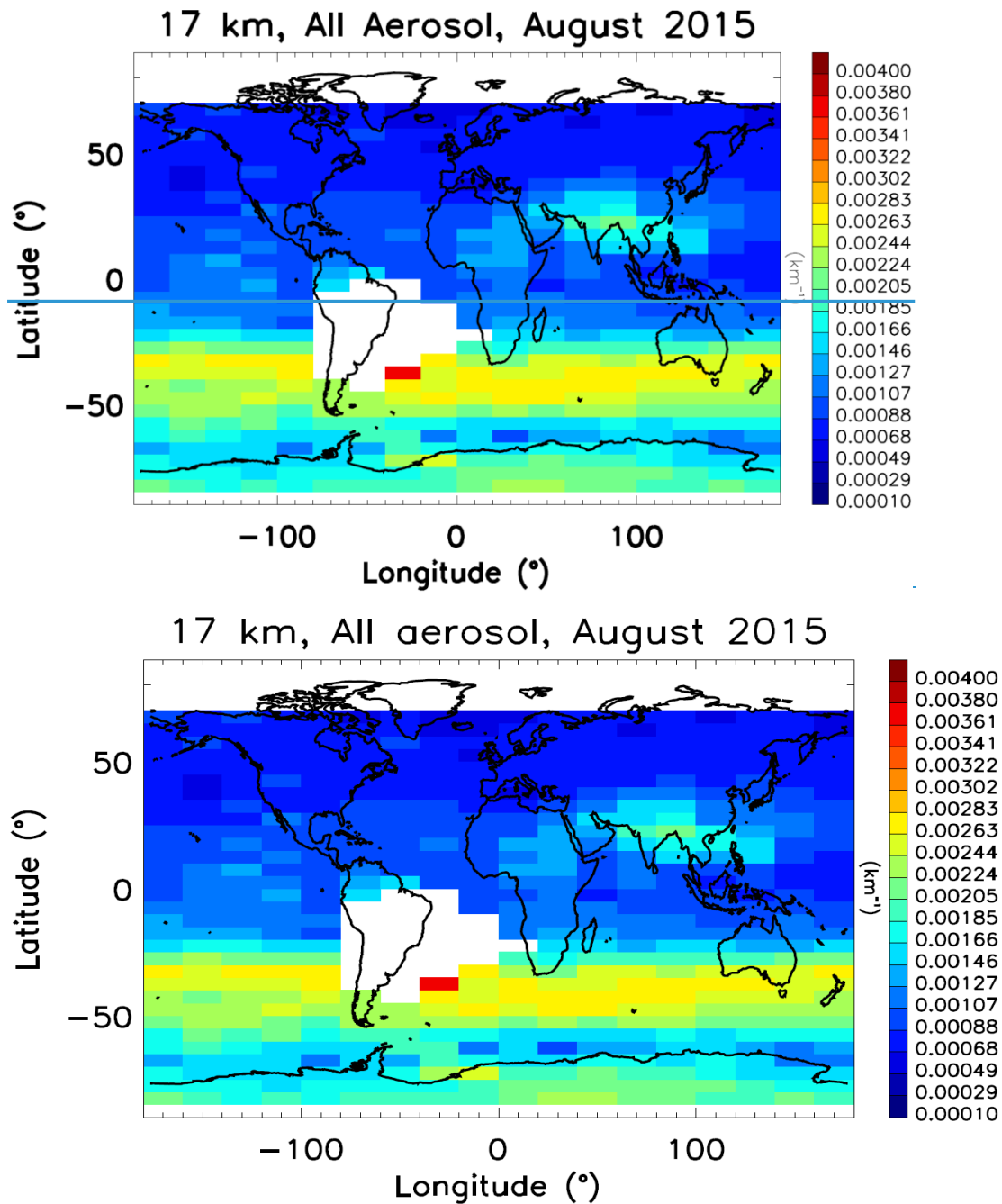


Figure 1011. Retrieved 532 nm extinction coefficients (km^{-1}) at 17 km for August 2015.

5

Figure 1011 shows the spatial distribution of the retrieved extinction coefficients at 17 km for the month of August 2015 for the “all aerosol” mode. Two strong perturbations of the lower stratosphere can be seen in this plot. The first is the plume from the Calbuco volcano in Chile

which erupted in April 2015—and. The initial plumes would be missed out in the level 3 stratospheric aerosol product because data over the SAA region were not included. However the plumes quickly spread around the southern hemisphere in a belt between 60°S to 30°S (Lopes et al., 2019) and can be seen in the level 3 stratospheric aerosol product from May 2015 onwards for several months. The other is the plume of high extinction over southeast Asia and extending to the Arabian peninsula to the west. This is the location of the Asian summer monsoon anticyclone which has been known to be a reservoir of pollution during the monsoon months and results from deep convective outflow of pollutants both gases and aerosols and their precursors from the surface layers (Kar et al., 2004, Vernier et al., 2011, 2011b).

3.2. Comparison with SAGE III on ISS

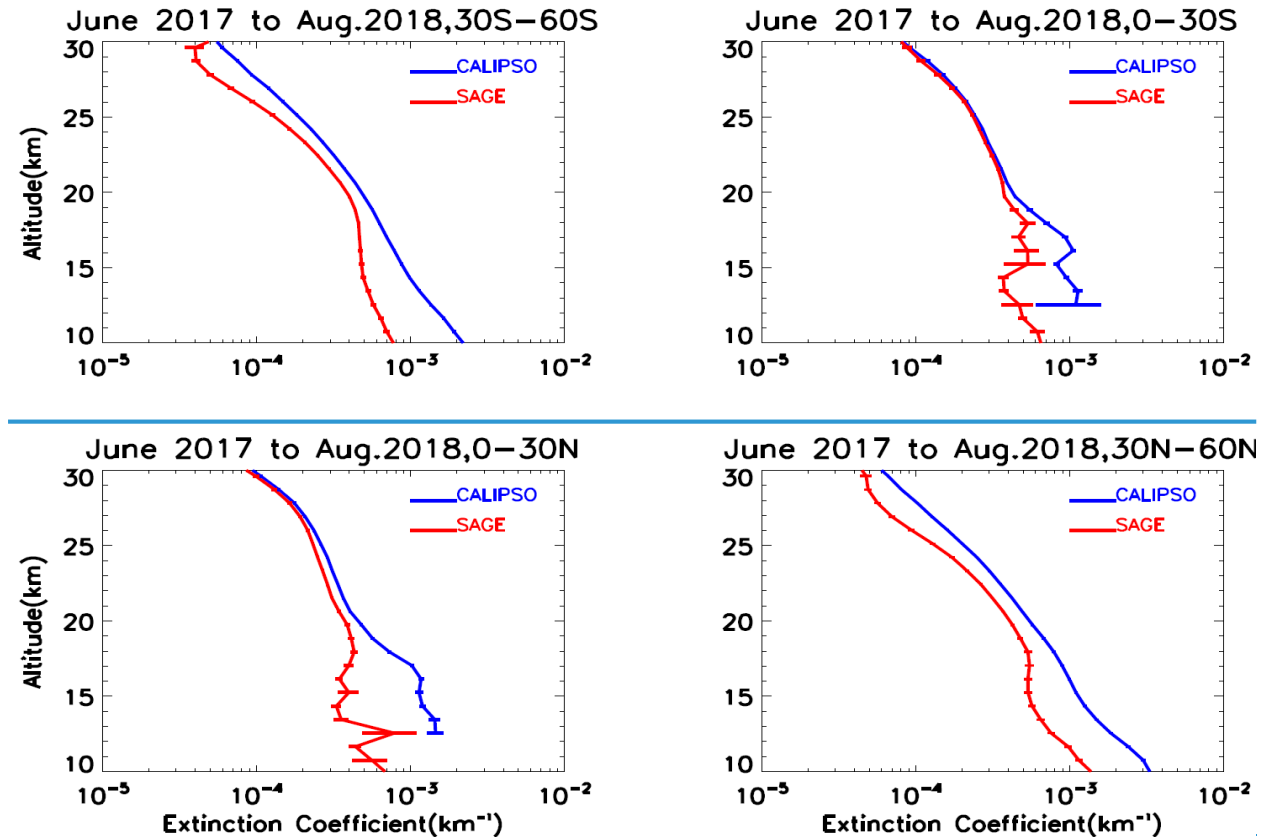
In this section we provide an initial quantitative assessment of the CALIPSO level 3 stratospheric aerosol product by inter-comparison of the retrieved extinction coefficients with those from the SAGE III instrument aboard ISS: (SAGE III-ISS). The SAGE III-ISS instrument was launched in February 2017 and has been providing measurements of ozone, NO₂, water vapor, and aerosols from its mount on the exterior of the ISS since March 2017 (Cisewski et al., 2014). The instrument derives its legacy from the long line of SAGE instruments which have been providing the most accurate retrievals of aerosol extinction in the stratosphere since 1984 (Chu et al., 1993; Thomason et al., 2008, 2010, Damadeo et al., 2013). SAGE III-ISS performs solar and lunar occultation measurements as the ISS orbits the Earth and covers the entire globe a broad latitude (90°S band (60°S to 90°N/60°N) and longitude range (180°W to 180°E). The aerosol extinction profiles are available from the solar occultation measurements in 9 channels from 384 nm to 1544 nm: starting June 2017. We use the latest version 5.1 extinction profiles reported in the 521 nm channel, which is closest to the CALIPSO 532 nm channel. In order to compare with the CALIPSO level 3 product, which reports gridded monthly averages, we average the daily data from SAGE III-ISS onto the same latitude grid (zonally averaged) as CALIPSO over a month and interpolate to the CALIPSO altitude grid. Data from both the sunrise and sunset occultations are used in the comparisons. Further, the data were filtered for cloud contamination by selecting only those data having a 521 nm to 1022 nm extinction ratio greater than 2 (Thomason and Vernier, 2013). We convert the SAGE III data-ISS data at 521 nm to 532 nm by using an Angstrom exponent (binned into 5° latitude bins and interpolated to CALIPSO altitude grid) derived from the extinctions retrieved at

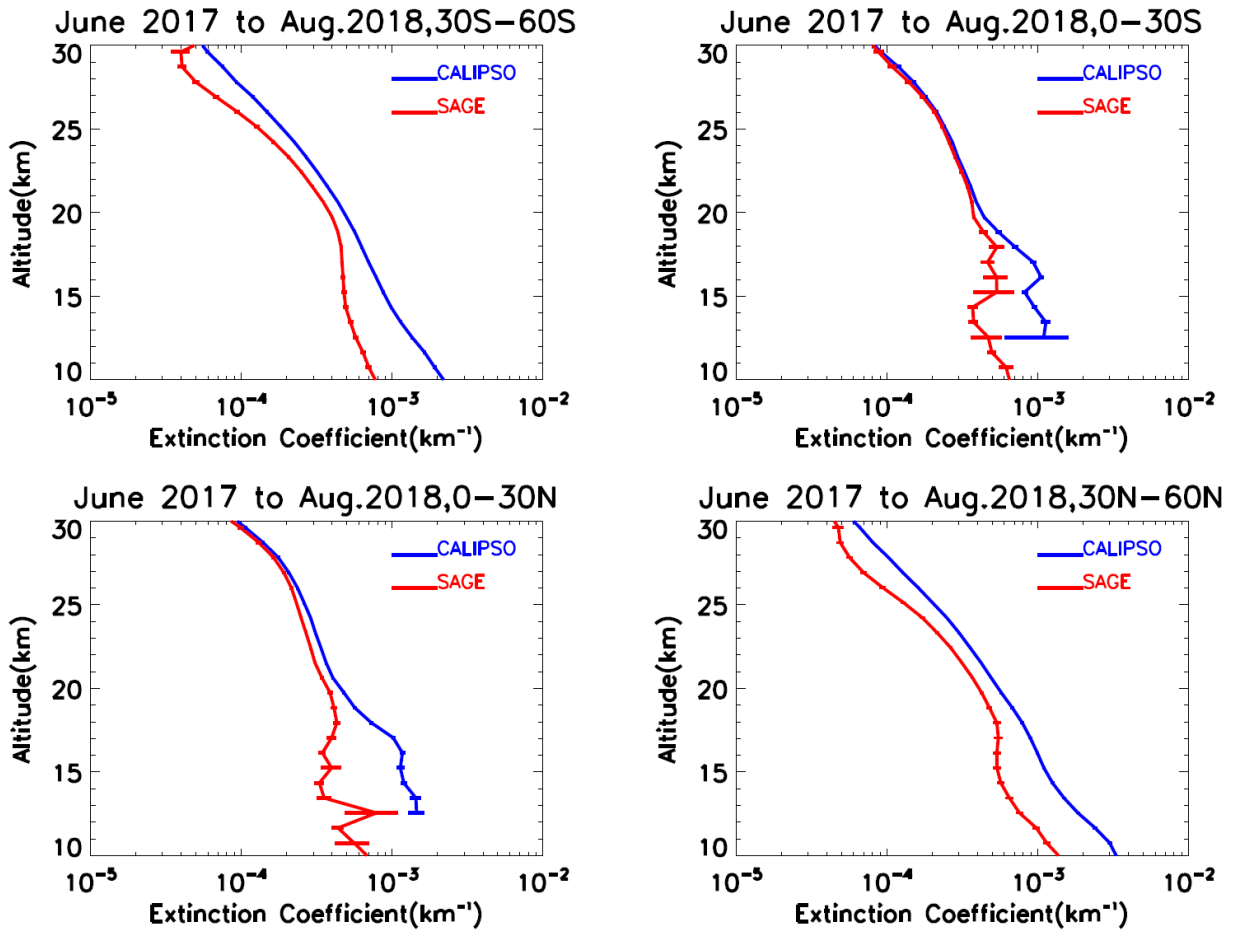
521 nm and 1022 nm by SAGE III-ISS for the same month. Measurements from both the instruments from June 2017 through August 2018 were used for this comparison. The globally averaged value of the Angstrom exponent (between 521 nm and 1022 nm) derived using all 15 months of data is about ~1.56, essentially the same as the constant value used by Khaykin et al. (2017) to convert SAGE II extinctions at 525 nm to 532 nm. We used only extinction values with corresponding fractional extinction uncertainty less than 100% for retrievals from both the instruments and calculate the differences between CALIPSO and SAGE III-ISS from the following equation:

$$\Delta(z) = 100 \times (\sigma(z)_{\text{CALIPSO}} - \sigma(z)_{\text{SAGE}}) / \sigma(z)_{\text{SAGE}} \quad (4)$$

where $\sigma(z)_{\text{CALIPSO}}$ is the extinction coefficient at altitude z from CALIPSO and $\sigma(z)_{\text{SAGE}}$ is the extinction coefficient from SAGE III-ISS at the same altitude. Further, we use zonally averaged (into 5° latitude bins) profiles for height resolved comparisons and only the “all aerosol” mode from CALIPSO product for the sake of compatibility.

a)





b)

5

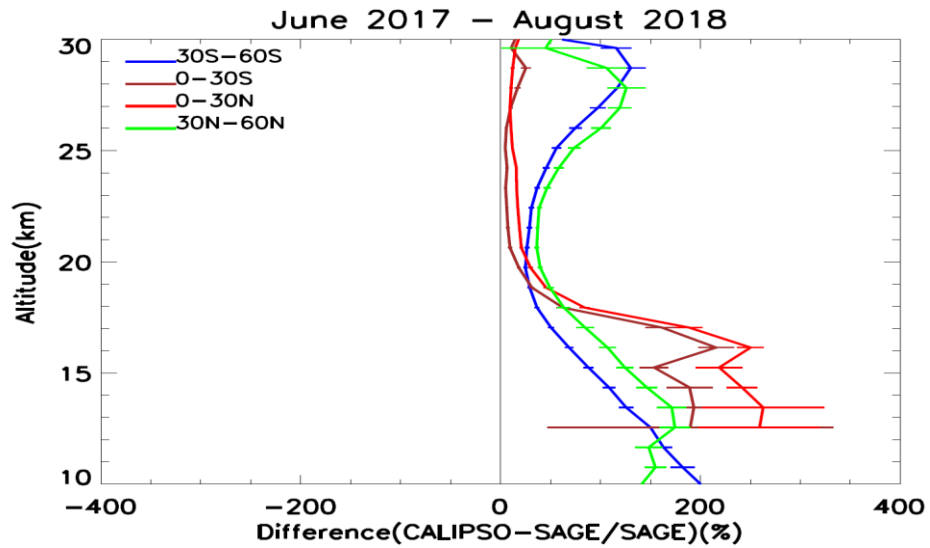


Figure 11.12a) Altitude-resolved profiles of the mean 532 nm extinction ~~coefficient~~ coefficients retrieved from CALIPSO and SAGE III-~~on~~-ISS using all available data between June 2017 and August 2018. The corresponding average differences are shown in panel b). The differences are calculated at each latitude and altitude grid for each month and then the average is taken over all the available months. The error bars represent the standard errors of the mean.

Figure 11.12a shows zonally averaged mean profiles of extinction coefficients retrieved from CALIPSO (in blue) and SAGE III-~~ISS~~ (in red) at 4 latitude bands using the same 15 months of measurements from the two instruments. Figure 11.12b shows the profiles of the fractional differences in the same latitude bands. The profiles for 0-30°S and 0-30°N, generally show fairly good agreement with the average difference within about 25% between 20 km and 30 km. The comparisons for 30°S-60°S and 30°N-60°N are similar and both show significant differences between CALIPSO and SAGE III-~~ISS~~ extinction ~~at all altitudes~~ with CALIPSO having a high bias of less than 50% near 20 km increasing to ~120% around 28 km. All the profiles diverge significantly at altitudes below 20 km, with the average difference often exceeding 100% and CALIPSO consistently overestimating SAGE III-~~Note that the aerosol retrievals from SAGE III-~~ISS. It is likely cloud removal artifacts in both the instruments are affecting these lower stratospheric comparisons. As pointed out in section 2.2.1, the filtering scheme that removes thin cirrus clouds in the all aerosol mode is not as efficient as the technique employed in the background mode. Consequently, scattering artifacts from undetected subvisible cirrus are more likely to appear in the all aerosol mode in the tropical lower stratosphere within a few kilometers above the tropopause. Using the extinction profiles from the background mode reduces the differences at these altitudes but does not completely eliminate them (not shown). Also, note that the aerosol retrievals from SAGE III-~~ISS~~(as for the legacy retrievals from SAGE II) are not directly filtered for the presence of clouds which may impact the retrievals in the lower stratosphere. Thomason and Vernier (2013) ~~discussed this issue~~ discuss the difficulties involved in ~~respect~~ cloud identification and clearing of the SAGE II ~~data. As these authors have pointed out, this is a difficult task and~~ measurements and conclude that it is not always possible to completely ~~remove the cloud effects.~~ eliminate cloud contamination of the aerosol extinction retrievals. Following their ~~analysis~~ recommendations, we have attempted to remove the cloud contamination in the extinction

retrievals by using only those data for which the ratio of extinctions at 521 nm and 1022 nm is greater than 2.0. SAGE III aerosol extinctions have not been validated as of now and it is not clear if there are any issues with the retrievals at lower altitudes near the tropopause. We further discuss the possible issues resulting from uncertainties in lidar ratios below.

5

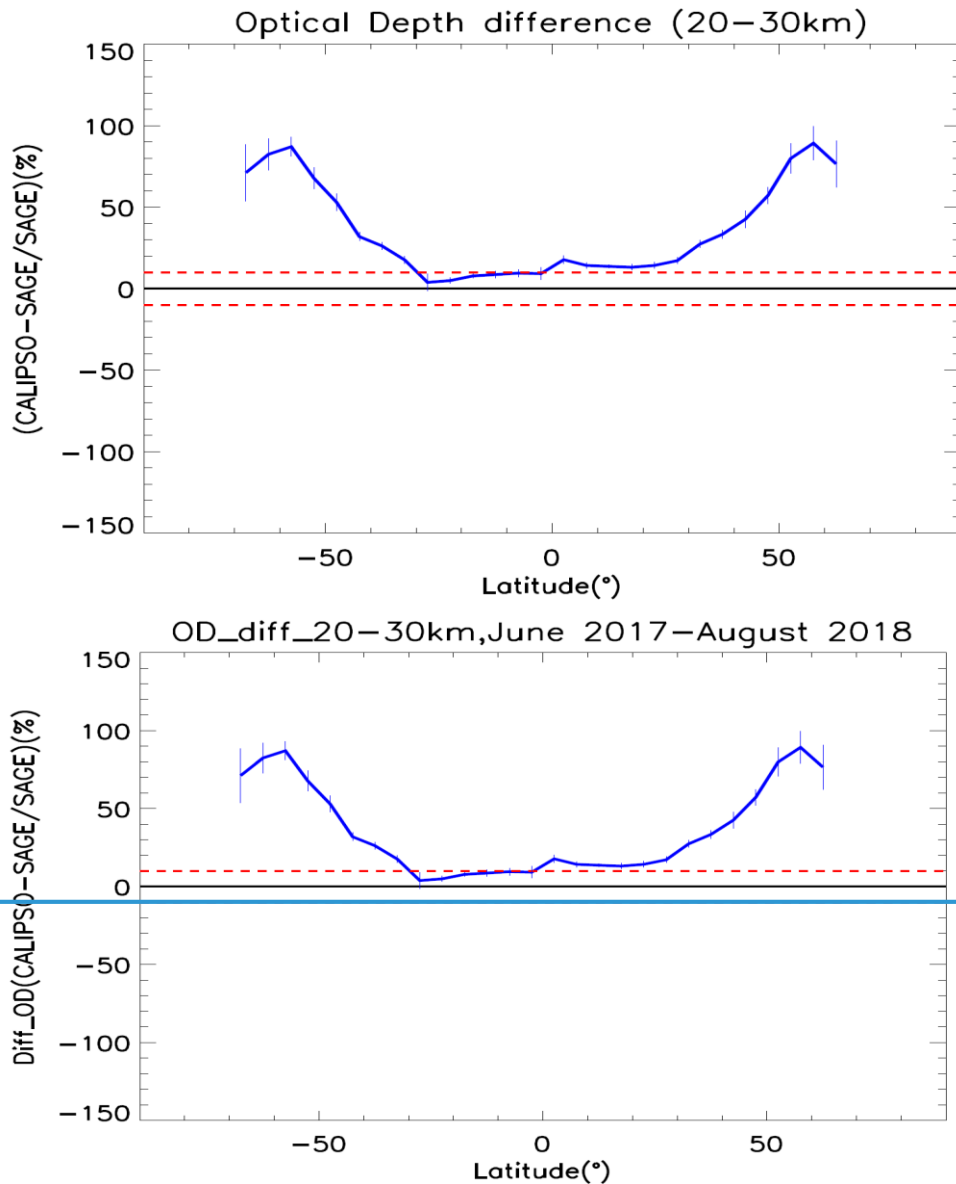


Figure 1213. Fractional difference in 532 nm optical depth between CALIPSO and SAGE III-ISS calculated using extinction coefficients from 20-30 km, as a function of latitude. The —dashed red lines demarcate the $\pm 10\%$ difference levels. The error bars represent the standard error of the mean.

10

Figure 4.13 shows the difference in the stratospheric optical depths between CALIPSO and SAGE III, calculated using the average extinction coefficient profiles between 20 km and 30 km. This region is not likely to be affected significantly by clouds and also is the region where most of the stratospheric aerosol resides, thus comparisons here are likely to be indicative of the overall performance differences between the two sensors. Between 30°S to 30°N the optical depths are in agreement to within about 10-20%, though the differences begin to rise substantially in the mid-latitudes of both hemispheres.

4. Discussion:

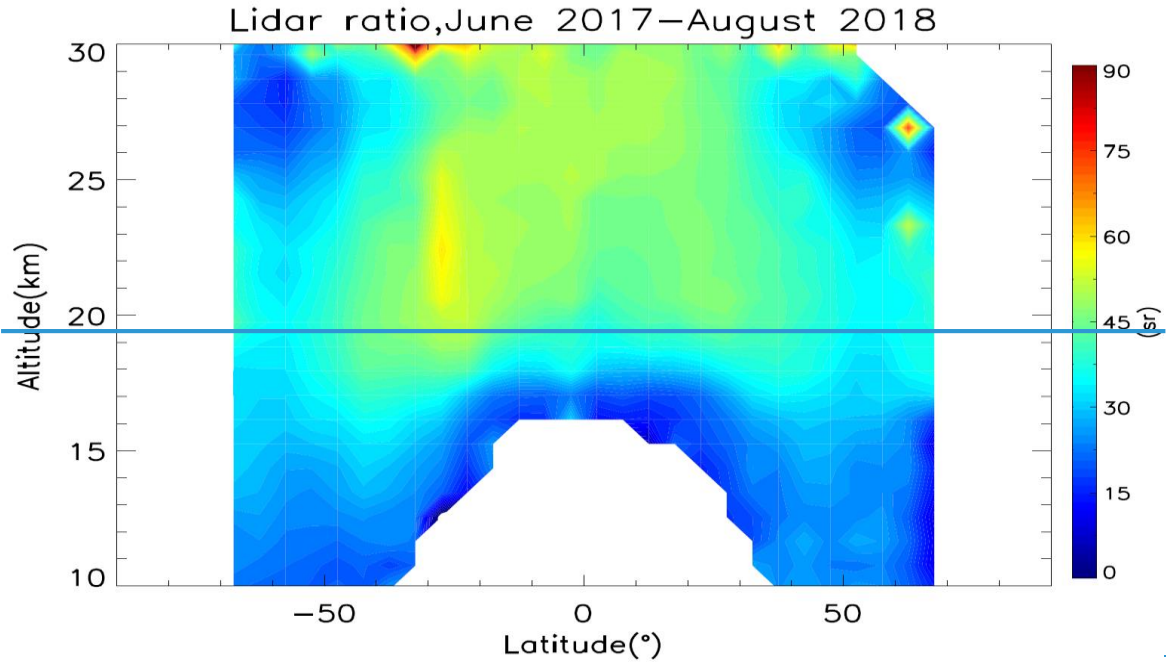
For an initial assessment of the CALIPSO stratospheric aerosol product, we have used the aerosol retrievals from SAGE III-~~on~~-ISS acquired between June 2017 and August 2018. The solar occultation technique used for SAGE III-~~ISS~~ retrievals does not rely on any assumptions on ~~the~~ aerosol ~~species~~ or size distribution. Further, the retrieval wavelengths from SAGE III-~~ISS~~ (521 nm) and CALIPSO (532 nm) are quite close and thus the comparison of the extinction retrievals will not be impacted significantly by errors in the Angstrom exponent. The previous section demonstrated that the retrieved aerosol extinction coefficients reported by the CALIPSO level 3 stratospheric aerosol product agree well with those reported by SAGE III-~~ISS~~ between 20 km and 30 km within tropical latitudes, (30°S-30°N), though the disparities between the two sets of measurements are significantly larger at higher latitudes, ~~and~~ ~~lower~~ altitudes. The primary parameter affecting the comparison with SAGE III-~~ISS~~ is likely to be the lidar ratio used in the CALIPSO retrieval. The CALIPSO extinction retrievals are quite sensitive to the lidar ratio used in the retrieval algorithm (Young et al., 2013, 2016), and the lidar ratio depends upon the optical and physical properties of the scattering particles. In the troposphere, a look-up table of lidar ratios is used by the CALIPSO extinction retrievals for various types of aerosols that might be encountered, ~~such as dust, smoke, marine aerosols etc.~~ (Omar et al., 2009, Kim et al., 2018). The version 1.00 level 3 stratospheric aerosol product uses a constant lidar ratio of 50 sr at all latitudes and altitudes for the stratospheric aerosol retrievals. While a lidar ratio of 50 sr has frequently been adopted for stratospheric analyses (e.g. ~~Trickle~~Trickl et al., 2013, Ridley et al., 2014, Sakai et al., 2016, Khaykin et al., 2017), it is not clear if this value is valid all over the stratosphere.

The adopted lidar ratio for the CALIOP stratospheric aerosol retrievals can be assessed by using the independent extinction retrievals from SAGE III-**ISS** and the attenuated backscatter measurements from CALIOP. For this we rewrite the Eq. (3c) as

$$T_p^2 = T_p^2(z) = \exp(-2 \int_0^z \sigma_p(r') dr'), \quad (5)$$

where $\sigma_p(z)$ is the particulate extinction coefficient as retrieved from the occultation measurements from SAGE III-**ISS**. Using these two-way transmittances from aerosols and computing all other terms in Eq. (2) and Eq. (3) from CALIOP data as earlier, we can obtain an estimate of the particulate backscatter $\beta_p(z)$. The **rangealtitude** dependent lidar ratio $S_p(z)$ may then be obtained from the expression:

$$S_p(z) = \sigma_p(z) / \beta_p(z) \quad (6)$$



15

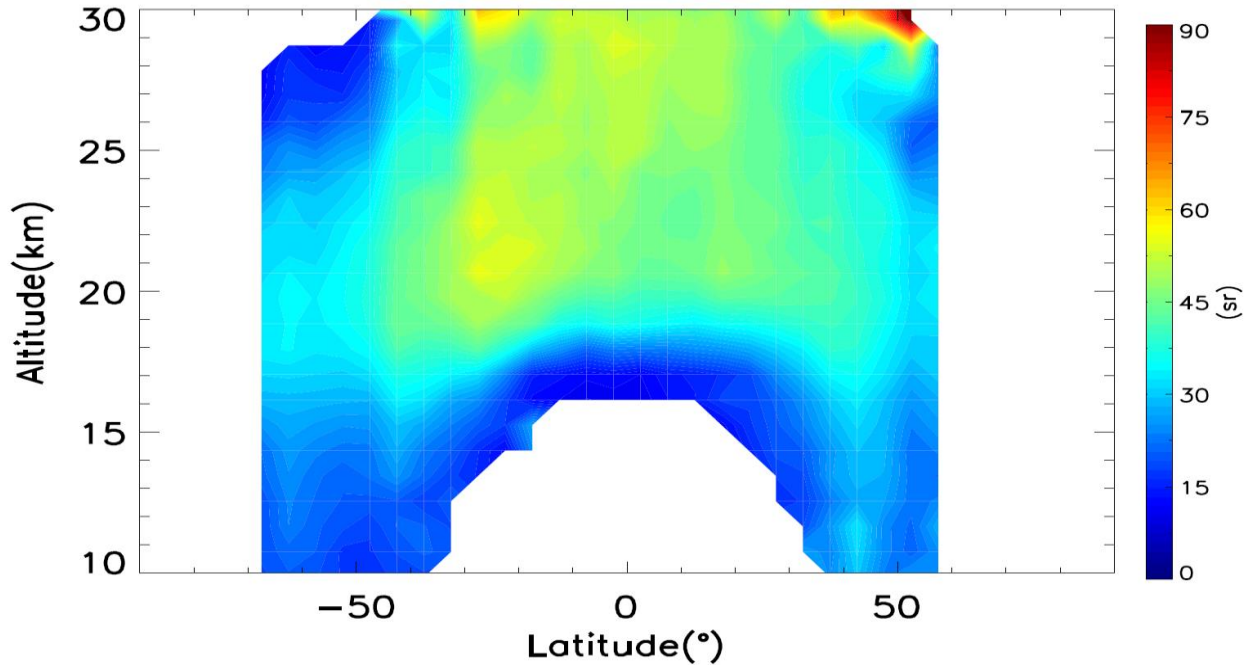


Figure 1314. Spatial distribution of the stratospheric aerosol 532 nm lidar ratio obtained from the extinction retrievals from SAGE III-ISS and backscatter measurements from CALIOP.

5

Figure 1314 shows the height-latitude cross section (averaged over June 2017–August 2018) of the estimated lidar ratios from the SAGE III-ISS and CALIOP measurements. For this figure, we have used data from both the instruments from June 2017 through March 2018, excluding data from August 2017 through November 2017 to avoid the effect of smoke from the strong pyroCb event of August–September, 2017 as discussed above. The data from both instruments beyond March 2018 were not used to avoid the impact of the Ambae volcano, which erupted in April 2018. As for the comparisons presented in section 3, we have averaged the SAGE III-ISS data over each month and interpolated to the CALIPSO altitude grid and computed the lidar ratios, which were then averaged to obtain the climatological distribution shown in Figure 14. As before, we have cloud cleared the SAGE III-ISS data below 20 km by only using the only those 521 nm extinction coefficients when the ratio of extinctions at for which 521 nm and to 1022 nm extinction ratio exceeded 2 and used an. The Angstrom exponent obtained from these two wavelengths was used to convert scale the SAGE III-ISS extinction at 521 nm to that at 532 nm. As can be seen, the lidar ratio values in the bulk of the stratosphere with significant aerosol loading are in the range 45–50 sr, quite similar to the canonical range in the stratosphere (Kremser et al., 2016), with the mean

10

15

20

value between 18-30 km and between 40°S and 40°N being -46 ± 56 sr. However, in the lowermost stratosphere at all latitudes and in ~~the~~ both the polar regions at essentially all altitudes, the estimated lidar ratio values are substantially lower (≤ 40 sr, Figure 1314). There may be several issues impacting these estimated lidar ratios. We have used the 521 nm aerosol extinction product from SAGE III-ISS, which is still an evolving product. In particular, any errors in the ozone retrievals from SAGE III-ISS are likely to adversely affect the 521 nm aerosol extinction retrievals. Further, in the lowermost stratosphere above the tropopause, mixtures of clouds and aerosols may exist and SAGE III-ISS aerosol data have not been cleared for clouds as such. We have used a simple cloud ~~clearance~~clearing procedure using the ratio of extinctions at 521 nm and 1022 nm, which might be of limited validity near the tropopause. **As mentioned above, incomplete thin cirrus removal artifacts in the CALIPSO stratospheric product, particularly in the “all aerosol” mode may also impact the estimates in the lower stratosphere within a few kilometers above the tropopause particularly in the tropics.** Similarly, at high altitudes in the polar regions the aerosol loading is expected to be quite small (extinction $\sim 10^{-5}$ km⁻¹) and both sensors are likely to experience difficulty in retrieving these very low extinction coefficients. In particular, CALIOP can have significantly enhanced noise at those altitudes in the polar regions (e.g., see Fig. 16 in Hunt et al., 2009) which may contribute to the differences. Note also that a lidar ratio that is in error at the highest altitudes would lead to incorrect extinction retrievals for CALIOP lower down, since the attenuation correction **that are propagated downward** would **also** be in error. In any case, using a lower lidar ratio in these areas, as suggested by Figure 1314, will lead to lower retrieved extinction coefficients from CALIOP and will alleviate the differences noted in section 3.

Is there any evidence of low lidar ratios in the high latitude stratosphere as seen in Figure 1314? O'Neill et al. (2012) studied aerosol plumes from ~~the~~ Sarychev volcano from high arctic observations from the Polar Environmental Atmospheric Research Laboratory (PEARL) station (80.05°N, 86.42°W) and estimated **a characteristic** lidar ratio of 59 sr using ~~size distribution from AERONET~~ **which was also close to the average lidar ratio of 55 sr estimated from the measurements.** The Arctic High Spectral Resolution (AHSRL) ~~lidar~~**also retrieved lidar ratio estimates ranging between ~ 51 sr and 59 sr from measurements acquired between 10- and 15 km.** **Similarly,** Kravitz et al. (2011) ~~also~~reported lidar ~~ratio~~**ratios** of 50 sr and 60 sr for Sarychev plumes **obtained** from the Koldewey Aerosol Raman Lidar (KARL) at Ny- Alesund, Svalbard (78.9°N, 11.9°W). Hoffmann et al. (2010) estimated a somewhat higher value of 65 sr for Kasatochi aerosol

plume near the tropopause over Ny-Alesund, in September 2008. Interestingly, **and in stark contrast**, for a clear day with no Kasatochi layers **present**, they obtained a background lidar ratio of 18 ± 6 sr ~~by fitting the integrated lidar extinction to coincident photometer optical depth measurements. At high altitudes (> 20 km) in polar regions during non-PSC conditions, volcanic influence is not likely to be significant;~~ however more **data may be measurements are clearly** needed ~~to verify the low lidar ratios at those~~ **all stratospheric** altitudes. There is also a paucity of measurements at the stratospheric altitudes over the southern high latitude regions.

In presence of large ash and even sulfate injections from volcanoes, ~~the~~ lidar **ratio ratios** can be significantly different and can evolve with time. From the so-called “constrained” retrievals, when the lidar ratios of layers can be obtained directly from the attenuation measurements from CALIOP (Young and Vaughan, 2009), the median lidar ratio of sulfate as well as ash-dominant layers from several volcanoes has been found to be ~ 60 - 69 sr (Prata et al., 2017, Kar et al., ~~2018~~). ~~We~~ **2018b**). **In constructing Fig. 14, we** have not ~~filtered the~~ **used** data from either instrument for the ~~presence~~ **period** of ~~volcanic and smoke particles, which can skew~~ **possible contamination from** the **strong pyroCb event in 2017 as well as after the eruption of Ambae volcano. We shall continue to refine** the lidar ratio estimates ~~shown in Figure 13. For~~ **using** the ~~data used~~ **methodology** described here (~~June 2017 through August 2018~~), ~~there were probably no significant injections of ash from volcanoes; however the large pyroCb event of August 2017 (as mentioned above) would contribute~~ **as more contemporaneous measurements from SAGE III-ISS and CALIPSO become** **available**. In future versions of the CALIOP level 3 stratospheric aerosol product we shall attempt to use a more representative lidar ratio over all of the stratosphere.

5. Conclusion

In this paper we have provided a detailed account of the algorithm used to construct the **recently released** CALIPSO level 3 stratospheric aerosol **profile** product version 1.00 ~~that was recently released~~. Further, we have given qualitative as well as an initial quantitative assessment of the aerosol extinction retrievals. We have shown that the product captures significant stratospheric aerosol injections (e.g., from volcanic eruptions **and wildfires**) and clearly illustrates perturbations from stratospheric dynamics over the lifetime of the mission. Comparisons with extinction retrievals obtained from SAGE III ~~on ISS show~~ **ISS show** quite good agreement to within about **25%** in the mean between 20-30 km and between about 30°S-30°N. However, the comparison

consistently indicates much larger deviations, exceeding 100-200% (CALIPSO higher), at mid-to-high latitudes (30°S-60°S and high30°N-60°N) and at low altitudes- (10-20 km). The role of the lidar ratio used for the extinction retrievals in the level 3 stratospheric aerosol product was also explored. Based on combined measurements by CALIPSO and SAGE III-ISS, the current lidar ratio of 50 sr is shown to be appropriate for background conditions above 20 km in the tropics. However, it may be unrepresentative of lidar ratios closer to the tropopause and at mid-to-high latitudes. Future versions of the CALIPSO level 3 stratospheric aerosol profile product may refine the lidar ratios based on these and forthcoming analyses.

10 Acknowledgements:

J. K. would like to thank Jean-Paul Vernier, M. C. Pitts and Larry Thomason for useful discussions during the development of the CALIPSO stratospheric product. SAGE III aerosol data were obtained from the Langley Atmospheric Science Data Center. The referees are thanked for useful comments and suggestions that significantly improved the manuscript. J.K. would like to acknowledge illuminating discussions with M. C. Pitts on PSCs.

References:

- 20 Ansmann, A., Baars, H., Chudnovsky, A., Mattis, I., Veselovskii, I., Haarig, M., Seifert, P., Engelmann, R. and Wandinger, U., Extreme levels of Canadian wildfire smoke in the stratosphere over central Europe on 21-22 August 2017, *Atmos. Chem. Phys.*, 18, 11831-11845, <https://doi.org/10.5194/acp-18-11831-2018>, 2018.
- Beyerle, G., Neuber, R., Schrems, O., Wittrock, F., and Knudsen, B.: Multiwavelength lidar measurements of stratospheric aerosols above Spitsbergen during winter 1992/93, *Geophys. Res. Lett.*, 21, 57-60, <https://doi.org/10.1029/93GL02846>, 1994.
- 25 Brock, C. A., Jonsson, H. H., Wilson, J. C., Dye, J. E., Baumgardner, D., Borrmann, S., Pitts, M. C., Osborn, M. T., Decoursey, R. J. and Woods, D. C.: Relations between optical extinction, backscatter and aerosol surface and volume in the stratosphere following the eruption of Mt. Pinatubo, *Geophys. Res. Lett.*, <https://doi.org/10.1029/93GL01691>, 1993.
- 30

- Bourassa, A., Rieger, L. A., Lloyd, N. D. and Degenstein, D. A.: Odin-OSIRIS stratospheric aerosol data product and SAGE III intercomparison, *Atmos. Chem. Phys.*, 12, 605-614, <https://doi.org/10.5194/acp-12-605-2012>, 2012.
- 5 Chazette, P., David, C., Lefrere, J., Godin, S., Pelon, J and Megie, G.: Comparative lidar study of the optical, geometrical and dynamical properties of stratospheric post-volcanic aerosols, following the eruptions of El Chichon and Mount Pinatubo, *J. Geophys. Res.*, 100, D11, 23195-23207, <https://doi.org/10.1029/95JD02268>, 1995.
- 10 Chu, W. P. and McCormick, M. P., Inversion of stratospheric aerosol and gaseous constituents from spacecraft solar extinction data in the 0.38-1.0 μm wavelength region, *Appl. Opt.*, 18, 1404-1413, 1979.
- Cisewski, M., Zawodny, J., Gasbarre, J., Eckman, R., Topiwala, N., Rodriguez-Alvarez, O., Cheek, D. and Hall, S., The Stratospheric Aerosol and Gas Experiment (SAGE III) on the International Space Station (ISS) mission, *Proc. of SPIE*, 9241, 924107, 2014.
- 15 Chen, Z., Bhartia, P. K., Loughman, R., Colarco, P. and Deland, M., Improvement of stratospheric aerosol extinction retrieval from OMPS/LP using a new aerosol model, *Atmos. Meas. Tech.*, 11, 6495-6509, <https://doi.org/10.5194/amt-11-6495-2018>, 2018.
- Chu, W. P., McCormick, M. P., Lenoble, J., Brogniez, C., and Pruvost, P.: SAGE II inversion algorithm, *J. Geophys. Res.*, 94(D6), 8339–8351, <https://doi.org/10.1029/89JD00113>, 1989.
- 20 Damadeo, R. P., Zawodny, J. M., Thomason, L. W. and Iyer, N., SAGE version 7.0 algorithm: Application to SAGE II, *Atmos. Meas. Tech.*, 6, 3539–3561, <https://doi.org/10.5194/amt-6-3539-2013>, 2013.

- de Laat, A. T. J., Stein Zweers, D. C., Boers, R., and Tuinder, O. N. E.: A solar escalator: Observational evidence of the self-lifting of smoke and aerosols by absorption of solar radiation in the February 2009 Australian Black Saturday plume, *J. Geophys. Res.*, 117, D04204, <https://doi.org/10.1029/2011JD017016>, 2012.
- 5 Deshler, T.: A review of global stratospheric aerosol: Measurements, importance, life cycle, And local stratospheric aerosol, *Atmos. Res.*, 90, 223-232, <https://doi.org/10.1016/j.atmosres.2008.03.016>, 2008.
- de Vries, M. J. M. Penning, Dorner, S., Pukite, J., Hormann, C., Formm, M. D. and Wagner, T., Characterisation of a stratospheric sulfate plume from the Nabro volcano using a combination of passive satellite measurements in nadir and limb geometry, *Atmos. Chem. Phys.*, 14, 8149-8163, <https://doi.org/10.5194/acp-14-8149-2014>, 2014.
- 10 Friberg, J., Martinsson, B. G., Andersson, S. M. and Sandvik, O. S., Volcanic impact on the climate—the stratospheric aerosol in the period 2006-2015, *Atmos. Chem. Phys.*, 18, 11149–11169, <https://doi.org/10.5194/acp-18-11149-2018>, 2018.
- 15 Fromm, M., Lindsey, D. T., Servranckx, R., Yue, G., ~~Trickle~~Trickl, T., Sica, R., Doucet, P., and Godin-Beekmann, S., The untold story of pyrocumulonimbus, *Bull. American Met. Soc.*, 1193-1209, <https://doi.org/10.1175/2010BAMS3004.1>, 2010.
- Gelaro, R., McCarty, W., Suarez, M. J., Todling, R., Molod, A., Takacs, L., Randles, C. A., Darmenov, A., Bosilovich, M. G., Reichle, R., Wargan, K., Coy, L., Cullather, R., Draper, C., Akella, S., Buchard, V., Conaty, A., Da Silva, A. M., Gu, W., Kim, G.-K., Koster, R., Lucchesi, R., Markova, D., Nielsen, J. E., Partyka, G., Pawson, S., Putman, W., Rienecker, M., Schubert, S. C., Sienkiewicz, M., and Zhao, B.: The Modern-Era Retrospective Analysis for Research and Applications, Version 2 (MERRA-2), *J. Climate*, 30, 5419–5454, <https://doi.org/10.1175/JCLI-D-16-0758.1>, 2017.
- 25 Glaccum, W., Lucke, R. L., Bevilacqua, R. M., Shettle, E. P., Hornstein, J. S., Chen, D. T., Lumpe, J. D., Hrigman, S. S., Debrestian, J. J., Fromm, M. D., Dalaudier, F., Chassefiere, F., Deniel, C., Randall, C. E., Rusch, D. W., Olivero, J. J., Brogniez, C., Lenoble, J., and Kremer, R., The polar ozone and aerosol measurement instrument, *J. Geophys. Res.*, 101, 14479-14487, 1996.
- 30 Glatthor, N., Höpfner, M., Semeniuk, K., Lupu, A., Palmer, P. I., McConnell, J. C., Kaminski, J. W., von Clarmann, T., Stiller, G. P., Funke, B., Kellmann, S., Linden, A., and Wiegeler, A.:

The Australian bushfires of February 2009: MIPAS observations and GEM-AQ model results, *Atmos. Chem. Phys.*, 13, 1637-1658, <https://doi.org/10.5194/acp-13-1637-2013>, 2013.

Grams, G. and Fiocco, G.: Stratospheric aerosol layer during 1964 and 1965, *J. Geophys. Res.*, 72, 3523– 3542, doi:10.1029/JZ072i014p03523, 1967.

Haarig, M., Ansmann, A., Baars, H., Jimenez, C., Veselovskii, I., Engelmann, R., and Althausen, D.: Depolarization and lidar ratios at 355, 532, and 1064 nm and microphysical properties of aged tropospheric and stratospheric Canadian wildfire smoke, *Atmos. Chem. Phys.*, 18, 11847-11861, <https://doi.org/10.5194/acp-18-11847-2018>, 2018.

Hofmann, D., Barnes, J., O'Neill, M., Trudeau, M., and Neely, R., Increase in background stratospheric aerosol observed with lidar at Mauna Loa observatory and Boulder, Colorado, *Geophys. Res. Lett.*, 36, L15808, <https://doi.org/10.1029/2009GL039008>, 2009.

Jaeger, H and Deshler, T., Lidar backscatter to extinction, mass and area conversions for stratospheric aerosols based on midlatitude balloonborne size distribution measurements, *Geophys. Res. Lett.*, 29, 1929, <https://doi.org/10.1029/2002GL015609>, 2002.

Junge, C. E., and Manson, J. E., Stratospheric aerosol studies, *J. Geophys. Res.*, 66, 2163–2182, <https://doi.org/10.1029/JZ066i007p02163>, 1961.

Kar, J. Bremer, H., Drummond, J. R., Rochon, Y. J., Jones, D. B. A., Nichitiu, F., Zou, J., Liu, J., Gille, J. C., Edwards, D. P., Deeter, M. N., Francis, G., Ziskin, D. and Warner, J., Evidence of vertical transport of carbon monoxide from Measurements of Pollution in the Troposphere, *Geophys. Res. Lett.*, 31, L23105, <https://doi.org/10.1029/2004GL021128>, 2004.

Kar, J., Vaughan, M. A., Lee, K.-P., Tackett, J. L., Avery, M. A., Garnier, A., Getzewich, B. J., Hunt, W. H., Josset, D., Liu, Z., Lucker, P. L., Magill, B., Omar, A. H., Pelon, J., Rogers, R. R., Toth, T. D., Trepte, C. R., Vernier, J.-P., Winker, D. M., and Young, S. A.: CALIPSO lidar calibration at 532 nm: version 4 nighttime algorithm, *Atmos. Meas. Tech.*, 11, 1459-1479, <https://doi.org/10.5194/amt-11-1459-2018>, 2018a.

Kar, J., Vaughan, M. A., Tackett, J. Omar, A., Trepte, C. R. and Lucker, P. L., Constrained lidar ratios for volcanic ash and sulfate layers in the stratosphere from CALIOP version 4.10 data, paper presented at the American Geophysical Union Fall Meeting, Washington, DC., Dec.10-14, 2018b.

Kent, G. S. and McCormick, M. P., SAGE and SAM II measurements of global stratospheric aerosol optical depth and mass loading, *J. Geophys. Res.*, 89, 5303-5314, 1984.

5 Khaykin, S. M., Godin-Beekmann, S., Keckhut, P., Hauchecorne, A., Jumelet, J., Vernier, J.-P., Bourassa, A., Degenstein, D. A., Rieger, L. A., Bingen, C., Vanhellemont, F., Robert, C., DeLand, M. and Bhartia, P. K., Variability and evolution of the midlatitude stratospheric aerosol budget from 22 years of ground-based lidar and satellite observations, *Atmos. Chem. Phys.*, 17, 1829–1845, <https://doi.org/10.5194/acp-17-1829-2017>, 2017.

10 Khaykin, S. M., Godin-Beekmann, S., Hauchecorne, A., Pelon, J., Ravetta, F. and Keckhut, P., Stratospheric smoke with unprecedentedly high backscatter observed by lidars above southern France, *Geophys. Res. Lett.*, <https://doi.org/10.1002/2017GL076763>, 2018.

15 Kremser, S., Thomason, L. W., von Hobe, M., Hermann, M., Deshler, T., Timmreck, C., Toohey, M., Stenke, A., Schwarz, J. P., Weigel, R., Fueglistaler, S., Prata, F. J., Vernier, J.-P., Schlager, H., Barnes, J. E., Antuna-Marrero, J.-C., Fairlie, D., Palm, M., Mahieu, E., Notholt, J., Rex, M., Bingen, C., Vanhellemont, F., Bourassa, A., Plane, J. M. C., Kolcke, D., Carn, S. A., Clarisse, L., Trickl, T., Neely, R., James, A. D., Rieger, L., Wilson, J. C., and Meland, B.: Stratospheric aerosol-Observations, processes and impact on climate, *Rev. Geophys.*, 54, 278–335, <https://doi.org/10.1002/2015RG000511>, 2016.

20 Liu, Z., Liu, D., Huang, J., Vaughan, M., Uno, I., Sugimoto, N., Kittaka, C., Trepte, C., Wang, Z., Hostetler, C. and Winker, D., Airborne dust distribution over the Tibetan Plateau and surrounding areas derived from the first year of CALIPSO lidar observations, *Atmos. Chem. Phys.*, 5045-5060, <https://doi.org/10.5194/acp-8-5045-2008>, 2008.

25 Liu, Z., Vaughan, M., Winker, D., Kittaka, C., Getzewich, B., Kuehn, R., Omar, A., Powell, K., Trepte, C., and Hostetler, C.: The CALIPSO lidar cloud and aerosol discrimination: Version 2 Algorithm and initial assessment of performance, *J. Atmos. Ocean. Tech.*, 26, 1198–1212, <https://doi.org/10.1175/2009JTECHA1229.1>, 2009.

Liu, Z., Kar, J., Zeng, S., Tackett, J., Vaughan, M., Avery, M., Pelon, J., Getzewich, B., Lee, K.-P., Magill, B., Omar, A., Lucker, P., Trepte, C., and Winker, D.: Discriminating between clouds and aerosols in the CALIOP version 4.1 data products, *Atmos. Meas. Tech.*, 12, 703-734, <https://doi.org/10.5194/amt-12-703-2019>, 2019.

- Lopes, F. J. S., Silva, J. J., Antuña Marrero, J. C., Taha, G. and Landulfo, E.: Synergetic Aerosol Layer Observation After the 2015 Calbuco Volcanic Eruption Event, *Remote Sens.*, **11**, 195, <https://doi.org/10.3390/rs11020195>, 2019.
- 5 Lucke, R. L. et al., The Polar Ozone and Aerosol Measurement (POAM III) instrument and early validation results, *J. Geophys. Res.*, **104**, 18785-18799, 1999.
- Mauldin III, L. E., Zaun, N. H., McCormick, M. P., Guy, J. H. and Vaughan, W. R.: Stratospheric aerosol and Gas Experiment II instruments: A functional description, *Opt. Eng.*, **24**, 307-312, <https://doi.org/10.1117/12.7973473>, 1985.
- 10 McCormick, M. P., Swissler, T. J., Fuller, W. H. and Osborn, M. T.: Airborne and Ground-Based lidar measurements of the El Chichón stratospheric aerosol from 90°N to 56°S, *Geofísica Internacional*, **23**, 187-221, 1984.
- McCormick, M. P., Thomason, L. W. and Trepte, C. R.: Atmospheric effects of the Mt Pinatubo eruption, *Nature*, **373**, 399–404, <https://doi.org/10.1038/373399a0>, 1995.
- 15 McElroy, C. T., Nowlan, C. R., Drummond, J. R., Bernath, P. F., Barton, D. V., Dufour, D. G., Midwinter, C., Hall, R. B., Ogyu, A., Ullberg, A., Wardle, D. I., Kar, J., Zou, J., Nichitiu, F., Boone, C. D., Walker, K. A., and Rowlands, N.: The ACE-MAESTRO instrument on SCISAT: Description, performance, and preliminary results, *Appl. Optics*, **46**(20), 4341–4356, 2007.
- 20 McGill, M. J., Vaughan, M. A., Trepte, C. R., Hart, W. D., Hlavka, D. L., Winker, D. M., and Kuehn, R.: Airborne validation of spatial properties measured by the CALIPSO lidar, *J. Geophys. Res.*, **112**, D20201, <https://doi.org/10.1029/2007JD008768>, 2007.
- Noel, V., Chepfer, H., Hoareau, C., Reverdy, M., and Cesana, G.: Effects of solar activity on noise in CALIOP profiles above the South Atlantic Anomaly, *Atmos. Meas. Tech.*, **7**, 1597-1603, <https://doi.org/10.5194/amt-7-1597-2014>, 2014.
- 25 Northam, G. B., Rosen, J. M., Melfi, S. H., Pepin, T. J., McCormick, M. P., Hofmann D. J. and Fuller, W. H.: Dustsonde and Lidar Measurements of Stratospheric Aerosols: a Comparison, *Applied Optics*, **13**, 2416-2421, <https://doi.org/10.1364/AO.13.002416>, 1974.
- 30 O'Neill, N. T., Perro, C., Saha, A., Lesins G., Duck, T. J., Eloranta, E. W., Nott, G. J., Hoffman, A., Karumudi, M. L., Ritter, C., Bourassa, A., Abboud, I., Carn, S. A., Savastiouk, V.:

Properties of Sarychev sulphate aerosols over the Arctic, *J. Geophys. Res.*, 117, D04203, doi:10.1029/2011JD016838, 2012.

- Peterson, D. A., Campbell, J. R., Hyer, E. J., Fromm, M. D., Kablick III, G. P., Cossuth, J. H., and DeLand, M. T.: Wildfire-driven thunderstorms cause a volcano-like stratospheric injection of smoke, *npj Climate and Atmospheric Science*, 1, <https://doi.org/10.1038/s41612-018-0039-3>, 2018.
- Pitts, M. C., Thomason, L. W., Poole, L. R., and Winker, D. M.: Characterization of Polar Stratospheric Clouds with spaceborne lidar: CALIPSO and the 2006 Antarctic season, *Atmos. Chem. Phys.*, 7, 5207-5228, <https://doi.org/10.5194/acp-7-5207-2007>, 2007.
- Pitts, M. C., Poole, L. R., and Thomason, L. W.: CALIPSO polar stratospheric cloud observations: second-generation detection algorithm and composition discrimination, *Atmos. Chem. Phys.*, 9, 7577-7589, <https://doi.org/10.5194/acp-9-7577-2009>, 2009.
- Powell, K. A.: *Development of the CALIPSO Lidar Simulator*, M.S. Thesis, Department of Applied Science, The College of William and Mary, 228 pp., 2005.
- Powell, K. A., Hostetler, C. A., Liu, Z., Vaughan, M. A., Kuehn, R. A., Hunt, W. H., Lee, K.-P. Trepte, C. R., Rogers, R. R., Young, S. A., and Winker, D. M.: CALIPSO Lidar calibration algorithms. Part I: Nighttime 532 nm parallel channel and 532 nm perpendicular channel, *J. Atmos. Ocean. Tech.*, 26, 2015–2033, <https://doi.org/10.1175/2009JTECHA1242.1>, 2009.
- Prata, A. T., Young, S. A., Siems, S. T and Manton, M. J., Lidar ratios of stratospheric volcanic ash and sulfate aerosols retrieved from CALIOP measurements, *Atmos. Chem. Phys.*, 17, 8599–8618, <https://doi.org/10.5194/acp-17-8599-2017>, 2017.
- Ridley, D. A., Solomon, S., Barnes, J. E., Burlakov, V. D., Deshler, T., Dolgii, S. I., Herber, A. B., Nagai, T., Neely, R. R., Nevzorov, A. V., Ritter, C., Sakai, T., Santer, B. D., Sato, M., Schmidt, A., Uchino, O., and Vernier, J. P.: Total volcanic stratospheric aerosol optical depths and implications for global climate change, *Geophys. Res. Lett.*, 41, 7763–7769, <https://doi.org/10.1002/2014GL061541>, 2014.
- Robock, A., Volcanic eruptions and climate, *Rev. Geophysics*, 38(2), 191-219, <https://doi.org/10.1029/1998RG000054>, 2000.
- Sakai, T., Uchino, O., Nagai, N., Liley, B., Morino, I., and Fujimoto, T.: Long-term variation of stratospheric aerosols observed with lidars over Tsukuba, Japan, from 1982 and Lauder,

New Zealand, from 1992 to 2015, *J. Geophys. Res. Atmos.*, 121, 10283–10293, <https://doi.org/10.1002/2016JD025132>, 2016.

5 **Sassen, K., Wang, Z. and Liu, D., Cirrus clouds and deep convection in the tropics: Insights from CALIPSO and CloudSat, *J. Geophys. Res.*, 114, <https://doi.org/10.1029/2009JD011916>, 2009.**

Solomon, S., Daniel, J. S., Neely III, R. R., Vernier, J. P., Dutton, E. G. and Thomason, L. W., : The persistently variable “background” stratospheric aerosol layer and global climate change, *Sci. Express*, <https://doi.org/10.1126/science.1206027>, 2011.

10 Thomason, L. W. and Peter, T., Assessment of stratospheric aerosol properties (ASAP), SPARC report no 4, WCRP-124, WMO/TD-No. 1295, 2006.

Thomason, L. W., Pitts, M. C., and Winker, D. M.: CALIPSO observations of stratospheric aerosols: a preliminary assessment, *Atmos. Chem. Phys.*, 7, 5283-5290, <https://doi.org/10.5194/acp-7-5283-2007>, 2007.

15 Thomason, L. W., Burton, S. P., Luo, B.-P. and Peter, T., SAGE II measurements of stratospheric aerosol properties at non-volcanic levels, *Atmos. Chem. Phys.*, 8, 983-995, <https://doi.org/10.5194/acp-8-983-2008>, 2008.

Thomason, L. W., Moore, J. R., Pitts, M. C., Zawodny, J. M. and Chiou, E. W., An evaluation of the SAGE III version 4 aerosol extinction coefficient and water vapor data products, *Atmos. Chem. Phys.*, 10, 2159-2173, <https://doi.org/10.5194/acp-10-2159-2010>, 2010.

20 **Thomason, L. W. and Vernier, J.-P.: Improved SAGE II cloud/aerosol categorization and observations of the Asian tropopause aerosol layer: 1989–2005, *Atmos. Chem. Phys.*, 13, 4605-4616, <https://doi.org/10.5194/acp-13-4605-2013>, 2013.**

Thomason, L. W., Ernest, N., Millan, L., Rieger, L., Bourassa, A., Vernier, J.-P., Manney, G., Luo, B., Arfeuille, F. and Peter, T., A global space-based stratospheric aerosol climatology: 1979-2016, *Earth Sys. Sci. Data*, 10, 469-492, <https://doi.org/10.5194/essd-10-469-2018>, 2018.

Trickl, T., Giehl, H., Jäger, H., and Vogelmann, H.: 35 yr of stratospheric aerosol measurements at Garmisch-Partenkirchen: from Fuego to Eyjafjallajökull, and beyond, *Atmos. Chem. Phys.*, 13, 5205–5225, <https://doi.org/10.5194/acp-13-5205-2013>, 2013.

30 Turco, R. P., Whitten, R. C., Toon, O. B., Pollack, J. B., and Hamill, P.: OCS, stratospheric aerosols and climate, *Nature*, 283, 283–285, <https://doi.org/10.1038/283283a0>, 1980.

- Winker, D. M., J. Pelon, J. A. Coakley, Jr., S. A. Ackerman, R. J. Charlson, P. R. Colarco, P. Flamant, Q. Fu, R. Hoff, C. Kittaka, T. L. Kubar, H. LeTreut, M. P. McCormick, G. Megie, L. Poole, K. Powell, C. Trepte, M. A. Vaughan, B. A. Wielicki: The CALIPSO Mission: A Global 3D View Of Aerosols And Clouds, *Bull. Am. Meteorol. Soc.*, 91, 1211–1229, <https://doi.org/10.1175/2010BAMS3009.1>, 2010.
- Winker, D. M., Liu, Z., Omar, A., Tackett, J. and Fairlie, D., CALIOP observations of the transport of ash from the Eyjafjallajökull volcano in April 2010, *J. Geophys. Res.*, 117, D00U15, <https://doi.org/10.1029/2011JD016499>, 2012.
- Winker, D. M., J. L. Tackett, B. J. Getzewich, Z. Liu, M. A. Vaughan, and R. R. Rogers, The global 3-D distribution of tropospheric aerosols as characterized by CALIOP, *Atmos. Chem. Phys.*, 13, 3345–3361, <https://doi.org/10.5194/acp-133345-2013>, 2013.
- Vaughan, M. A., Powell, K. A., Kuehn, R. E., Young, S. A., Winker, D. M., Hostetler, C. A., Hunt, W. H., Liu, Z., McGill, M. J., and Getzewich, B. J.: Fully automated detection of cloud and aerosol layers in the CALIPSO lidar measurements, *J. Atmos. Ocean. Tech.*, 26, 2034–2050, <https://doi.org/10.1175/2009JTECHA1228.1>, 2009.
- Vaughan, M. A., Pitts, M., Trepte, C., Winker, D., Detweiler, P., Garnier, A., Getzewich, B., Hunt, W., Lambeth, J., Lee, K.-P., Lucker, P., Murray, T., Rodier, S., Tremas, T., Bazureau, A., and Pelon, J., Cloud-Aerosol LIDAR Infrared Pathfinder Satellite Observations (CALIPSO) data management system data products catalog, Release 4.10, NASA Langley Research Center Document PC-SCI-503, Hampton, Va., USA, 2016.
- Vernier, J. P., Pommereau, J. P., Garnier, A., Pelon, J., Larsen, N., Nielsen, J., Christiansen, T., Cairo, F., Thomason, L. W., Leblanc, T., and McDermid, I. S.: Tropical stratospheric aerosol layer from CALIPSO lidar observations, *J. Geophys. Res.*, 114, D00H10, <https://doi.org/10.1029/2009JD011946>, 2009.
- Vernier, J. P., Thomason, L. W., Pommereau, J.-P., Bourassa, A., Pelon, J., Garnier, A., Hauchecorne, A., Blanot, L., Trepte, C., Degenstein, D. and Vargas, F., Major influence of tropical volcanic eruptions on the stratospheric aerosol layer during the last decade, *Geophys. Res. Lett.*, 38, L12807, <https://doi.org/10.1029/2011GL047563>, ~~2011~~2011a.
- Vernier, J.-P., Thomason, L. W. and Kar, J., CALIPSO detection of an Asian tropopause aerosol layer, *Geophysical Research Letters*, 38, L07804, <https://doi.org/10.1029/2010GL046614>, ~~2011~~2011b.

- Vernier, J. P., Fairlie, T. D., Murray, J. J., Tupper, A., Trepte, C., Winker, D., Pelon, J., Garnier, A., Jumelet, J., Pavolonis, M., Omar, A. H. and Powell, K.A., An advanced system to monitor the 3D structure of diffuse volcanic ash clouds, *J. Appl. Meteor. Climatol.*, **52**, 2125-2138, <https://doi.org/10.1175/JAMC-D-12-0279.1>, 2013.
- 5 Vernier, J.-P., Fairlie, T. D., Deshler, T., Natarajan, M., Knepp, T., Foster, K., Weinhold, F. G., Bedka, K. M., Thomason, L. and Trepte, C., In situ and space based observations of the Kelud volcanic plume: The persistence of ash in the lower stratosphere, *J. Geophys. Res.*, **121**, 11104-11118, <https://doi.org/doi:10.1002/2016JD025344>, 2016.
- 10 Young, S. A. and Vaughan, M. A.: The retrieval of profiles of particulate extinction from Cloud Aerosol Lidar Infrared Pathfinder Satellite Observations (CALIPSO) data: Algorithm description, *J. Atmos. Ocean. Tech.*, **26**, 1105–1119, <https://doi.org/10.1175/2008JTECHA1221.1>, 2009.
- 15 Young, S. A., Vaughan, M. A., Kuehn, R. E., and Winker, D. M.: The retrieval of profiles of particulate extinction from Cloud–Aerosol Lidar Infrared Pathfinder Satellite Observations (CALIPSO) data: Uncertainty and error sensitivity analyses. *J. Atmos. Ocean. Tech.*, **30**, 395–428, <https://doi.org/10.1175/JTECH-D-12-00046.1>, 2013.
- Young, S. A., Vaughan, M. A., Kuehn, R. E., and Winker, D. M.: Corrigendum, *J. Atmos. Ocean. Tech.*, **33**, 1795–1798, <https://doi.org/10.1175/JTECH-D-16-0081.1>, 2016.
- 20 Young, S. A., Vaughan, M. A., Garnier, A., Tackett, J. L., Lambeth, J. D., and Powell, K. A.: Extinction and optical depth retrievals for CALIPSO’s Version 4 data release, *Atmos. Meas. Tech.*, **11**, 5701-5727, <https://doi.org/10.5194/amt-11-5701-2018>, 2018.

Response to Referee #1

5 Hereafter Kar et al. will be shortened to K19. K19 introduce a level 3 stratospheric aerosol product based on CALIOP data. This initial version was developed since the production of the version 4 CALIOP level 1B and 2 data sets. K19 summarize the CALIOP product history and point out the major advance in
10 version 4 that enables a stratospheric L3 product that extends completely through the Junge layer (calibration based on measurements between 36-39 km). They describe how they employ previously documented CALIOP cloud and PSC masks to isolate aerosols, and an additional screen based on a depolarization ratio threshold for creating a separate background aerosol L3 data set and a background+plume data set. The manuscript is well composed and written. The L3 algorithm is logical and described adequately. K19 offer it as a first version and acknowledge some key areas that may justify refinements. This manuscript is appropriate for AMT. It represents a useful new contribution to the resources that atmospheric and climate scientists need for large-scale studies of the stratosphere. I would recommend publication after K19 satisfactorily address the following issues, one of which I classify as major. Next I characterize this concern, followed by some minor concerns. Finally a list of
15 technical items to address.

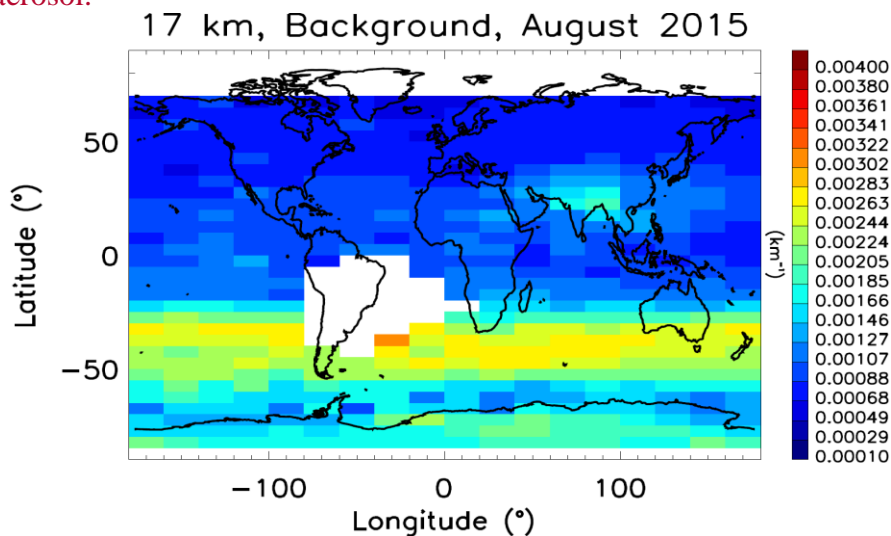
Thanks very much for a careful reading of the manuscript and for your useful suggestions.

20 *Major concern: It is apparent from several figures and K19's discussion of them that there may be a significant bias in the L3 products (both background and all-aerosol). My attention was drawn to the residual PSC signature in Figures 4, 8, 9. K19 acknowledge this residual and attribute the signature to "particles in the process of becoming PSC." The residual itself is a dominant feature in all the figure panels where PSC presence is expected. This undoubtedly reveals an incomplete masking of weak but meaningful scattering. In the high-latitude winter realm it is straightforward to dismiss these as tenuous cloud particles, but at lower latitudes and especially the lowermost stratosphere, any residual that may survive cloud screening cannot be simply classified as aerosol. Given that the L3 aerosol algorithm is globally based on the L2 merged layer data, any tenuous cloud (analogous to the acknowledged PSC residual) will be in the L3 dataset and considered aerosol. Just like PSCs, cirrus clouds in their formative and sublimation phase will naturally present a scene that will contain scatterers outside the layer-detection algorithm's thresholds. An ad hoc inspection of L1B quicklooks reveals this to be fairly common. Hence to the extent that a particular scene is subject to thin, patchy, formative or sublimating cirrus, the L3 background and "all aerosol" data sets are at risk for false-positive aerosol detections. This vulnerability reaches its greatest likelihood in regimes of high-frequency, high-altitude cloud. The most prevalent of these is the Asian summer monsoon region, one of the cloudiest on Earth for high cirrus. To the extent that the PSC analogy is accurate for non-polar high-cloud regimes, the L3 background and all-aerosol data may be cloud biased like the PSC signatures alluded to here. If this concern is well founded, it is essentially impossible to confidently argue that extinction enhancements such as those displayed in Figure 10 in the Asian monsoon sector are aerosols and not tenuous clouds. K19 are encouraged to consider the revelations they showed with respect to PSC residual and assess the applicability of that analogy to the potential for cloud contamination in the lowermost stratosphere, especially where/when cirrus cloud occurrence frequency is high. It might also be instructive to compare Figure 10 with an identical rendering based on the L3 background realization. Ideally the stratospheric background should have no imprint of clouds or aerosol perturbations. The amount of similarity between a background rendering of Figure 10 and the manuscript's rendering would be informative as to how well the L3 algorithm is performing in cirrus-cloudy areas.*
25
30
35
40
45

50 *This concern was also informed by Figure 3, which shows a layer-like peak in background scattering ratio at the same altitude as the all-aerosol data set in the Sarychev Peak-influenced stratosphere. It led me to wonder what the blue background plot would look like for the same period and geographic cell but for a year without a known volcanic plume. If there is a significant reduction in peak scattering and a monotonic decrease with altitude, it would be suggestive of extra-background aerosols getting into the background data set. Akin to the cloud-detection-threshold conundrum, stratospheric aerosol features absent a feature-detection, yet visible to the eye in quicklook images, are common. To the extent that this is true and quantifiable, L3 background aerosol abundance will be high biased, especially when there are large/widespread tenuous plumes. This may be manifested in Figure 4a, which shows hints of the Nabro plume in the same place as the stronger Nabro feature in the less-screened realizations.*
55

Your concern about cloud contamination is a perennial problem with all satellite instruments attempting to retrieve aerosol in the lower stratosphere below about 20 km. We tried our best to remove cloud contamination by using several different filters. As mentioned in the manuscript, the first filter removes the layers as detected by the CALIPSO layer detection module and then classified as “cloud”s by the Cloud-Aerosol-Discrimination (CAD) module. Clearly, the efficiency of removal of cloud layers in this dataset depends upon the efficiency of both these algorithms. In particular the CAD algorithm uses the optical properties of the layers, specifically the volume depolarization ratio and attenuated color ratio with both measurements becoming noisy at increasing altitudes above the local tropopause. The second filter removes the PSCs as identified by the separate PSC Mask product and again depends upon the robustness of the PSC product. Note that we have used v1.0 of the PSC product which has since been updated into V1.5 and we will use the latter in the future versions of the stratospheric aerosol product. For this version of the product and for the sake of uniformity, we decided to use the clouds (PSCs or otherwise) as detected by the available CALIPSO layer products. Note that in the polar regions, particularly over Antarctica, layers detected as “clouds” by the CAD algorithm and independently as PSCs have been removed. As has been clearly stated in the manuscript, scattering from particles below the threshold of detection for both the regular layers as well as the PSC layers will remain in the product. In particular, in winter over Antarctica, it may not be easy to define the point when the background aerosol transitions into a detectable PSC.

As you mentioned and as is well-known, it is very difficult to remove the tenuous cirrus clouds which occur within a few kilometers near the tropical tropopause. Our third filter attempts to do this using a threshold on either volume depolarization ratio or attenuated color ratio. We discuss these filters further below. However, we would like to point out that presence of aerosols within the Asian summer monsoon anticyclone between ~13-18 km (the so-called Asian Tropopause Aerosol Layer, ATAL), formed from gas phase precursors or primary aerosols related to deep convection has been confirmed from balloon and aircraft observations, although some ice clouds are likely present over this same area (Tobo et al., 2007, Vernier et al., 2011, 2015, 2018, Hopfner et al., 2019). Therefore most of this plume as e.g. seen in Fig 10 (Fig. 11 in revised version) is likely aerosol.



The figure above shows the spatial distribution of the “background” aerosol mode for July 2015 at 17 km. As can be seen, the Asian summer monsoon plume as well as the signature of the Calbuco volcano between 30°S and 50°S appear even in the background mode. As discussed above, any signal that is below the layer detection threshold and survives the different filters mentioned above will be included in our background product.

Regarding the depolarization ratio filter adopted by K19, Vernier et al. (2009) (“V09”) applied a 5% screen to profiles that are an average of 300-600 L1b profiles. The argumentation therein for 5% was based on an assessment of depol. ratio typical for L1B data. By definition the average depol. ratio in the gridded averaged data is going to be shifted low with respect to the L1B data. The probability distribution of depol. ratio in the V09 gridded data set is unreported and thus unknown, but it is likely to have a very small mean since it is composed of many clear-sky pixels as well as cloud fringes and weak-cloud pixels. It is unclear how a 5% depol. ratio in such an average distribution maps to 5% in L1B data. Consequently a depol. ratio threshold based on the gridded data may have to be much smaller than even 5%. Neither V09 nor K19 provide any testing in defense of the 5% threshold, hence any conclusions regarding aerosol abundance or cloud contamination in the L3 data set are subject to considerable uncertainty. An analogous argument applies to the color-ratio filtering described. K19 apply a color ratio screen based on gridded, averaged data but chose a threshold that is justified in relation to L1B data. Hence some amount of cloud contamination would be systemic in the L3 all-aerosol data set. K19 are encouraged to assess the veracity of my concern, and if it is valid, to take steps to quantify the biases resulting from inadequate screening.

As mentioned above and stated in the manuscript, the depolarization and the color ratio filters were primarily designed to remove the thin cirrus near the tropopause. This is a non-trivial issue if at the same time you are trying to capture the signals of volcanic ash in the stratosphere in the early part of the plume evolution which is important to characterize from the point of view of aviation safety. Firstly the aerosol/cloud discrimination depends upon the scattering ratio or the strength of the plume, and in particular there is generally a large overlap between aerosols and clouds at low scattering ratios. Clearly no single number can be optimal for all situations or at all scattering ratios. We used the cirrus filter at the gridded level to avoid the noise at the profile-by-profile basis. We used June 2011 for testing the filters because of the two representative cases, Nabro being mostly sulfate and Puyehue-Cordon Caulle (PCC) being mostly ash and we wanted to capture both of these stratospheric perturbations. In particular it was a good test case for capturing ash plumes from PCC, since the ash plumes were observed ~12 km, near the cruising altitudes of most airline flights. As explained in the text it was not possible to achieve this using only a depolarization filter to remove the cirrus clouds—indeed the volume depolarization ratio of optically thin cirrus clouds can be as low as 0.1, so even using a very low volume depolarization ratio it would not be possible to get rid of all cirrus. On the other hand, as shown in Figure 4 (Figure 3 in revised version), the attenuated color ratio filter with threshold at 0.5 at the gridded level (which may include both high and low scattering ratios), did capture the ash plumes of PCC also retaining the Nabro plumes at the same time. Lowering the threshold to, say 0.1 for the attenuated color ratio, signals from both the volcanoes essentially disappear and using a higher threshold (e.g. 0.8 which might be more appropriate for higher scattering ratios as also pointed out by referee#2) may retain much more clouds. However, for tenuous plumes, the adopted threshold of 0.5 is likely to retain some cirrus cloud at the tropics near the tropopause, which cannot be helped since we use the same threshold uniformly for all cases. We have now explained this in the text using a new Figure (Figure 4). As shown in that Figure, for such tenuous plumes, the aerosol extinction does not change significantly between the “all aerosol” and “background” modes, but the depolarization filter in the background mode removes the cirrus more efficiently. Thus it might be better to use the “background” mode for volcanically quiet years or for sulfate volcanoes, particularly after several weeks when the

plumes become tenuous. In any case, as seen in the climatology of thin cirrus (Sassen et al. 2008), this will primarily impact only the tropics and in the vicinity of the tropopause (up to ~17-18km). In particular, any bias seen in comparisons with other datasets above ~ 20 km will have nothing to do with this cirrus filter and there may be other sources for such a bias.

Minor concerns:

P2, L26-30. This survey of important solar occultation instruments for aerosol measurement is missing a callout for SAM II and POAM II, III. SAM II was especially central to stratospheric aerosol and cloud research. Please consider augmenting this survey.

We have revised the relevant paragraph in the revised version as:

“Most of our current knowledge of the global distribution of stratospheric aerosols comes from satellite measurements. The earliest such measurements were carried out by the Stratospheric Aerosol Measurement II (SAM II) on board the Nimbus 7 spacecraft which provided the vertical profiles of aerosol extinction at 1 μm and were followed by the Stratospheric Aerosol and Gas Experiment (SAGE) series of instruments (Chu and McCormick, 1979, Kent and McCormick, 1984, Mauldin et al., 1985; Chu et al., 1993; Damadeo et al., 2013). The basic principle employed in these instruments is solar occultation, wherein the vertical profile of stratospheric aerosols is retrieved from measurement of sunlight as the rays pass through the atmosphere during sunrise and sunset events as observed from the orbiting spacecraft. Stratospheric aerosols have been characterized using this technique from SAGE instruments on Earth Radiation Budget Satellite (ERBS) and Meteor-3M as well as from the International Space Station (ISS). Among other spaceborne instruments that use this technique are the Polar Ozone and Aerosol Measurement (POAM II, POAM III, Glaccum et al., 1996, Lucke et al., 1999) and Measurement of Aerosol Extinction in the Stratosphere and Troposphere Retrieved by Occultation (MAESTRO, McElroy et al., 2009). In addition, the Optical Spectrograph and InfraRed Imager System (OSIRIS) and the Ozone Mapping and Profiler Suite (OMPS) have used a limb scatter technique to obtain the aerosol extinction profiles (Bourassa et al., 2012, Chen et al., 2018).”

P5, L23: The L3 data set extends to 85 N and S. This is beyond CALIPSO’s orbit extrema of 82 N and S. Please explain the apparent extrapolation.

Since the data are binned in 5° in latitude, the first and the last bins imply available data averaged between 85° and 80° in both hemispheres.

P8, L07. Two questions regarding the tropopause boundary. Please report the tropopause data that are used. K19 say that tropospheric data are removed. How does that reconcile with Figure 6, which shows

an essentially continuous record of tropical aerosol data at 15-16 km? Isn't the tropical tropopause minimally variant and higher than 16 km? Perhaps there are enough tropical profiles where the tropopause is < 15 km. Some words of clarification are requested.

5 We have added the following:

“The tropopause heights were taken from the Modern-Era Retrospective analysis for Research and Applications 2 (MERRA-2) reanalyses as in all V4 products (Gelaro et al., 2017).”

10 Please note that Figure 6 has been revised (now Figure 7) and two new panels have been added showing the distribution at mid-high latitudes in both hemispheres. Also, the stratospheric retrievals for this first version were carried out up to one km below the local tropopause for use in UTLS studies which would explain the extinction data below 16 km. In any case the tropical distribution is now shown starting at 17 km.

15 *P11, L10. Regarding the discussion of the June 2011 situation. K19 might consider mentioning Grimsvotn (May 2011, just a bit earlier than June) given that these aerosols are apparently evident in Fig. 4 in the northern extratropics.*

20 Thanks for this information. We have added the following:

“Further, the high scattering ratios near 50°N are likely due to the Grimsvotn volcano, which erupted in May 2011.”

25 *P12, discussion of Figure 5. The relative differences are not evident to my eyes. It might be a good idea to show a third panel, A-B. Or perhaps use another color scale to make it more evident.*

Figure 5. These sample sizes are huge. Might K19 consider increasing the temporal granularity?

Per your suggestion, we have now added a third panel showing the difference in samples between the “all aerosol” and “background” modes.

30 We are not exactly sure what you mean by “temporal granularity”. Figure 6 (previously Figure 5) shows the number of samples accumulated at an altitude of 17 km in each horizontal grid cell for the month of July 2009. Since the level 3 stratospheric aerosol data product reports monthly averages aggregated on 5° latitude × 20° longitude spatial grid, the “temporal granularity” of the product is one month.

35 *P12, L22. “. . .particles which are in the process forming PSCs.” The same might be said of PSCs in sublimation/evaporation mode. Please consider a minor rewording taking this into account.*

40 We have deleted this sentence and revised the previous sentence as:

“Also note the high number of samples over parts of Antarctica, partly from oversampling due to orbital configuration and related to small particles below the detectability of PSCs by the PSC mask algorithm.”

P13, L22-30. Discussion of lidar ratio. I did not see any attention to the differences between the lidar ratio for smoke as compared to sulfate. Please augment the discussion in that regard.

We have added the following in the text:

5
“Note that the lidar ratios could also be significantly different for stratospheric perturbations resulting from smoke intrusion from pyroCb events (Peterson et al., 2018, Khaykin et al., 2018). For this first version of CALIPSO stratospheric aerosol product we have used only a single lidar ratio.”

10
Discussion of Figure 6. This is an unfair comparison between Kelud, a tropical volcano, and a set of extratropical volcanoes. Hence it doesn't seem to be of any value to compare the relative imprints of these plumes. Consider removing this discussion or providing a stronger argument.

15
We have deleted the relevant sentence. As already mentioned above, we have now added a couple of new panels (new Figure 7) showing the time altitude plots at mid/high latitudes in both hemispheres, per the second referee's suggestion. The discussion has been modified accordingly.

20
Figure 6. K19 label and point out some of the obvious features but not all. There seems to be no rationale for this, so please consider labeling the dramatic plumes in J07, J11 (between Sarychev Peak and Nabro), and J16.

25
We wanted to point out the outstanding features without cluttering the plot with too many labels. In any case, we have now added labels for the features you have mentioned.

30
P15, L09. Discussion of Black Saturday. K19 rightly acknowledge the pyrocumulonimbus source of this stratospheric plume. Dowdy et al., <https://doi.org/10.1002/2017JD026577>) provide a detailed characterization of the pyroconvection. Please consider citing this paper if K19 consider it important to do so.

35
Dowdy et al. mostly deal with lightnings associated with the Black Saturday event as well as fires ignited by the event and don't quite directly address the stratospheric aerosol plumes being discussed in Figure 6 (now Figure 7) and so we have not cited this paper.

P15, L09. “. . .reached altitudes of 16–20 km. . .” To my eye the plume reached ~22 km. Am I looking at this correctly? If so, please adjust the description accordingly.

40
That sentence referred to the findings from the cited works. We have added the following sentence: “The signature of this event can also be identified in Figure 7b, reaching up to nearly 22 km”.

P15, L10-11. “These pyrocumulonimbus events seem to be increasing in frequency. . .” If K19 have support for that statement please provide it. Perhaps there is a paper to cite?

45
We have deleted this sentence in the revised version.

50
Figure 7 and discussion thereof. Two points. 1. Please provide a tropopause line or marker. 2. This is a very interesting item to understand but it seems to be out of place with the rest of the paper. Perhaps can offer a strong motivation for including it. If not, consider removing it and making it part of future work.

P16, L13. “. . .telltale signature of smoke. . .” the differential 532 nm attenuation is as evident in sulfate plumes as smoke. If this discussion is to remain, it should be expanded to include sulfate.

Per your suggestion, we have now added the tropopause lines in all the four panels in this figure (now Figure 8). We believe it is a relevant figure in that it sets the stage for the height-latitude cross sections of scattering ratios we show in the following figure. We can designate the encircled plumes in Figure 9 as smoke only on the basis of the discussion of this figure.

The level 2 stratospheric aerosol classification algorithm classifies most of the layers as “smoke” or “ash”. As mentioned in the manuscript, some of the “ash” has been misclassified because of high depolarization. However we did not mention “sulfate” anywhere.

P18, discussion of Kelud. It should be acknowledged, thanks to CALIPSO, that the injection of Kelud went to 26+km. See Kristiansen et al. (doi:10.1002/2014GL062307). That paper also shows MLS SO2 to 31 mb, so some injected material was up in the mid 20s of km. This means that there may have been no lofting at all, just time-lagged conversion. If K19 agree with this assessment, please consider modifying the discussion accordingly.

Kristiansen et al. point out that most of the ash injection was around 17 km. Also from our Figure 9 (Figure 10 in revised version), the slow ascent of the plume can be clearly seen which is consistent with the upward branch of the Brewer-Dobson circulation. Friberg et al. (2018) also support this explanation. Therefore we have not modified the discussion as such.

P18, L01. “17 km” This is inconsistent with the Fig. First panel shows aerosol to 21 km. Am I looking at this correctly?

We have modified the sentence as follows:

“The gradual lofting of the plume, with its top rising from ~21 km over the tropics in March to ~24 km in the same general location several months later, shows the signature of stratospheric dynamics in the CALIPSO stratospheric aerosol product.”

Figure 13 and attendant analysis. A few questions and concerns. 1. It wasn't clear to me how K19 matched up the SAGE III data with CALIOP. It's not self evident how that would be done. Please clarify. 2. This figure and text comes in a section called “Discussion” but it is fundamentally a distinct analysis followed by discussion. It would be more logically set off in another titled section. 3. During this analysis timeframe there were background sulfates and fresher smokes from BC2017. The lidar ratios would not be a constant. How have K19 considered this situation?

This figure is the first attempt to obtain the stratospheric lidar ratio using backscatter measurements from CALIPSO and extinction data from SAGE III, using the limited amount of contemporaneous data available at this time. Hence we have done it only in a climatological sense. In other words, we have not used strictly coincident profiles from each instrument as such. We have added the following to clarify this:

“As for the comparisons presented in section 3, we have averaged the SAGE III data over each month and interpolated to the CALIPSO altitude grid and computed the lidar ratios, which were then averaged to obtain the climatological distribution shown in Figure 14.”

Even though it is a new result, it fits in better in the context of the discussion on the lidar ratios. So we have decided to let this be a part of the discussion itself.

Please note that we have now replotted this figure by not using data from the biomass burning months of August through November 2017 and also all data after March 2018 to avoid

contamination from the Ambae volcano. As can be seen in the revised figure, the results remain much the same despite loss of data.

Technical Matters:

5

In a few places Thomas Trickl's name is misspelled "Trickle."

P2, L14: "number" is a singular subject.

10

P5, L13: "The V4 data attenuated. . ." Delete "data."

P6, L21: ". . .the primary input files used for this product is. . ." Replace "is" with "are."

15

P9, L25: "The distribution. . .suggest.." Replace "suggest" with "suggests."

These points have been taken care of.

20

Figure 4 and other plots with latitude on x-axis: Please explain why the data in summer hemisphere don't extend as far poleward as in the winter hemisphere.

Added a sentence in the legend clarifying lack of data at high northern latitudes during nighttime in summer months.

25

P14, L13: "rising trend" This may suggest a nonlinear trend. Perhaps "positive trend" instead?

Done.

Figure 7. Show the tropopause.

30

Done.

Figure 8, bottom panels: What's causing the rainbow edge in the SH? Perhaps trim this off, or explain what is responsible for it.

35

Done.

P18, L1: ". . .lofting. . .plume from around 17 km. . ." The figure shows the plume starting out at _21 km, not 17 km. Please clarify.

40

We have revised the text as:

"The gradual lofting of the plume, with its top rising from ~21 km over the tropics in March to ~24 km in the same general location several months later, shows the signature of stratospheric dynamics in the CALIPSO stratospheric aerosol product."

45

P19, L19: Regarding SAGE III ISS providing data "since March 2017. . ." The SAGE results reported herein start in June 2017. Please clarify.

50

Although the ASDC archives state the temporal coverage for the SAGE III aerosol data start from March 2017, the available data actually begins in June 2017 after commissioning. We have modified the sentence as: "The aerosol extinction profiles are available from the solar occultation measurements in 9 channels from 384 nm to 1544 nm starting June 2017."

References:

- 5 Friberg, J., et al., Atmos. Chem. Phys., 18, 11149, <https://doi.org/10.5194/acp-18-11149-2018>, 2018.
- Hopfner, M., et al., Nature Geosc., <https://doi.org/10.1038/s41561-019-0385-8>, 2019.
- Tobo, Y et al., Atmos. Res., 84, 233-241, <https://doi.org/10.1016/j.atmosres.2006.08.003>, 2007.
- Vernier, J.-P. et al., Geophys. Res. Lett., 38, L07804, <https://doi.org/10.1029/2010GL046614>, 2011.
- 10 Vernier, J.-P., et al., J. Geophys. Res. Atmos., 120, 1608, doi:10.1002/2014JD022372, 2015.
- Vernier, J.-P., et al., Bull. Am. Meteorol. Soc. **99**, 955–973, <https://doi.org/10.1175/BAMS-D-17-0014.1>, 2018.

15

Response to Referee #2

20 **General comments**

25 *In this contribution, Kar et al. present the new level 3 stratospheric aerosol product for the CALIPSO mission. The details of the science algorithm used to construct the level 3 product are presented. In addition, a preliminary quantitative assessment of the product is made through an inter-comparison of the CALIPSO and SAGE-III (ISS) extinction coefficient retrievals. Some nice observations of volcanic and wildfire smoke aerosols are also described. The paper is well structured and well written and the assumptions used in the retrieval are clearly articulated. This contribution is important because the level 3 aerosol product could potentially be used in radiative forcing studies that consider the impacts of aerosol loading in the stratosphere. I recommend publication after addressing some minor revisions suggested below.*

30

Thanks very much for a careful reading of the manuscript and for your useful suggestions.

Specific comments

35 *When describing the time-series of stratospheric perturbations due to major volcanic eruptions and wildfires shown in Figure 6, I think it's important to stress in the text (and Abstract) that this analysis is representative of aerosols in the tropical (25_S-25_N) stratosphere. Kasatochi and Sarychev were high latitude eruptions and so most of their sulfates were confined to mid-high latitudes. In addition, Kelud and Nabro are located within tropical latitudes and so their signatures are exaggerated relative to Kasatochi and Sarychev in the figure. Figure 6 would be much more illuminating if panels representing mid-high latitude bands were added.*

40

Per your suggestion, we have revised this Figure (now Figure 7) with two new panels on mid-high southern (40°S-60°S) and northern latitudes (40°N-60°N). We have also revised the relevant sentence in the abstract as:

“Further, we show that the extinction profiles (retrieved using a constant lidar ratio of 50 sr) capture the major stratospheric perturbations in both hemispheres over the last decade resulting from volcanic eruptions, extreme smoke events, and signatures of stratospheric dynamics.”

The discussion on the high bias of the CALIPSO retrievals relative to the SAGE-III retrievals is very interesting. Figure 13 shows that this is largely due to the assumption of a constant lidar ratio set to 50 sr in the CALIPSO product. The authors point out that there were ‘probably no significant injections of ash from volcanoes’ during their analysis period (June 2017 - August 2018); however, there was a significant ($\sim 0.15\text{Tg SO}_2$) eruption of Ambae (15.389_S, 167.835_E) in Vanuatu in April 2018 (Global Volcanism Program, 2018). This event may have affected the analysis and should be noted in the discussion section. Another point that could be mentioned is the effect of averaging the data over 15 months. Wouldn’t this ‘smooth out’ the influence of volcanic/smoke aerosols on the derived lidar ratios shown in Figure 13?

Thank you for pointing this out. We have now replotted this figure (now Figure 14) by not using data from the biomass burning months of August through November 2017 and also all data after March 2018 to avoid contamination from the Ambae volcano. As can be seen in the revised figure, the results remain much the same despite loss of data.

Another factor that would impact the new aerosol product is the choice of the color ratio threshold. The authors use a color ratio threshold of 0.5 to remove clouds and retain volcanic ash clouds. However, several authors (Winker et al. 2012; Vernier et al. 2013; Prata et al., 2017) have shown that volcanic ash colour ratios can be as high as 0.80. Setting this threshold too low may therefore remove volcanic ash from the ‘all aerosol’ product. This point should be addressed when introducing the choice of their selected threshold.

We have discussed this issue in detail in response to the first referee’s comments. Essentially the problem stems from using one single hard number as threshold for all situations, which is what we have done for this first version of the stratospheric data product. Pueyhue Cordon Caulle (PCC) volcano had a large number of plumes with strong scattering. So using a larger threshold for the attenuated color ratio like 0.8 will capture more of those plumes. However, the larger particles with such high attenuated color ratios will sediment out relatively rapidly leaving more diffuse ash with low scattering ratios. As mentioned in the response to the first referee, at low scattering ratios there can be a significant overlap between the thin cirrus and aerosols. Using a attenuated color ratio threshold of 0.8 will thus include a larger contribution from the cirrus for the tenuous plumes for PCC. The problem will be exacerbated for other volcanoes with relatively tenuous plumes, since we use the same threshold for all cases. We found using the color ratio threshold of 0.5 does a reasonably good job of retaining the ash and sulfate plumes from PCC and Nabro volcanoes.

Specific comments about figures

In a lot of the figures the axes and colorbar labels are missing. Also some of the labels are not written clearly. For example, the authors use underscores and abbreviations. I think using proper label names with appropriate variable symbol definitions and units would make the figures clearer. Also latitude/longitude units should use the degree symbol (not the abbreviated ‘deg’). At the very least, the labelling should be consistent throughout the paper.

We have addressed these issues in the revised version.

P1L28-30: There is also large disagreement (>100%) between CALIPSO and SAGE-III at altitudes below 20 km (Figure 11b). This should be stated in the abstract.

We have added the following to the abstract:

“Similarly there are large differences ($\geq 100\%$) within 2 to 3 kilometers above the tropopause which might be due to cloud contamination issues.”

5 ***P3L26: I see two Kar et al. (2018)s in the references section. Please use 'a' and 'b' to differentiate between them.***

Done.

10 ***P4L10-11: 'The consequences of this change...' - I suggest adding the V3 zonally and vertically averaged attenuated scattering ratio (for the same time period) to Fig. 1. This would make the change from V3 to V4 very clear.***

Per your suggestion we have now revised Figure 1. We are now showing the median values, as they better represent the distribution of CALIPSO data.

15

P4L17: Change 'over this latitude' to 'over each latitude'.

Done.

P5L17: 'accurate to about 1%' - do you have a reference for this?

20 It is actually 1.6% and we have corrected this in the revised version. This is from Kar et al. (2018a) and we have added the reference here.

P5L28: Delete 'going'.

P6L8: Replace 'i.e.' with 'such as'.

Done.

25 ***P6L11: 'Vaughan et al. (2009)' - Is there a new reference for the V4 level two layer detection algorithm that you could add?***

The layer detection algorithm has not changed in version 4.

P6L14: Replace 'but' with 'however'.

30 ***P6L18: Change 'product' to 'level 3 stratospheric aerosol product'.***

P6L21: Change 'the primary input files used for this product' to 'the primary input file used for the present product'.

Done.

35 ***P7, Figure 2: For consistency, should use small 'b' in the 'Write results to Background component' box.***

Done.

P7L7: Please define the 'local tropopause'. E.g. is this taken from GMAO?

40 We have added the following:

“The tropopause heights were taken from the Modern-Era Retrospective analysis for Research and Applications 2 (MERRA-2) reanalyses as in all V4 products (Gelaro et al., 2017).”

P8L4: Change 'Antarctica' to 'Antarctic'. Change 'both the hemispheres' to 'both hemispheres'.

Done.

5

P9L24: Shouldn't this be 'Vernier et al. 2013'?

Actually it was first described in Vernier et al., 2009.

10

P9L25: The Puyehue ash did not reach 17 km. Maximum heights observed by CALIOP were _13 km (Vernier et al., 2013; Prata et al., 2017).

This sentence has been deleted in the revised version and the text has been restructured.

15

P9L26: Threshold of 0.5 seems too low. Vernier et al. (2013) use a threshold of 0.8 to discriminate between clouds and volcanic ash. I think the impact of this threshold should be mentioned (see specific comments above).

We have already responded to this above.

20

P10L11: Change 'threshold' to 'threshold of the level 2 layer detection algorithm'.

Done.

25

P11, Figure 4: Can you comment on what's causing the high scattering ratios just above 10 km at _50_N?

The first referee has pointed out that this could be due to the Grímsvötn volcano and we have added the following:

30

“Further, the high scattering ratios near 50°N are likely due to the Grímsvötn volcano, which erupted in May 2011.”

35

P12L3: What does this look like for a threshold of 0.75-0.80? You may get more of a signal for the Puyehue event.

As we mentioned above, taking a higher threshold also increases the cirrus contamination.

40

P12L4: Change 'Nabro' to 'Nabro (near 30_N)'.

Done.

45

P12, Figure 5: I think the labels are wrong here i.e. Figure 5b looks like 'background' and Figure 5a looks like 'all aerosol'.

P12L19-21: I don't see a high number of samples over North America in Figure 5b (see above Figure 5 comment).

50

Actually, the labels are correct, as can be verified from the attached color scale. In order to make it more clear and per the first referee's suggestion, we have now added an additional plot showing the difference in sample numbers between the two modes. We are now showing the sample number distribution at 17 km, showing enhanced sampling over the Asian summer monsoon plume area.

P13L27: Change 'significant ash' to 'significant ash and sulfate'.

Done.

P14L22: Change 'image' to 'figure'.

P14L23: Change '(Kasatochi, Nabro etc.) to '(e.g. Kasatochi and Nabro)'.

The text has been revised here in view of two new panels and these words do not appear in the new text.

P15L10: 'quite clearly seen' - I'm not sure it is that clear. There are several other features in the figure that are more apparent than the Black Saturday bushfires, which aren't commented on. I suggest changing to 'can be identified'.

Done.

P15, Figure 6: I think you could add panels representing middle and high latitude bands to better represent the major stratospheric perturbations on a global scale (see specific comments above). Also, there's a significant feature around December 2010 that's not mentioned. This was probably due to the Merapi (7.54_S, 110.446_E) eruption in Indonesia in November 2010. Surono et al. (2012) estimate 0.44 Tg of SO2 in the upper troposphere and the plume reached heights of 16-17 km. Another feature that's not explained is the one around July 2015. It seems quite significant. Do you know what's causing it?

Per your suggestion we have now added two new plots (now Figure 7) showing the stratospheric features at mid/high latitudes (40°S-60°S and 40°N-60°N). Originally we were only trying to point out the most prominent cases without cluttering it too much with labels. However we have now pointed out Merapi as well as some other features in the plot. The feature near July 2015 is the signature of Calbuco volcano (also shown now in Figure 7). The Calbuco signature at these latitudes could be seen for several months afterwards.

P16, Figure 7d: Please fix the cropping at the bottom of the figure - some text has been cropped.

Done.

P16L15-16: 'irregular shapes' - could this also be due to ice particles?

While the differential attenuation strongly suggests these are mostly smoke particles, there is always the possibility of ice formation from the pyroconvection event. This sentence has been modified as:

“The high volume depolarization ratio (≥ 0.1) seen in Figure 7b is somewhat unusual for smoke and suggests the presence of irregular soot particles and mineral dust and possibly some ice particles, with fast adiabatic lifting possibly retaining the initial irregular shapes (Haarig et al., 2018, Khaykin et al., 2018).”

P17L6: 'smoke spreads globally' - I don't see this in the figure. It looks like the smoke spreads throughout the Northern Hemisphere but the Southern Hemisphere scattering ratio remains unchanged.

What we meant was that the plume spread at all longitudes and at lower latitudes---in any case “globally” has now been deleted and the new text reads as:

“After the original injection of smoke in August 2017 at mid-latitudes, the smoke spreads to lower latitudes as can be seen in these monthly mean spatial distributions from the level 3 stratospheric aerosol product.”

P17, Figure 8: What is the cause of the high scattering ratio from 25-30 km over the equator?

The high scattering ratios at 25-30 km (now in Figure 9) reflect the tropical stratospheric reservoir. We have added the following:

“As in Figure 4, the feature with high attenuated scattering ratio near 25-30 km seen in all the four panels is the signature of the tropical reservoir of stratospheric aerosols, maintained by a complex interplay of transport from the troposphere and stratospheric dynamics as well as microphysical processes including the Brewer-Dobson circulation, the QBO, evaporation and sedimentation (Trepte and Hitchman, 1992, Kremser et al., 2016).”

P17L17: Kelud erupted in February 2014 not April 2014 (see Kristiansen et al., 2015).

Thank you—we have corrected this in the text.

P18L1: ‘The gradual lofting of the plume from around 17 km over the tropics to nearly 24 km over several months...’. This seems to imply a rise of 7 km, which I think is misleading. Measuring from the top of the aerosol feature it looks like it rises from 21 to 24 km from March-December 2014 (a rise of 3 km). Please clarify this in the text.

We have now revised the sentence as:

“The gradual lofting of the plume, with its top rising from ~21 km over the tropics in March to ~24 km in the same general location several months later, shows the signature of stratospheric dynamics in the CALIPSO stratospheric aerosol product.”

P19L7-9: The Calbuco volcanic cloud actually went almost directly through the SAA (see <http://nicarnicaaviation.com/calbuco-eruption-april-2015>). Eventually it spread through the Southern Hemisphere but due to the rejection of data in the SAA region a large proportion of the Calbuco signal may not be captured in the CALIPSO level 3 stratospheric aerosol product. I think this is worth mentioning here.

We have revised the text as follows:

“The initial plumes would be missed out in the level 3 stratospheric aerosol product because data over the SAA region were not included. However the plumes quickly spread around the southern hemisphere in a belt between 60°S to 30°S (Lopes et al., 2019) and can be seen in the level 3 stratospheric aerosol product from May 2015 onwards for several months.”

P20L18: Change ‘essentially same’ to ‘essentially the same’.

Done.

P20, Equation (4): I got slightly confused here with the notation. What’s the difference between $\alpha_p(r)$ (defined at P13L24) and $\sigma(z)_{\text{CALIPSO}}$? And which variable is the one that corresponds to the ‘all aerosol’ profile product?

Thanks for pointing out this oversight—we have replaced α by σ , which would make it consistent everywhere. The same variable will represent the extinction coefficient in both the components and for comparisons with SAGE III we have used only the “all aerosol” component, since the latter includes extinctions from all sources.

P22, Figure 11 caption: 'the mean 532 nm extinction coefficient' is this what $\sigma(z)_{\text{CALIPSO}}$ is? In Eq. (4) the definition is the 'extinction coefficient at altitude z'. I would use the same wording to avoid confusion or put the symbols ($\sigma(z)_{\text{CALIPSO}}$ and $\sigma(z)_{\text{SAGE}}$) in parentheses in the figure caption.

The extinction coefficient as a function of altitude is $\sigma(z)$ with subscripts either CALIPSO or SAGE. The curves in Figure 11 (now Figure 12) represent the mean taken over all the profiles of $\sigma(z)$ using all the data as mentioned in the legend. We think it is generally clear.

P22L18: 'the presence of clouds which may impact the retrievals' - Please provide a little more information on how clouds impact the retrieval. If some clouds weren't removed, wouldn't this bias SAGE-III aerosol extinction high? Thus compensating for the difference seen in the comparison with CALIPSO below 20 km?

In the revised version, we have discussed the possible impacts of cloud clearance issues in our product in section 2.2.1 and added a new figure (Figure 4). Further we have added the following “As pointed out in section 2.2.1, the filtering scheme that removes thin cirrus clouds in the all aerosol mode is not as efficient as the technique employed in the background mode. Consequently, scattering artifacts from undetected subvisible cirrus are more likely to appear in the all aerosol mode in the tropical lower stratosphere within a few kilometers above the tropopause. Using the extinction profiles from the background mode reduces the differences at these altitudes but does not completely eliminate them (not shown).”

P22L23: Change '2.0' to '2'.

Done.

P22L24: On my first read through, I immediately thought the assumption of constant lidar ratio was the issue. You go on to discuss this but it's not mentioned here. Perhaps it's worth adding a sentence and referencing the discussion that comes later.

We have added the following:

“We further discuss the possible issues resulting from uncertainties in lidar ratios below.”

P23L15: Change 'Discussion:' to 'Discussion'.

Done.

P24L3-5: Change 'tropical latitudes' to 'tropical latitudes (30_S–30_N)'.

Done.

P24L5: Change 'higher latitudes' to 'higher latitudes and lower altitudes'.

Done.

P24L10: 'smoke, marine aerosols etc' - please list all the aerosol types considered by references cited.

All the different types of aerosols in the troposphere are really not relevant in the stratosphere, so we have simply deleted “such as smoke, marine aerosols etc.”

5 ***P24, Eq. (5): In Eq. (3), the two-way particulate transmittance is range-dependent. I assume it would be range-dependent ($T_{2p}(r)$) here too?***

Thank you and this has been corrected.

10 ***P25L16: 'substantially lower' - Could you put a number to this? E.g. what's the mean lidar ratio in the lowermost stratosphere? I think it is important to give a number or range given the discussion that follows.***

We have added “ ≤ 40 sr” to incorporate both the lowermost stratosphere as well as the high latitudes.

15 ***P27L3: 'no significant injections of ash from volcanoes' - this is probably true, but there were significant injections of SO₂ and therefore sulfate. For example, Ambae (Vanuatu) in April 2018 underwent a significant SO₂-rich eruption (see specific comments above).***

20 We have now revised Figure 13 (now Figure 14) by removing possibly contaminated data from the pyroCb event of 2017 and all data after March 2018 to avoid effects from Ambae volcano.

P27L12: Change 'volcanic eruptions' to 'volcanic eruptions and wildfires'.

25 Done.

P27L16: Change 'mid-to-high latitudes' to 'mid-to-high latitudes (30_S–60_S and 30_N–60_N)'

30 Done.

P27L16: Change 'high altitudes' to 'high altitudes (10–20 km)'

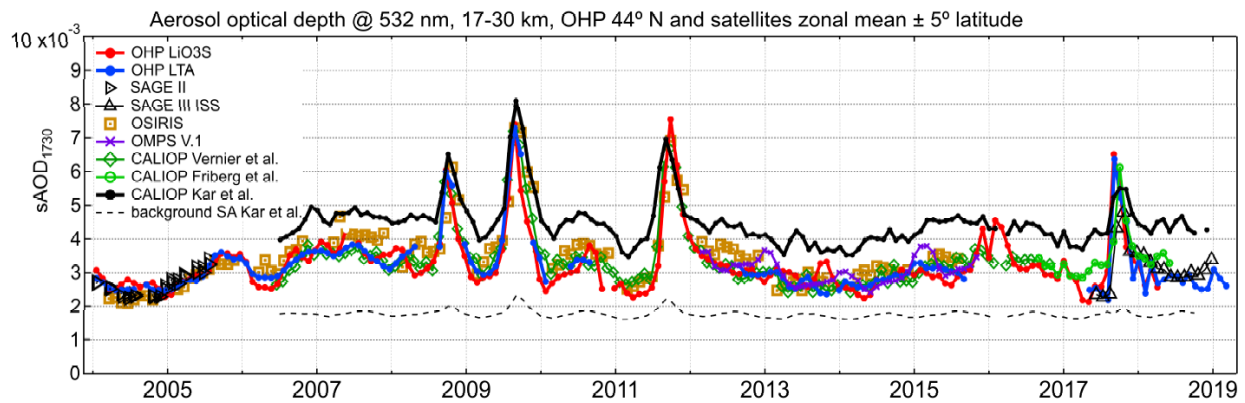
35 Done.

Response to Referee#3

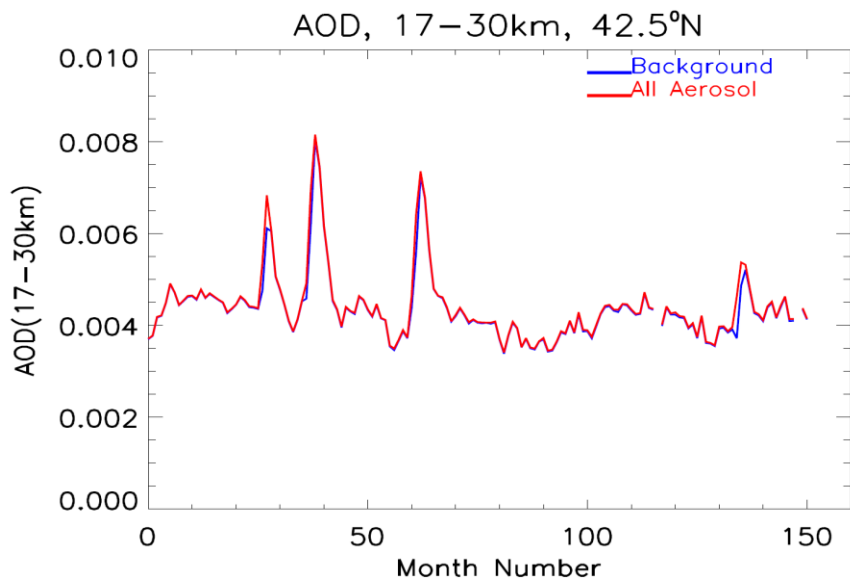
The article by Jayanta Kar and coauthors presents the new stratospheric aerosol (SA) product based on CALIOP measurements, describes the data handling procedure and provides an initial assessment of the data quality through intercomparison with ISS SAGE III measurements of aerosol extinction. With nearly 12 years of continuous operation, CALIOP measurement record represents a valuable source of near-global information on the stratospheric aerosol variability at seasonal to decadal time scales. An obvious advantage of CALIOP measurements is their higher vertical resolution compared to other space-based aerosol sensors (e.g. SAGE, OSIRIS, OMPS etc.) exploiting passive remote sensing techniques. This is why an official release of CALIOP SA data product has been long awaited by stratospheric community and thus the article represents a valuable contribution. The manuscript is well organized and easy to follow, the data retrieval is comprehensively described and the procedure of cloud screening together with the choice of assumption are well discussed. A novel and valuable result is the latitude-height distribution of extinction to backscatter (lidar) ratio inferred by coupling zonally-averaged CALIOP and SAGE III observations.

Thanks very much for a careful reading of the manuscript and for your useful suggestions.

That said, I have a major concern on the data product as such. The very day I found out about the release of L3 CALIOP stratospheric aerosol product, I incorporated the data into the intercomparison of stratospheric AOD series at NH midlatitudes from various satellites and Haute Provence (OHP) lidars in a way we did it in (Khaykin et al., ACP, 2017). The result came quite surprising to me as the new L3 series were remarkably high-biased with respect to all other data sets, including CALIOP SA data product by Vernier et al. I actually thought that I somehow mistreat these data. However, having read this article I realized that this bias is real and amounts to 30-40% at 45 N (Fig. 12), which is consistent with my estimates. A figure below shows time series of AOD of the 17-30 km layer within a 5 deg. latitude belt centered at 44 N as obtained from OHP lidars and various satellite sensors. It includes the CALIOP SA data product by Vernier et al. as well as a more recent one by Friberg et al., (ACP, 2018). While all the data series - independently of the measurement technique (lidar, solar occultation, limb scattering), data handling and the principal measurand (backscatter or extinction) - are in a good agreement, the new L3 CALIOP series stands out high-biased. With that, the background AOD appears low-biased with respect to the well identified clean periods, e.g. 2013-2014.



We would like to point out two things regarding the intercomparisons plot of AOD you provided. First is the reasonably close match between the CALIPSO L3 product "all aerosol mode" with others for the strong volcanic perturbations. Secondly there is some error in the "background" AOD curve you have plotted. The "background" extinctions do not differ that much from the "all aerosol" mode for quiet conditions. In particular there would be essentially no difference between the two modes above 25 km, since aerosol "layers" hardly ever occur above this altitude and there are no thin cirrus above 25 km. The figure below shows the AODs calculated between 17-30 km from the two modes for the grid cell at 42.5°N:



General remarks.

The article reports the observed bias with respect to SAGE III in an honest and comprehensive way, however the discussion of its possible reasons is not satisfying. Basically, it appeals to inaccurate knowledge of the lidar ratio, cloud screening issues and potential errors in the early version of SAGE III extinction product. However, this can in no way explain the discrepancy with other versions of CALIOP SA products by Vernier et al and Friberg et al., nor with OHP lidar operating at the same wavelength. Obviously, there are other reasons for the positive bias beside the error in lidar ratio or that of SAGE III extinction product. These reasons are neither identified nor hypothesized upon, leaving one wonder about the credibility of the L3 SA product as a whole and strongly limiting its scientific value, particularly for radiative forcing studies. Another missing item is the discussion on the quality of the "background aerosol" product. I suggest that the authors attempt to investigate the possible reasons for the latitude and altitude dependent bias and try to eliminate it if possible or at least sketch the envisaged changes/improvements in the future version of CALIOP L3 SA product, other than refinement of lidar ratios. In order to isolate the lidar ratio issue, the validation of the L3 data product could be done on integrated backscatter available from NDACC ground-based lidars at various latitudes.

As described in the text, we rigorously solve the lidar equation from 36 km downwards to 1 km below the tropopause using the same extinction retrieval module as for the standard CALIPSO tropospheric retrieval. In contrast, the Vernier et al. product does not solve the lidar equation, but instead compute the extinction by multiplying the gridded attenuated backscatter by a lidar ratio

of 50 sr. As a result, they do not correct the attenuated backscatter for the particulate attenuation at the successive range bins. This may not make significant difference in the retrieved extinction above 20 km under low aerosol loading. However the attenuation can quickly build up below 20 km and under high aerosol loading leading to a significant low bias in the Vernier et al. extinction profiles. Friberg et al. (2018) recognized this and pointed out the large underestimation in AOD that can result from this effect, particularly in the lowermost stratosphere. Friberg et al.(2018) did apply an approximate particulate attenuation correction to their product, nonetheless, even they did not rigorously solve the lidar equation.

In the manuscript, we have pointed out the high bias in our extinction values in mid-high latitude. Some of this can come from cloud clearance issues, either from the inadequacies of our CAD algorithm or from difficulties in complete removal of thin cirrus clouds, the latter mostly affecting a few kilometers above the tropopause in the tropics. We have now added a new figure (Figure 4) and discussed possible cloud contamination issues in both the modes. However, what needs to be appreciated is the retrieval of extremely low values of extinction ($\sim 10^{-4} - 10^{-5} \text{ km}^{-1}$) that is being attempted using the CALIOP backscatter measurements with significantly lower SNR than in the troposphere. We believe we have discussed the possible issues impacting the differences with SAGE III to the best of our knowledge at this time. However, we do believe that the more significant contributor to this bias at mid-high latitudes is the lidar ratio, as also becomes quite clear from Figure 13 (now Figure 14) in the manuscript. In any case we shall continue to investigate the reasons for these biases further using stratospheric extinction retrievals from other satellites and NDACC ground based lidars at various locations (as you have suggested). However that is beyond the scope of this manuscript; here we are primarily describing the algorithm involved in retrieving the extinction profiles.

Specific remarks

Figure 4. A strong signal above southern high latitudes is certainly due to PSC and I believe these are type 1b PSC (supercooled ternary solution, STS), which are non depolarizing and thus may be aliased as stratospheric aerosol. The interpretation in p.12 l.5-7 (signature of particles in the process of becoming PSCs) is thus incorrect. I wonder, why the PSCs could not be screened out using temperature threshold for PSC formation, which are relatively well known.

As mentioned in the text, we have used the level 1 CALIOP data for this product while using the level 2 products to filter out the cloud layers. Globally we have used the level 2 clouds as detected by our CAD algorithm and for consistency we decided to use the level 2 CALIPSO PSC mask product to remove the PSCs. Clearly the backscatter is from residual material below the detection limit of the PSC algorithm and likely to be the background aerosol particles which are transitioning into full blown detectable PSC layers. There is only a fine line between background stratospheric aerosol and when it starts growing by HNO_3 uptake and thus may be considered a PSC particle. We have modified the sentence in line 5, page 12 as:

“Since all PSC layers detected by the dedicated PSC detection algorithm were removed, what remains are the signatures of only those particles below the detectability threshold of the PSC mask data product.”

Also, using the temperatures from MERRA-2 at these high latitudes as a threshold for detecting PSCs may have its own caveats. For this first version of the product, we have not taken that approach.

5 **Figure 8 and 9, both showing latitude-height sections. Is there a particular reason why the former reports the attenuated scattering ratio, whereas the latter reports extinction coefficient? It would be easier to compare them had they presented the same units.**

10 The attenuated scattering ratio and the retrieved extinction coefficient are both part of the product and we wanted to show examples from both the variables.

Figure 9. What causes the strong signal around the tropopause at midlatitudes? If this is cloud contamination, this should be carefully discussed.

15 We have added the following:

“Note the high extinction values near 50°N-60°N in the lower stratosphere (~10-15km). These are similar to the summer rise in extinctions at these latitudes as discussed earlier (Figure 7) and are possibly due to biomass burning effects but could also be related to possible cloud clearance issues. As also mentioned above, the high extinctions at high southern latitudes could be related to scattering from particles below the PSC detection threshold as well as to transported volcanic material from Kelud.”

20

Response to Referee#4

25 **The paper “CALIPSO Level 3 Stratospheric Aerosol Product: Version 1.00 Algorithm Description and Initial Assessment” presents and discusses the new science algorithm and data handling techniques that are developed to generate the CALIPSO version 1.00 level 3 stratospheric aerosol profile product. The study falls within the scope of AMT. The authors have done a thorough job, the manuscript is well-written/structured, the presentation clear, the language fluent, the quality of the figures high. The result support the conclusions.**

30

35 Thanks very much for carefully reading the manuscript and for your useful suggestions.

Two major deficiencies are the implementation of a constant stratospheric aerosol lidar ratio (50 sr), regardless of an aerosol type classification, and the evaluation of the stratospheric aerosol product against SAGEIII extinction coefficient observations, a product which has not been validated (including issues of SAGEIII such as cloud contamination propagating in the comparison). However the stratospheric aerosol product and all the issues are properly and extensively discussed in the manuscript, thus I recommend publication in AMT, under minor revisions before it can proceed to be published.

40

45 For this first version of the product we have used a constant lidar ratio of 50 sr globally. In future versions we hope to incorporate a more informed lidar ratio distribution. As shown in Figure 14, by making use of the extinction retrievals from SAGE III and backscatter measurements from

CALIPSO, an initial estimate of the stratospheric aerosol lidar comes out to be $\sim 46 \pm 6$ sr, quite close to the value we have adopted. Although not validated yet, the SAGE III extinction retrievals are still the gold standard for stratospheric aerosol data and so we have used them in our initial comparisons.

Minor comments:

1) P1L17-18: “gridded level 3 product is based on version 4.2 of the CALIOP level 1 and level 2 data products”. According to this sentence CALIOP level 1 V4.2 is used. It is not clear whether the authors refer to Level 1B or Level 1.5 Profile Data. In the case of L1B, please provide a web link to the used data repository.

Added 1B in P1 and given the link to the data repository in section 2.1.

2) P1L27: “where the average difference between zonal mean extinction profiles is typically less than 25% between 20km and 30km”. Please rephrase to provide also whether the sentence refers to overestimation or underestimation compared to SAGEIII.

We have added “(CALIPSO biased high)” within brackets.

3) P3L29-30: “This is a level 3 monthly averaged product gridded in latitude (5o), longitude (20o) and altitude (900m)”. Although the justification of the 900m vertical resolution is sufficient, the authors should provide explanation on the reasons why the spatial resolution of 5ox20o deg2 grids was selected. How much the selected spatial (horizontal), vertical and temporal resolution affect the final dataset (in terms of backscatter and extinction coefficient profiles at 532nm)?

We have added the following in the text:

“Given the low SNR in the stratospheric backscatter measurements, it is necessary to average the data substantially, both spatially and temporally. Averaging the backscatter data over 5° in latitude increases the SNR by a factor of 40 (compared to single shot profiles) and provides a reasonable depiction of stratospheric aerosol distribution. This is also consistent with the early results of Thomason et al. (2007), who used the early CALIPSO measurements together with data from the CALIPSO simulator (Powell, 2005) to show that averaging the data over 5° in latitude and about 1 km in the vertical resulted in fairly representative stratospheric distribution. Further, spatial distributions of stratospheric species tend to be zonally symmetric (e.g. Kremser et al., 2016). In order to capture the signature of any possible longitudinal variation, e.g., the Asian Tropopause Aerosol Layer (ATAL) which occurs over Asia every summer during the monsoon months, we have used a longitudinal grid of 20° .”

It is important to remember that we are trying to retrieve very low extinction coefficients ($\sim 10^{-4}$ - 10^{-5} km^{-1}) in the stratosphere using the backscatter measurements with low SNR at those altitudes. This cannot be achieved without a significant amount of averaging of the data spatially and temporally. It may be mentioned that the currently available Global Space-based Stratospheric Aerosol Climatology (GLOSSAC) product that uses CALIPSO data as well as OSIRIS data is zonally invariant and binned in 5 degree in latitude and produced on monthly basis, consistent with the needs of the climate modelling community.

We believe the justification for the adopted grid lies in capturing the various stratospheric perturbations in the retrieved products, to the extent possible. As shown in the manuscript, seasonal

and regional perturbations like the Asian Tropopause Aerosol Layer (ATAL) as well as the pyroCb events and volcanic signatures are well captured in the product, vindicating the spatial and temporal resolution adopted for the product.

5 **4) P5L26: “Note that the range of altitudes to be covered in the stratosphere at various latitudes is from 8.2 km to 36 km, the latter being the lower limit of the calibration region”. Please mention the applied methodology of decoupling stratospheric and tropospheric layers, since the altitude of 8.2 km frequently lies below Tropopause? Does it rely on MERRA-2 by GMAO?**

10 We have added the following:

“The altitude resolution of the CALIOP level 1 profiles varies with altitude from 60 m between 8.3 km and 20.2 km to 180 m between 20.2 km and 30.1 km and finally to 300 m between 30.1 km and 40.0 km. In order to achieve a uniform altitude resolution, the vertical grid resolution was set to 900 m. Note that the tropopause can occur below 8.3 km at high latitudes, but the vertical resolution of level 1 profiles changes again below this altitude and the lower limit was kept at 8.3 km as a trade-off between computational complexity and the stratospheric information content, while the upper limit was set at 36 km, which is the lower limit of the calibration region. The tropopause heights were taken from the Modern-Era Retrospective analysis for Research and Applications 2 (MERRA-2) reanalyses as in all V4 products (Gelaro et al., 2017).”

25 **5) P8L8-9: “Further, all L1B profiles within the South Atlantic Anomaly (SAA) region are also removed”: Why do the authors remove CALIOP observations over the SAA region. Based on Kar et al., 2017 (CALIPSO lidar calibration at 532nm: version 4 nighttime algorithm), the new nighttime CALIOP calibration technique compensates for the higher NSR values, resulting in reliable calibration coefficients even over the SAA region. The authors it is suggested to include the justification in the manuscript.**

30 While the version 4 calibrations were done over SAA region also, the stratospheric profiles over this area may still be noisy. Therefore, for this first version of the product, we decided to remove all data over the SAA region. In fact this issue has been discussed in detail in the second paragraph on this page.

35 **6) P8L25: “. . . leading to generally lower CAD scores (Liu et al., 252019).”. Since CAD ranges between -100 and 100, it is not clear whether the authors refer to more aerosol reliable retrievals (CAD -> -100) or to absolute values of CAD score, therefore, CAD values closer to zero.**

We have revised the text as “generally lower absolute values of CAD scores”.

40 **7) P9L4-7: Although the authors provide the Vaughan et al., 2009 reference, some information on the noise filter should also be included in the manuscript, even if briefly.**

We have modified the text adding some information on the noise filters as:

45 “Essentially a range dependent threshold array of attenuated scattering ratios is constructed, which incorporates noise from two types of sources. The first category is the range invariant noise and

includes detector dark noise and noise from the solar background light. The second category is the range dependent noise from single shot measurements and is calculated from the molecular models. Using this range dependent threshold, outliers are removed (for details see Vaughan et al., 2009, section 2c). After removing the outliers, the 5 km profile is assigned to the appropriate spatial grid.”

8) Figure 4: Based on the manuscript, Figure 4b and 4c refer to the aerosol mode, however it is not clear neither in the caption nor in the manuscript whether they refer to the background or the aerosol mode. In addition, high stratospheric values are observed at 0o latitude, between 25 and 30 km height. Where do the authors attribute the observed values?

Figure 4 (now Figure 3 in the revised version) is showing the effects of the various filters. Figure 3a is the standard background mode where a depolarization filter is employed after removing all layers or features. Figure 3b is not really part of the product but is only meant to show the result, if we had employed a depolarization filter after retaining the aerosol layers in the stratosphere—clearly the Cordon plume is being missed here. Figure 3c is the standard “all aerosol” mode” where a color ratio filter is used after retaining the aerosol layers and shows that this filter captures both the volcanoes. We have modified the caption as:

“Zonally averaged height-latitude cross sections of attenuated scattering ratio for June 2011: a) after removing all detected layers and using a volume depolarization ratio filter (i.e., background aerosol only); b) including aerosol layers in the stratosphere detected by the level 2 algorithms with a 5% volume depolarization ratio filter applied; and c) including the level 2 aerosol layers but using an attenuated color ratio filter instead of the volume depolarization ratio filter. The white area in the northern high latitudes in summer indicates lack of nighttime data.”

As regards the high values over the tropics we have added the following sentence:

“Note that the enhanced scattering ratios near 25-30 km represent the tropical reservoir of stratospheric aerosols (Trepte and Hitchman, 1992, Kremser et al., 2016).”

9) P12L5: “Note the high scattering ratio values in the Antarctic latitudes between 15 km and 25 km”. The authors are kindly requested to provide a reference for this statement.

No reference is available for this statement---essentially this is what we are pointing out from CALIOP measurements.

10) P12L17-18: “The white grid cells over southeast Asia occur because the tropopause is higher than 16 km in this region”. The authors are kindly requested to provide a reference for this statement, including the typical tropopause height over this region.

Note that this Figure has now been revised and we are now showing the sample number distribution at 17 km, where no data drop out can be seen from tropopause-related issues.

11) P12L21-22: “This is again likely due to small particles which are in the process forming PSCs”. The authors are kindly requested to provide a reference for this statement.

This particular sentence has now been deleted and the sentence preceding this has been modified as:

“Also note the high number of samples over parts of Antarctica, partly due to oversampling from orbital configuration and related to small particles below the detectability of PSCs by the PSC mask algorithm.”

5

12) P13L13: “For the CALIPSO stratospheric aerosol product, the particulate multiple scattering factor is taken as 1 for all species of stratospheric aerosols”. The authors are kindly requested to provide a reference for this statement. Which is quantitative the effect of this assumption on the discussed stratospheric aerosol product?

10

We expect the single scattering assumption to hold in the stratosphere most of the time, except may be for the early part of the plume injection. This is also consistent with the retrievals in the version 4 level 2 aerosol retrievals

15

We have revised the relevant text as:

“For the CALIPSO stratospheric aerosol product, the particulate multiple scattering factor is taken as 1 for all species of stratospheric aerosols, consistent with the approach taken in the CALIPSO level 2 aerosol retrievals (Young et al., 2013; Young et al., 2016; Young et al., 2018).”

20

A quantitative discussion of this is examined in the comprehensive error analysis detailed in Young et al., (2013).

13) P13 - Stratospheric Aerosol Lidar Ratio of 50 sr is used. Although the authors explain in detail the selection of the specific lidar ratio value and evaluate against SAGEIII observations, it is expected that the uniform value used globally, regardless of the aerosol type, introduces large uncertainties. Which is the effect of this assumption to the stratospheric aerosol product? The authors mention that appropriate LR values for different aerosol subtypes will be introduced in future versions of the stratospheric product, however the assumption of constant LR value highly affects the reliability of the extinction coefficient profiles and should be mentioned in the abstract.

25

30

We believe we have adequately discussed the lidar ratio issue in the discussion section. In particular the lidar ratio obtained by using the extinction from SAGE III and backscatter from CALIOP gives a value quite close to the adopted lidar ratio in much of the stratosphere.

35

We have revised the relevant sentence in abstract as:

“Further, we show that the extinction profiles (retrieved using a constant lidar ratio of 50 sr) capture the major stratospheric perturbations in both hemispheres over the last decade resulting from volcanic eruptions, extreme smoke events, and signatures of stratospheric dynamics.”

40

14) Figure 8: The authors should discuss on the high values of attenuated scattering ratios observed over the equator, including the proper references.

We have added the following:

45

“As in Figure 3, the feature with high attenuated scattering ratio near 25-30 km seen in all the four panels is the signature of the tropical reservoir of stratospheric aerosols, maintained by a complex interplay of transport from the troposphere and stratospheric dynamics as well as microphysical

processes including the Brewer-Dobson circulation, the QBO, evaporation and sedimentation (Trepte and Hitchman, 1992, Kremser et al., 2016).”

5 **15) P18L1-5: “The persistence of the stratospheric perturbation for several months is consistent with the results of Vernier et al. (2016) who found the presence of ash in the lower stratosphere 3 months after the Kelud eruption from balloon observations”. The observed features are qualitative consistent with the results of Verner et al. (2016). Is it possible to the authors to include a quantitative comparison?**

10 It is not possible to do a comparative comparison, because we are using a monthly averaged product at 5° latitude by 20 ° longitude—for a proper profile by profile comparison we need to have proper collocations. In any case, this paper is primarily devoted to a description of the algorithm and data product. While we offer an initial assessment of data product quality by providing multiple comparisons to SAGE III measurements, this paper is not intended as a comprehensive validation of all possible results that could be retrieved from this product.

15 **16) P20L3-5: “SAGE III performs solar and lunar occultation measurements as the ISS orbits the Earth and covers the entire global latitude (90oS to 90oN) and longitude range (180oW to 180oE).” ISS orbital characteristics are characterized by 51.6o inclination, therefore the authors it is suggested to check the global latitude coverage (90oS to 90oN).**

20 We have modified this sentence to:

25 “SAGE III performs solar and lunar occultation measurements as the ISS orbits the Earth and covers a broad latitude band (60°S to 60°N) and longitude range (180°W to 180°E).”

30 **17) P20L15-17: “The globally averaged value of the Angstrom exponent derived using all 15 months of data is about 1.56”. Please mention between which wavelengths.**

In the preceding sentence we had already mentioned that the Angstrom exponent was derived from 521 nm and 1022 nm. In any case we have added “(between 521 nm and 1022 nm)” once again.

35 **18) P20L22: “ $\sigma(z) = 100 \times (\sigma(z)_{\text{CALIPSO}} - \sigma(z)_{\text{SAGE}}) / \sigma(z)_{\text{SAGE}}$ ”. How are extreme cases treated? Which computational filters are applied? For instance, cases with $\sigma(z)_{\text{CALIPSO}} = 0$ ($\sigma(z) = -1$), or cases with very low values of $\sigma(z)_{\text{SAGE}}$ are also included? In case of applied filters in the dataset used prior to the results, the authors should mention them in the manuscript.**

40 As clearly mentioned in the text, we have used the extinction coefficients with fractional uncertainties less than 100% as retrieved from both SAGE III and CALIPSO. No other filters were used for these comparisons.

45 **19) P22L14: “between CALIPSO and SAGE III extinction at all altitudes with CALIPSO having a high bias”. Wherever the manuscript refers to statistical indicators, such as the “high bias” here, the authors should mention the corresponding computed values.**

Done.

50 **20) P23L8: “calculated using the average extinction coefficient profiles between 20 km and 30 km”. The reason of selecting vertically the region between 20km and 30km and not the region from 20 km up to 34 km, hence including the stratospheric region of V3 calibration, is not clear nor justified in the manuscript, since it is proven in Kar et al. (2017) that this region is not aerosol free.**

5 The retrieved profiles above 30 km are often quite noisy from both the instruments and were not used. Once again, retrieving aerosol extinction coefficients $\sim 10^{-5} \text{ km}^{-1}$ from these measurements is stretching the limits of the instruments' measurement capabilities while at the same time not adding anything significant to the stratospheric optical depth estimates. The purpose of this figure is to show the difference in the retrieved optical depths within the altitudes where much of the stratospheric aerosol generally resides.

10 **21) P2314: "though the differences begin to rise substantially in the midlatitudes of both hemispheres". Please include explanation on the observed features, including the necessary references.**

15 We don't completely understand the cause of these differences at this time. Further validation work using data from other instruments providing extinction retrievals might be of help in determining these.

20 **References:**

Thomason, L.W. et al., Atmos. Chem. Phys., 7, 5283-5290, <https://doi.org/10.5194/acp-7-5283-2007>, 2007.

Powell, K. A., Development of the CALIPSO lidar simulator, M. S. thesis, College of William and Mary, 228 pp. available at <http://www-calipso.larc.nasa.gov/resources/publications.php>